Dynamics and interactions of infections on networks

Moore, Sam

Award date:
2020

Awarding institution:
University of Bath

Dynamics and interactions of infections on networks

submitted by

Sam Moore

for the degree of Doctor of Philosophy

of the

University of Bath

Department of Mathematical Sciences

January 17, 2020

INCLUSION OF PUBLISHED MATERIAL

This thesis includes material from the following published articles:

S. MOORE, P. MÖRTERS AND T. ROGERS, *A re-entrant phase transition in the survival of secondary infections on networks*, Journal of Statistical Physics, 2018, pp. 1 - 14

This thesis is dedicated to my mum, Ginny, who forged for me the greatest world she knew. Every achievement I make within it stands as her legacy.

SUMMARY

In the mathematical modelling of epidemics, networks are frequently used to represent population structure and the effects of heterogeneity. The ideal network infection model presents dynamically consistent but mathematically tractable representations of both the population structure, usually by way of a random graph, and a stochastic spreading process on it. High levels of observed social and biological complexity, however, mean that compromises must be made dependent on the primary quantity of interest. This has led to a plethora of models and techniques in the literature.

In this thesis the primary interest is in models that track infection timings; how quickly will an infection cross the network and how long after person A is infected might person B become infected also? We shall see how models tracking infection time prove effective in capturing the dynamics of multiple coevolving contagions as, in order to study infection interactions, it must be known where their time frames overlap.

To this end, we shall consider three main models. Firstly, we use a multi-type branching process to analyse a secondary infection with dependence upon a primary infection host; this enables us to determine a window of relative speed in which the infections must develop in order to have secondary survival. Secondly, we develop a multi-type variant of the time tracking message passing equations; these enable us to answer questions about local susceptibility in a model with several interacting infection strains. Finally, by analysing the simplest version of these same message passing equations, we succeed in presenting some new theory for tracking infection timings with a calculation for the asymptotic speed of an infection wave front and an approximation of the expected infection time offset for heterogeneous individuals in the population bulk.

ACKNOWLEDGEMENTS

The considerable degree of drama that began my postgraduate life means that I owe a great deal of thanks for help, of peculiar sorts along with the expected and for the toleration for a great amount of inconvenience, by a great many people. That is far too many to mention by name, but includes the following.

I must firstly thank my supervisor Tim Rogers, I genuinely couldn't have hoped for anyone better. Tim somehow always seemed to know the right thing to do, even when that was apparently different from one day to the next. I must also thank Peter Mörters who set me off on the right course.

Next, I must thank the people of SAMBa. Shortly after joining Bath University an unfortunate altercation between bicycle and Land Rover left me with a broken neck. It was no small part to the people of SAMBa that life seemed to continue on much as before, albeit from a 2 foot lower perspective. I must give a special mention here to Susie who fought every battle for me, even when I assured her there was no problem. In a similar vein, I must also thank the charities *Special Effect*, who enabled me to stay connected with the world using just my eyes, and *Regain* who helped get me back on my bike again– a PhD without this would have surely been impossible.

My gratitude goes also to all my friends and colleagues from my time in Bath; to name just a few, Marcus, who found me a pen I could write with, Alge, who once bought me 5 kg of cheese, Fred, who also gave me cheese, Will and the people of 4w 1.15, who helped me open jars, lift things into cars and cheerily mocked me at every available opportunity and the inhabitants of Livingstone Terrace who fed and sheltered me when I was forced to live in halls with undergraduates.

Finally, I must thank my family, my brothers on whom I know I can always rely, and my Dad for nearly single-handedly putting up with all my complaints, for getting me to this point in life despite much adversity, and, with some help from Jane, for some proofreading (although "iff" isn't actually a typo).

I would like to reiterate that to thank everyone who deserves it from my time at Bath University would require these acknowledgements to become a substantial chapter. I have been blessed and humbled by a great deal of kindness and generosity from a great many people. None of you will be forgotten.

CONTENTS

CHAPTER 1

INTRODUCTION

Networks, it may be argued, are a hallmark of civilisation. The Romans connected our cities with roads, distributed fresh water via aquaducts and pipes and introduced sanitation via complex sewer systems [1]. As the world was mapped empires became established on the back of highly developed trade networks between ports, canals, and eventually rail. Then, during the 19th century, communication networks proliferated; first in the form of ever more sophisticated telegraph networks, followed by radio and telephone lines, mobile communication and satellites.

The 20th century brought us power grids and with them an explosion in technology sending us into the digital age. Information now travels rapidly throughout the world via the internet; a network of far reaching lines of copper wire, fibre optic cables and wireless hubs supporting countless non-physical networks in the form of the Web, numerous subsets of social media, emails and databases.

The operation of today's society is shaped by the ability to travel rapidly across the globe and send correspondence and disseminate ideas almost anywhere near instantaneously. While this globalisation creates countless new possibilities, it also opens new vulnerabilities; creating pathways for the rapid spread of bacterial infection, digital viruses and radical ideas. As observed by the writer Frigyes Karinthy [2],

> *Planet earth has never been as tiny as it is now. It is shrunk– relatively speaking of course– due to the quickening pulse of both physical and verbal communication.*

Understanding the dynamics of how contagions spread through networks, both individually and collectively, is therefore essential in allowing us to fully utilise and advance our capabilities, defend against attack and mitigate disaster.

Networks of interest are often big, even global in scale and rich in complexity. To study dynamics on them then requires a certain degree of approximation and, in seeking to do this effectively, mathematicians have developed a diverse tool kit. One such tool

is the random graph. The aim of the random graph is an algorithm to grow a structure with properties reminiscent of the object of study. Perhaps most simply this is to reflect what a network looks like on average or, for more sophisticated models, on a local scale– given knowledge of someone's friends, what do we expect the friends of their friends to look like?

The study of spreading quantities meanwhile is most often framed in the language of infection. Their prevalence throughout the history of mankind, combined with their potential for destruction, leaves little persuasion for their worth of study. The first proposed infection models neglected many aspects of population structure but nevertheless provided a first answer to the question of how large an outbreak may become given knowledge of its infectivity and longevity [3, 4]. The importance of population structure in infection modelling becoming quickly apparent, however, soon led to studying infections in the context of networks. This is the most dominant and successful approach used today and it is in this context that this thesis presents a trio of papers.

Infections are diverse in both their dynamics and effects, their interactions and how they spread; the common cold represents some 200 different viruses transmitted by saliva in close proximity [5]; bubonic plague was carried through our cities by rats to devastating effect; we frequently, inadvertently but actively, distribute E. coli bacteria in food products (a record of such instances may be found in [6]). Bearing this in mind, chapters 2 and 3 are concerned with epidemic complexity.

In Chapter 2 we will consider secondary infections– one infection that follows on from another. It is well appreciated that when we fall ill we are weakened, our immune systems compromised, leaving us open to super infections that can be devastating; this is seen for instance in the case of the wave of pneumonia that followed the Spanish flu outbreak of 1918 [7]. Despite their impact, little has previously been done to translate simple epidemic models to the application of secondary infection waves.

The main parameter of interest here is perhaps the relative infection time-scales between the primary and secondary infection waves. The most instructive model to be previously found on this interplay is by way of stacked SIS dynamics on the lattice [8, 9]. In the first paper presented, we use the machinery of branching processes to investigate a translation of this model to SIR dynamics on a random graph. The resulting interplay is both interesting and perhaps surprising as we found that the most successful secondary infection will progress at a speed proportional to its primary predecessor. We will see that infections either too slow or too fast are unable to persist.

The bacteria population on earth has been estimated at 5×10^{30} cells [10] and, with such a weight of coexistence, interactions are common. Besides the mono-directional relationship described by our super infection model, bacteria may also enjoy symbiosis, be pressured by competition or mutate between variants. The second paper, presented in Chapter 3, considers such relationships in the creation of a model of coevolving infection types. While infection interaction has been modelled previously, for instance with cooperation in [11] and with competition in [12, 13], our approach seeks to include aspects of

population structure to assess heterogeneous quantities such as who will be reached by which strain first, and for models with competition, its impact on type dominance.

The key to advancement in both these papers are models that keep track of time. Infections are usually ephemeral and, to gauge interaction, it's not enough to just know whether they arrive somewhere, but also when.

In Chapter 4 a final paper is presented that examines infection timing in more detail by evaluating how long it is expected to take the infection to travel in network based distance measures; if you are six degrees of separation away from a disease carrier, how long until you should be considered at risk? Who out of your friends will become infected first?

As a prelude to these papers, in this introductory chapter we shall begin by acquainting ourselves with the mathematical landscape from where our models are drawn. The first half of this chapter is devoted to a discussion of the theory of random graphs, an effective tool in the study of large real world networks. Before any technical discussion, however, we shall first consider the somewhat related topic of the branching process, their use thereafter demonstrated with a proof one of the most fundamental results in the study of the classic random graph– the emergence of the giant component.

Following this we turn our attention to the many variants of the random graph model, which have been introduced to more closely match the topology of commonly observed network structures, and show the phase transition for connectivity is in fact a common phenomena. The discussion of graphs is concluded with an introduction to the theory of percolation, essentially stochasticity added to an instance of a graph structure leading to the possible break down of the giant component.

We shall then move on to consider the modelling of infections, first with historical models that assume a homogeneous population, before moving onto discussing attempts to introduce heterogeneity. We finally wed epidemic modelling with that of networks in so called network epidemiology where results from percolation theory, and the exploration of connected components by a branching process, may be drawn upon. We conclude the introduction by discussing some recent techniques in modelling infections with sparse network approximations, a framework we will use extensively in the following research.

Throughout the rest of this introduction the focus shall be on insight over technical rigour. Results are presented to build the reader's understanding of the state of the literature and create an appreciation of the strengths and weaknesses of differing models and techniques. The reader wanting more technical details to complete the picture shall be referred where appropriate to the original sources in which this is given.

1.1 Networks and graphs

The network scientist is frequently hindered by objects of study too large and complex to analyse or even measure effectively. The world wide web for example is composed of over 1.5 billion active websites [14], a similar number to that of the active daily users on the social network of Facebook [15], and epidemiologists are tasked with modelling a human population moving towards 8 billion. This is a problem circumvented by the approximation to a simple representative model, the random graph, the study of which has led, over the past 60 years, to growth in the now rich field of graph theory.

An attempt to study a mathematically abstracted version of real networks was first made by Rapoport and Solomonoff in the early 1950s [16] with the first systematic study of what we now recognise as a random graph. In their paper they consider the size of what we now term the connected components of the graph and, by studying how properties of the graph structure change with edge density, they are able to allude to one of the most seminal results in graph theory– the existence of a phase transition at which the graph goes from being comprised of many small disconnected clusters to forming a single large connected body, the formation of the *giant component*. Determining the existence of large connected components will become of particular interest later when we start discussing infection spread; when considering the sub-network of infected nodes, for instance, the existence of the giant component is equivalent to a large scale epidemic outbreak. In laying the grounds for infection modelling, connectivity will hence dominate much of our discussion of random graphs.

Rapoport and Solomonoff's results however remained largely unnoticed until the end of the decade when they were resurrected and expanded upon simultaneously by both Gilbert [17] and, the pair largely celebrated as the founding fathers of random graph theory, Erdős and Rényi [18]. While Gilbert and Erdős and Rényi simultaneously introduced two very similar graph models, they differed in their approach to them. Gilbert's model, which he called the binomial model $\mathcal{G}(n,p)$, has become the most prevalent of the two formulations. To take a sample, $G(n,p)$, from the family $\mathcal{G}(n,p)$, Gilbert takes n vertices and includes each possible edge independently at random with probability p. Gilbert studied the probable form of such a sample by using generating functions and successfully derived expressions for a number of properties such as the event some $G(n,p)$ is connected.

Erdős and Rényi meanwhile were interested in graphs with prescribed numbers of edges as well as vertices. This gave rise to the family, $\hat{\mathcal{G}}(n,m)$, of all possible graphs with n vertices and m edges, thus any one configuration may be chosen uniformly at random with probability $1/\binom{\binom{n}{2}}{m}$. While Gilbert's, as well as Solomonoff and Rapoport's, results relied on the derivation of complex expressions for the exact number of graphs with certain properties, Erdős and Rényi's legacy was insightful in that asymptotic results for large graphs may be best obtained by probabilistic means. Their method asks questions like: what do most graphs in the family $\hat{\mathcal{G}}(n,m)$ look like?

It is worth noting that asymptotically, for large n, these two classical graph models,

$\mathcal{G}(n,p)$ and $\hat{\mathcal{G}}(n,m)$, are roughly equivalent with $m = np$. Furthermore, it is a historical quirk, due to this equivalence and the importance of Erdős and Rényi's work that, while Gilbert's formulation is most frequently used, the model is often referred to as an Erdős-Rényi graph, or simply a random graph. This is the custom we shall conform to throughout the remainder of this thesis.

In studying infections on networks, the only parts of the network of interest are those which are connected to the source of the outbreak; a large epidemic may only occur in a largely connected society. Moreover, as an infection spreads, its pathway defines a connected subgraph. The study of infection on networks is therefore all about the probabilistic size of connected components– this quantity will then dominate much of our preliminary discussion.

Perhaps the most important of Erdős and Rényi's results in their seminal paper *On the evolution of random graphs* [19] was the observation of a variety of phase transitions, arising with an increase of the mean degree in their model. Most importantly they show that in the large graph limit, there exist degree thresholds above which structures will exist with probability 1 and below which they won't be seen. For large n, if $pn < 1$ the largest connected component of a random graph $G(n,p)$ is with high probability of size $O(\log n)$, jumping to $O(n)$ above the threshold $pn = 1$. The component of order n, when it exists, is known as the *giant component* of the graph. Furthermore, they show the giant component is unique; if $np > 1$ then we have a single giant component of order n with all other components of order $\log n$.

This is a well studied phenomenon, and many alternative proofs have since been given, for example Nachmias and Peres [20] give a simple proof using Martingales and Karp [21] via an exploration process which may be seen analogous to a branching process. Later we will return to consider this manner of proof. Let us first turn now though to formally introducing the branching process.

1.1.1 Branching processes

As we have already touched upon, in both the study of random graphs and infection processes, and certainly the interface between the two [22, 23, 24, 25], we shall frequently find branching processes to make a useful approximation. In particular, as we shall see in the subsequent section 1.1.2, the number of vertices in an Erdős-Rényi graph at a distance less than d away from a given starting node may be well approximated by the total size of a branching process after d generations. Furthermore, considering a subgraph of individuals that ever get reached by an infection, the branching process approximation may still be made by restricting its offspring distribution. In Chapter 2 we shall take advantage of this duality in the creation of an infection model. Before going further, however, we shall first take the opportunity to introduce branching process theory in terms of their background, definition and a few key results which we shall find useful.

While similar earlier models do exist, Bienayme in 1845 [26] being a known example, the

origin of the branching process is generally attributed [27] to a paper by Galton and Watson published in 1875 [28]. The original motivation for the model was in the consideration of male lineage and two associated questions suggested by Galton [29]. These were posed as follows:

> *Problem 4001. A large nation, of whom we will only concern ourselves with the adult males, N in number, and who each bear separate surnames, colonise a district. Their law of population is such that, in each generation, a_o per cent of the adult males have no male children who reach adult life; a_1 have one such male child; a_2 have two; and so on up to a_5, who have five. Find (1) what proportion of the surnames will have become extinct after r generations; and (2) how many instances there will be of the same surname being held by m persons.*

Watson's idea was to approach the problem using a Markov chain over the state space of positive integers, $\{Z_n\}_{n=0,1,2,\ldots}$, representing the size of the population after n generations. The chain is then given transition probabilities of the form

$$\mathbb{P}[Z_{n+1} = j | Z_n = i] = \sum_{k_1+\ldots+k_i=j} p_{k_1} \ldots p_{k_i} \,. \tag{1.1}$$

These transition probabilities then describe the evolution of the population. An individual has a random number of offspring, i, with probabilities assigned by its *offspring distribution*, $\{p_i\}_{i=0,1,2,\ldots}$ such that $\sum p_i = 1$.

In the context of Galton's problem, the offspring distribution is simply given by the a_i percentiles, with $a_i = 0$ for $i > 5$. For example, the chance of going from a population of $Z_n = 2$ to $Z_n = 4$ in a single time step would be given by

$$\mathbb{P}[Z_{n+1} = 4 | Z_n = 2] = \frac{1}{100} \left(2a_1a_3 + a_2a_2 + 2a_4a_0\right) \,. \tag{1.2}$$

We would expect the population to increase in each generation by a factor of the mean, m, of the offspring distribution. So in n generations we would expect the population to have increased by a factor of m^n. It seems then that if $m < 1$ we have good reason to suppose that the population size will tend to 0, that is, extinction.

This is not to say that extinction will be avoided if $m > 1$. Indeed any process starting from a population of size one will go extinct in a single generation with probability p_0. The long term survival probability is a non trivial question then, one which has been successfully tracked by the use of generating functions [28, 30].

The generating function for the offspring distribution (or equivalently of Z_1 given

$Z_0 = 1$) is given by

$$f(s) = \sum_{k=0}^{\infty} p_k s^k, \text{ such that } |s| \leq 1\,, \tag{1.3}$$

from which we may read, for instance, that the expectation of Z_1 starting from the state $Z_0 = 1$ as

$$m = \mathbb{E}[Z_1] = \sum_{k=0}^{\infty} k p_k\,. \tag{1.4}$$

Usefully the function may be iterated to find the generating function for subsequent generations. If we define the n^{th} iterate of f as

$$f_n(s) = \begin{cases} s & \text{for } n = 0 \\ f[f_{n-1}(s)] \text{ for } n = 1, 2, ... \end{cases} \tag{1.5}$$

so

$$f_{n+1}(s) = f_n[f(s)] \tag{1.6}$$

and from this we may attain the following lemma:

Lemma 1.1. The generating function of Z_n is $f_n(s)$ (the n^{th} iterate).

Proof. Let us consider the generating function for the n^{th} generation, Z_n, which we shall call $f_{[n]}$. Now since the generating functions for multiple individuals is simply the product of their individual generating functions, it follows that the conditional generating function for Z_{n+1} given $Z_n = k$ would be given by $(f(s))^k$. Hence the generating function of Z_{n+1} is given by

$$f_{[n+1]}(s) = \sum_{k=0}^{\infty} \mathbb{P}(Z_n = k)(f(s))^k = f_{[n]}[f(s)]\,. \tag{1.7}$$

Thus, we see by definition of the generating function's iterates and by uniqueness of generating functions, that we have $f_{[0]} = f_0$ and thus inductively

$$f_{[n]}(s) = f_n(s)\,. \tag{1.8}$$

□

Using this result enables the finding of the sought extinction probabilities. This is achieved by the following theorem, more details of which may be found in [30].

Theorem 1.2. The extinction probability, q, is the smallest non-negative root of the equation $f(s) = s$. Furthermore, if m denotes the mean of the offspring distribution, then

$$m < 1 \Rightarrow q = 1 \tag{1.9}$$

$$m > 1 \Rightarrow q < 1 \tag{1.10}$$

and

$$\mathbb{P}(Z_n \to \infty) = 1 - q\,. \tag{1.11}$$

Proof. Now

$$\mathbb{P}(Z_n \to 0) = \lim f_n(0) = q\,. \tag{1.12}$$

Since also $Z_n = 0 \Rightarrow Z_{n+1} = 0$ and thus $\mathbb{P}(Z_n = 0) \leq \mathbb{P}(Z_{n+1} = 0)$, we see that

$$0 \leq f_0(0) \leq f_1(0) \leq f_2(0) \leq ... \leq q = \lim f_n(0) \tag{1.13}$$

Then since $\lim f_{n+1}(0) = \lim f_n(0)$ and $f_{n+1}(0) = f[f_n(0)]$, we may conclude that $f(q) = q$.

For some other root a, since f is non-decreasing, $f(0) \leq f(a)$. If also $f_n(0) \leq a$ for some n, it follows that

$$\begin{aligned} f_{n+1}(0) &= f[f_n(0)] \\ &\leq f(a) = a\,. \end{aligned} \tag{1.14}$$

Hence the first part of the theorem follows by induction.

If $m < 1$ then for every s such that $0 \leq s < 1$ it follows that $f'(s) < f'(1) = m < 1$, since f' is increasing on $\mathbb{R}^+$. Thus, by the mean value theorem $f(s) < s$. We may then conclude that in this case $q = 1$.

If $m = f'(1) > 1$, this means that at $f(1) = 1$ f is increasing more rapidly than s. So by the continuity of f, it follows that $f(s) < s$ for a left neighbourhood of $s = 1$. Further since $f(0) \geq 0$, we may conclude that $f(s) = s$ for some $0 \leq s < 1$ as required.

For the final part assume we are in this case $q < 1$ and $f'(q) < 1$, else the result is trivial. If we consider the probability of Z_n lying in the interval $[1, k]$, for the case when

$q > 0$ that is

$$\mathbb{P}[1 \leq Z_n \leq k] = \sum_{j=1}^{k} \mathbb{P}[Z_n = j] \tag{1.15}$$

$$\leq \sum_{j=1}^{k} \mathbb{P}[Z_n = j] \frac{q^{j-1} j}{q^k} \tag{1.16}$$

$$\leq \frac{f_n'(q)}{q^k} \tag{1.17}$$

$$= f'(q) n q^{n-1} \to 0 \tag{1.18}$$

and hence,

$$\lim_{n \to \infty} \mathbb{P}(1 \leq Z_n \leq k) = 0\,. \tag{1.19}$$

Thus, any reachable state in this interval may only be visited finitely often, and, since k was arbitrary, the result follows. For the case when $q = 0$, we must have that Z_n is non-decreasing and so $Z_n \to \infty$. □

It is worth noticing here that, although $q = 1$ for both the cases when $m = 1$ and $m < 1$, it is sensible to deal with the case $m = 1$ separately. This is because while extinction may be certain for the $m = 1$ case the process will be highly unstable. This is seen by considering the second derivative of the generating function to show that

$$\mathrm{Var}(Z_n | m = 1) \xrightarrow[n \to \infty]{} \infty\,. \tag{1.20}$$

All three cases of the basic Galton Watson process are well understood in the literature [30, 31, 32], though the most basic results, as already discussed, will prove sufficient for our needs. Let us instead turn our attention to some useful generalisations of the process.

Multi-type branching

The branching process may be modified to account for a heterogeneous population by introducing a number of different *types*. The multi-type branching process proceeds similarly to the Galton Watson process, except now we assign each individual a discrete type with an associated offspring distribution which describes both the number and type composition of that type's children. In chapters 2 and 3 we will model multiple interacting infections and find that the multi-type branching process creates additional parameters necessary in order to capture the dynamics of such complex infection systems.

The multi-type process is again a Markov process similar to that introduced previously, except over the space of vectors in $\mathbb{N}^k$, as opposed to in $\mathbb{N}$. As before we shall let Z_n be the overall number of individuals in the n^{th} generation, where entry Z_n^i gives the number of individuals of type i.

To describe the process we consider most basically the transition from a single individual of type i to the subsequent generation. That is, if $Z_0 = e_i$, what is the distribution of the subsequent state Z_1? Here e_i is, as typical, the vector with 1 in the i^{th} position and zeros elsewhere. We then define the transition probability

$$\mathbb{P}[Z_1 = (r_1, ..., r_n)|Z_0 = e_i] = p^i(r_1, ..., r_n)\,. \tag{1.21}$$

Where r_i is the number of individuals of type i. In this case, the generating function for Z_1 will be given by

$$f^i(s_1..., s_k) = \sum_{r_1,...,r_k=0}^{\infty} p^i_{(r_1,...,r_k)} s_1^{r_1} \dots s_k^{r_k} \;\; |s_1|, ..., |s_k| \leq 1\,. \tag{1.22}$$

Then we may formulate the vector equivalents of the offspring distribution and associated generating function as

$$\mathbf{p}(\mathbf{r}) = (p^1(\mathbf{r}), ..., p^k(\mathbf{r})) \tag{1.23}$$

and

$$\mathbf{f}(\mathbf{s}) = (f^1(\mathbf{s}), ..., f^k(\mathbf{s}))\,. \tag{1.24}$$

We retain many of the basic properties as for the original Galton Watson process. Firstly, it may be seen that the generating function still follows the same recursive behaviour. If we take $\mathbf{f_n}$ as the generating function for Z_n, then

$$\mathbf{f_{n+1}} = \mathbf{f}[\mathbf{f_n}]\,. \tag{1.25}$$

Define the mean matrix, M, with entries given by:

$$M_{ij} = \mathbb{E}(Z_1^j | Z_0 = e_i) = \frac{\partial f^i(1, ..., 1)}{\partial s_j}$$

So if we have N types, then the mean matrix will take the form

$$M = \begin{pmatrix} m_{1,1} & \dots & m_{1,N} \\ \vdots & \ddots & \\ m_{N,1} & & m_{N,N} \end{pmatrix}, \tag{1.26}$$

with entry $m_{i,j}$ giving the expected number of type j children from a type i parent. Further, by following similar arguments to before (details for instance in [30]), we may

find that

$$\mathbb{E}[Z_n] = M^n Z_0 \,. \tag{1.27}$$

Thus, the make up of the n^{th} generation is expected to be given by the n^{th} iterate of the mean matrix applied to the initial condition Z_0. A consequence of the Perron-Frobenius theorem [33] tells us that, for a matrix with positive entries (such as our mean matrix, M), we have a positive absolutely maximal eigenvalue ρ. It is worth mentioning that, while the Perron Frobenius theorem in its original form only accounts for matrices with strictly positive entries, the result has been generalised to allow zero entries by decomposing M into positive sub-matrices [34].

Since the expected population is described by iterates of M, it is reasonable to assume that if $\rho < 1$ then the population size will tend to zero, and if $\rho > 1$ it may possibly become large. Indeed this is the case, and moreover an analogue of Theorem 1.2 may be shown to hold with ρ taking the place of the offspring distribution mean, m, for the Galton Watson process.

In some situations the desired type space, $\mathcal{T}$, may actually be continuous. Consider for instance cosmic ray cascades; this is a process in which energetic particles strike other particles, energising them in turn and causing a chain reaction. The type here is a particle's energy, this dictating the degree of scattering at a collision point. One simple model for this phenomena has been made by discretising the type space to gain an approximation using standard multi type theory [35].

An alternative approach, and the one we shall use in Chapter 2, may be found by making the number of offspring a deterministic quantity (this may just be the expected value) dependent on the parent's type, but allowing a continuous type space. We may then introduce a production kernel, $\mu(s, s') = \eta(s)\phi(s, s')$, where $\phi(s, s')$ gives the probability density function for a child of a type s parent being of type s', and $\eta(s)$ the number of offspring coming from an individual of type s.

Suppose we have a population given by ψ, where $\psi(s)$ is equal to the number of individuals of type s. The density of type s individuals in the subsequent generation will then be given by the production operator

$$M[\psi](s') = \int_{\mathcal{T}} \psi(s)\mu(s, s')\mathrm{d}s \,. \tag{1.28}$$

This production operator then takes the place of the mean matrix in the discrete multi-type branching process and similar conditions on the survival of the process may be found relative to the largest eigenvalue of this operator, ρ_M. Specifically then, if again q gives the probability of extinction, we have

$$\rho_M \leq 1 \Rightarrow q = 1 \tag{1.29}$$

$$\rho_M > 1 \Rightarrow q < 1 \,. \tag{1.30}$$

1.1.2 The size of giant component

We have introduced branching processes at this juncture for their useful application to sparse networks. We call a network sparse, or alternatively tree-like, if there is typically only one path between any two nodes (not allowing for backtracking). In families of random graphs sparsity is often to be found in the large scale limit; if the degree sequence is fixed then the number of cycles will decrease with an increase in vertex numbers.

Consider a Poisson branching process, $\mathcal{X}(\lambda)$, that is a branching process with a Pois(λ) offspring distribution. For large, sparse, Erdős-Rényi graphs a connection between the branching process $\mathcal{X}(\lambda)$ and the graph $G(n, \frac{\lambda}{n})$ may then be described by considering a *vertex exploration process* [21]. Importantly to us, this is also an idea that has been used by Kendall [23] to study the spread of infection on graphs, something we shall make full use of in Chapter 2 where we show how even complex disease dynamics may be represented in this manner.

The exploration process is an algorithm to determine the connected component $C(v)$ containing some particular vertex v in the graph $G(n, \frac{\lambda}{n})$. It proceeds as follows:

1. Start with the vertex v, which we label *unexplored*, with every other vertex labelled as *new*.

2. Next, consider every possible edge out of v to some vertex w in the list of *new* vertices to establish which are present. All the neighbours found at this step are then relabelled as *unexplored*, and vertex v as *explored*.

3. Repeat the process starting from some randomly chosen unexplored vertex at each step until this list becomes exhausted. The resulting list of explored nodes gives the desired component, $C(v)$.

Now at step t of the exploration process it follows that the number, $X(t)$, of neighbouring vertices we shall add to the list of *unexplored* vertices will have the binomial distribution $B(n_t, \lambda/n)$, where n_t denotes the number of *new* vertices at the start of this step. In the early stages of this process, or if the size of $C(v)$ is relatively small compared to n, then we may approximate $n_t \approx n$, and thus $\mathbb{E}[X(t)] \approx \lambda$. As n becomes large (so $\frac{\lambda}{n} \to 0$) it follows that X_t may be coupled with a Poisson(λ) random variable Y_t with probability $1 - o(1)$. In this way we may conclude that in its early stages, or for relatively small $C(v)$, the exploration process matches the Poisson branching process $\mathcal{X}(\lambda)$ with probability $1 - o(1)$.

This means for some k fixed, when $k \ll n$, by the above we should have a close match between the branching and vertex exploration processes in any component of size at most k. Thus, the probability that the processes disagree before reaching size $k + 1$ is $o(1)$ and so

$$\mathbb{P}[|C(v)| = k] = \mathbb{P}[|\mathcal{X}(\lambda)| = k] + o(1)\,. \tag{1.31}$$

Furthermore, if we take $N_k(G(n, \frac{\lambda}{n}))$ to be the number of vertices in components of the graph $G(n, \frac{\lambda}{n})$ of size k then, for v chosen uniformly at random, we have

$$\mathbb{E}\left[\frac{1}{n}N_k(G(n,\lambda/n))\right] = \mathbb{P}[|C(v)| = k]\,, \tag{1.32}$$

and thus for $n \to \infty$

$$\mathbb{E}\left[\frac{1}{n}N_k(G(n,\lambda/n))\right] \to \mathbb{P}[|\mathcal{X}(\lambda)| = k]\,. \tag{1.33}$$

Then

$$\mathbb{E}[N_k(G(n,\lambda/n))^2] = n^2\mathbb{P}[|C(v)| = k, |C(w)| = k]\,, \tag{1.34}$$

where $C(v)$ and $C(w)$ are the connected components of two independently chosen vertices v and w respectively. By observing that for two separate explorations starting from v and w, the probability that they share a vertex before both reaching size k is again $o(1)$. It follows that

$$\frac{1}{n^2}\mathbb{E}[N_k(G(n,\lambda/n))^2] \to \mathbb{P}[|\mathcal{X}(\lambda)| = k]^2\,, \tag{1.35}$$

so by (1.33) then $\mathrm{Var}\left[\frac{N_k(G(n,\lambda/n))}{n}\right] = o(1)$, and thus we may also conclude convergence in probability

$$\frac{1}{n}N_k(G(n,\lambda/n)) \xrightarrow{p} \mathbb{P}[|\mathcal{X}(\lambda)| = k]\,. \tag{1.36}$$

The fact that the random graph matches a branching process locally is perhaps unsurprising; it is not too difficult to see that a large graph will be locally tree-like in structure. However, when we start considering large components of order n, it is reasonable to assume the coupling will break down. As the exploration process becomes large the distribution of X_t will be affected by both a declining number of new vertices left and the encountering of a progressive number of cycles.

Even here though it turns out that the branching process is still informative and in fact can tell us about the size of any large components of the graph, in particular, when it forms, the size of the giant component, C_g. Equivalently this means, as we shall make full use of in Chapter 2, the survival probability of a branching process which matches infection spread on a large Erdős-Rényi graph well approximates the probability of a large epidemic outbreak.

Let us now then turn to the promised proof of the emergence of the giant component. Bollobás and Riordan [36] succeed in connecting the probability that the total size of the branching process is infinite to the giant component size via the following theorem:

Theorem 1.3. For λ fixed as $n \to \infty$ the proportional size of the largest component of

the graph converges in probability,

$$\frac{1}{n}C_g(G(n,\lambda/n)) \xrightarrow{p} \rho(\lambda)\,, \tag{1.37}$$

where $\rho(\lambda)$ is the survival probability of a Poisson branching process with mean λ (so $\rho(\lambda) = 1 - q$ for the extinction probability q discussed above).

Thus, by Theorem 1.2, if $\lambda \leq 1$ then no large component exists, and if $\lambda > 1$ a large component exists with high probability.

Proof. We start by showing that the total proportion of vertices in all components of size greater than some given ω must converge in probability to $\rho(\lambda)$, so the proportional size of the giant component may be at most $\rho(\lambda)$. The proportion of vertices in components of at least size ω is

$$\frac{N_{\geq\omega}}{n} = 1 - \frac{1}{n}\sum_{k=1}^{\omega-1} N_k(G(n,\lambda/n))\,. \tag{1.38}$$

Abbreviating $G_n = G(n,\lambda/n)$, $\mathcal{X}(\lambda) = \mathcal{X}$, for some function $\omega(n) \to \infty$ we have

$$\left|\frac{1}{n}N_{\geq\omega(n)}(G_n) - \mathbb{P}[\mathcal{X} \geq \omega(n)]\right| = \left|\frac{1}{n}N_{<\omega(n)}(G_n) - \mathbb{P}[|\mathcal{X}| < \omega(n)]\right| \tag{1.39}$$

$$= \sum_{k=1}^{\omega(n)-1}\left|\frac{1}{n}N_k(G_n) - \mathbb{P}[|\mathcal{X}| = k]\right|\,. \tag{1.40}$$

Now by equation (1.36) for any fixed k

$$\left|\frac{1}{n}N_k(G_n) - \mathbb{P}[|\mathcal{X}| = k]\right| \xrightarrow{p} 0\,. \tag{1.41}$$

Thus, following the method of Bollobás and Riordan [36], we may choose the function $\omega(n)$ to grow slowly enough so that

$$\sum_{k=1}^{\omega(n)-1}\left|\frac{1}{n}N_k(G_n) - \mathbb{P}[|\mathcal{X}| = k]\right| \xrightarrow{p} 0\,. \tag{1.42}$$

By definition

$$\begin{aligned}\rho(\lambda) =& \mathbb{P}[\mathcal{X}(\lambda) = \infty] \\ =& \lim_{k\to\infty}\mathbb{P}[\mathcal{X}(\lambda) \geq k]\,,\end{aligned} \tag{1.43}$$

and since we have $\omega(n) \to \infty$, then $\mathbb{P}[\mathcal{X}(\lambda) \geq \omega(n)] \to \rho(\lambda)$ and we may conclude that

$$\frac{N_{\geq\omega(n)}}{n} \xrightarrow{p} \rho(n)\,. \tag{1.44}$$

We have then shown the result for the total of all large components containing more than $\omega(n)$ vertices. It then remains to show that, as $n \to \infty$, with high probability there exists only a single such component.

Suppose for contradiction we have multiple large components. If this were the case then we must have

$$C_g(G(n, \lambda/n)) \leq (\rho(\lambda) - \epsilon)\, n \tag{1.45}$$

for some $\epsilon > 0$.

For some random graph $H' = G(n, \lambda'/n)$ with $\lambda' < \lambda$. Observe that if we then add every other possible edge not already present with probability $\frac{\lambda - \lambda'}{n - \lambda'}$, then the subsequent graph will be equivalent to some $H = G(n, \lambda/n)$.

Consider the subset of vertices contained in large components of H', B. By equation (1.44), as $n \to \infty$, we have that

$$|B| \geq (\rho(\lambda'))n = (\rho(\lambda) - \epsilon/2)n\,. \tag{1.46}$$

for some $\epsilon > 0$. Suppose we find a partition of B into two disjoint subsets B_1 and B_2, so $B = B_1 \sqcup B_2$. Now by the assumption (1.45) and equation (1.46), B_1 and B_2 may be chosen to be disconnected in H with $|B_1|, |B_2| \geq \frac{\epsilon}{2}n$. Since there are $|B_1||B_2|$ possible ways to connect the two vertex sets, if B_1 and B_2 are disconnected in H' the probability that they are also disconnected in H is

$$\begin{aligned}
\frac{\lambda - \lambda'}{n - \lambda'}^{|B_1||B_2|} &\leq \left(1 - \frac{\lambda - \lambda'}{n}\right)^{\frac{\eta}{2}n(1-\frac{\eta}{2})n} && (1.47)\\
&= \left(1 - \frac{\lambda - \lambda'}{n}\right)^{\Theta(n^2)} && (1.48)\\
&= e^{-\Theta(n)}\,. && (1.49)
\end{aligned}$$

Finally, since there are at most $o(n)$ large components of H', which may be partitioned in at most $2^{o(n)}$ ways, then the expected number of suitable partitions is

$$2^{o(n)} e^{-\Theta(n)} = e^{-\Theta(n)} = o(1)\,. \tag{1.50}$$

Thus as $n \to \infty$, with high probability no such partition exists, so the assumption must not hold and we have a single large component as required.

□

In addition to the size of the largest component, branching processes have also been useful in describing other graph properties important in the study of infection, for instance the longest shortest path between any two vertices, the graph's *diameter*. When $\lambda < 1$, in the large graph limit Luczak [37] shows the diameter is equal almost surely to the diameter of the largest *tree component* of the graph, that is the largest subgraph which is

a tree. In this sub-critical case in fact the largest component is known to be a tree with approximately $\frac{\log(n)(1-np)^3}{np-1-\log(np)}$ vertices [38, 39, 40].)

This analysis was later extended to the super-critical case by Riordan and Wormald [41] using branching process arguments. In particular they prove that for $\lambda > 1$, the diameter of the random graph $G(n, \lambda/n)$ will be given by

$$\mathrm{diam}(G(n,\lambda/n)) = \frac{\log n}{\log \lambda} + \frac{2\log n}{\log(1/\lambda^*)} + O_p(1) \tag{1.51}$$

where λ^* is the branching number of the graph, defined by $\lambda^* = \lambda(1-\rho(\lambda))$.

1.1.3 Random graph variants

So far we have discussed only the classic random graph model, $G(n,p)$. The persistence of this model is perhaps due to how easy it is to handle, later we shall find results from infection spread on such networks readily attainable, however the Erdős-Rényi graph may often be a poor reflection of reality. In Chapter 4 we shall consider simulations on some real network structures, structures that have properties very different from the classic random graph.

The degree distribution for the random graph $G(n,p)$ may be represented by the probability some randomly chosen node has degree k,

$$p_k = \binom{n}{k} p^k (1-p)^{n-k}\,. \tag{1.52}$$

For large n then

$$p_k \approx fracn^k k! \left(\frac{p}{1-p}\right)^k (1-p)^n \xrightarrow[n\to\infty]{} \frac{\lambda^k e^{-z}}{k!}\,. \tag{1.53}$$

So in the Erdős-Rényi model, every node looks probabilistically the same and the distribution of node degrees is Poisson– certainly not something to be assumed for a general network.

Many alternative classes of random graph have been proposed to address this. One simple idea is to create a random graph from a deterministic degree sequence, often referred to as the configuration model [42]. This is constructed as follows:

> Suppose you have a degree sequence $k_1, ..., k_n$ where k_i is the number of edges connected to the i^{th} node. Create a list of the vertices with i included k_i times. Pair entries uniformly at random to get a list of edges. Since there are $\prod_i k_i!$ ways of making any one unique pattern, this samples a graph uniformly at random from the degree sequence.

If it is instead desirable to sample a graph from a degree distribution, rather than a given degree sequence, one might simply sample first a degree sequence then proceed as

above. Alternatively this could be done directly by taking the expected degree sequence, $l_1, ..., l_n$, then proceed by connecting i to j with probability $\frac{l_i l_j}{\sum_m l_m}$ [43].

Controlling the degree sequence isn't enough on its own to represent any observed network structure. Doing so in the manner described spreads nodes of differing degrees uniformly throughout the graph. However, it is quite reasonable that there may be some heterogeneity in the graph structure; perhaps it may be split into sparse and dense neighborhoods with low degree nodes more likely to be connected to other low degree nodes and high degree preferentially connected to high degree.

A simple method to reflect such inhomogeneity has been proposed by Söderberg [44], the aptly named Inhomogeneous Random Graph model. Here nodes are assigned types from a finite type space, $\mathbf{c}$, of size K, according to a vector of probabilities, $\mathbf{r} = \{r_1, ..., r_K\}$, with entries summing to 1. Similarly to a classical random graph formalisation, then each possible edge is included with independent probability, though now one that is inhomogeneous. The edge connecting vertex of type c to a vertex of type d is included with probability $\frac{m_{cd}}{n}$, where the m's are the entries of the $K \times K$ matrix, M, of elements in $[0, n]$.

The Inhomogeneous Random Graph $IRG(n, M, \mathbf{r}, \mathbf{c})$ defines a random graph with highly tunable structure. $IRG(n, p, 1, 1)$ for instance would return the classic Erdős-Rényi graph, while $IRG\left(n, \binom{m_{11}\, m_{12}}{m_{21}\, m_{22}}, [r_1, r_2], [1, 2]\right)$ for $m_{11} > m_{22} > m_{21}, m_{12}$ would produce a graph with a special case of connection inhomogeneity known as *assortative mixing* [45, 46]. An assortatively mixed network is one in which high degree vertices tend to connect to other high degree vertices, and low to low. Newman [45] observes that social networks tend to be assortative, while technological and biological networks are typically disassortative.

Of all variants to the Erdős-Rényi model however, perhaps two are most important in terms of scope and impact: the Watts-Strogatz model, which spans between highly localised and small world network regimes, and the Barabási-Albert model, an algorithm for the generation of a *scale-free* network.

Watts-Strogatz

Aside from problems of degree distribution, random graph structures have both strengths and weaknesses in their accuracy of reflecting real network dynamics. Heuristically, for a sparse Erdős-Rényi graph of average degree c, by the branching process approximation, we expect approximately c^m individuals at distance m. Hence, in a graph exploration, the number of vertices reached increases exponentially with distance and equivalently the average path length between any two nodes may be expected to scale logarithmically– this is a result proven in [39, 51, 52].

As may be observed in Table 1-1, this same scaling is in fact a property seen in many real networks [53] where average path lengths are typically short [54]. Often called the small world phenomenon, this is for instance the reason behind the famous 6 degrees of

Network	Average path length	Clustering coefficient	Size
Facebook sites [47]	4.3884	0.2954	27917
Condensed Matter collaboration [48]	5.3519	0.6417	21363
High school [49]	1.6198	0.4988	788
Facebook companies [47]	5.3098	0.2392	14113
Facebook athletes [47]	4.2745	0.2762	13866
Astrophysics collaboration [48]	4.1938	0.6328	17903
Facebook ego [50]	3.6916	0.6055	4039
1000 node circular lattice	62.875	0.6429	1000
1000 node Erdős-Rényi	5.1063	0.0032	1000

Figure 1-1: *Table showing graph properties measured for a selection of real networks and random graph models.*

separation, hypothesised by Karinthy [2] and investigated by Milgram [55], that a random pair of people are on average within 6 social contacts from one another. However, seemingly counter to this, real networks are similarly observed, again demonstrated in Table 1-1, to have a high level of clustering. From the graph perspective this is a common occurrence of triangles. In the language of social networks this means the friend of a friend has an increased probability of being your friend too.

Clustering is typically measured by way of the clustering coefficient, C, an expression of the proportion of vertices with a common neighbour that form a triangle [56, 57]. That is

$$C = \frac{\#\text{triangles}}{\#\text{connected triples}}\,, \tag{1.54}$$

where a connected triple is a vertex together with a pair of neighbours. In an Erdős-Rényi graph $G(n,p)$, the probability of the edge being present between the two neighbours required to complete the triangle is simply $\frac{c}{n}$, which for large graphs is arbitrarily small. The challenge then taken up by Watts and Strogatz was to produce a random graph model with mean vertex to vertex distance logarithmically proportional to graph size, but with clustering coefficient much greater than that seen in a classic random graph.

Watts and Strogatz's important observation was that, for a highly localised graph structure, the introduction of a relatively small number of random edges will dramatically decrease the average path length. They implemented this by starting with a regular graph with a high clustering coefficient that is purely locally connected, then adjusting it to create short paths across the whole network. Their chosen starting point for this model was a ring lattice created by connecting each vertex to its k clockwise nearest neighbours. In such a graph, since every connected pair of vertices may be seen to have $k-1$ additional neighbours in common, it follows that the lattice will have $\frac{nk(k-1)}{2}$ triangles, and, since each vertex will have $\frac{2k(2k-1)}{2}$ unordered neighbouring pairs, there will be $nk(2k-1)$

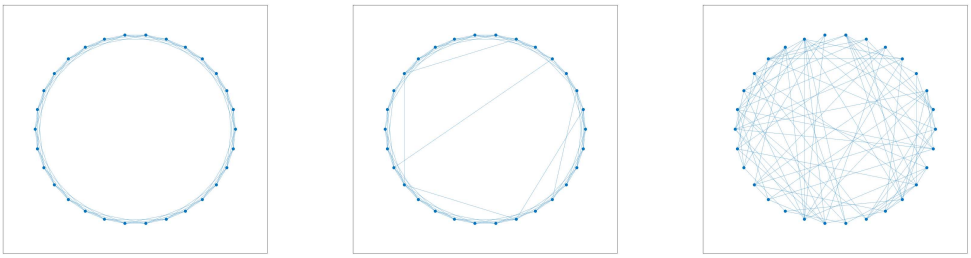

(a) $p = 0$ **(b)** $p = 0.1$ **(c)** $p = 1$

Figure 1-2: *Plot of three Watts-Strogatz graphs on 1000 nodes with degree 6. The graphs have rewiring probabilities of* $p = 0, 0.1, 1$*, average path lengths of* $83.6670, 6.1867, 4.0983$ *and clustering coefficients of* $0.6000, 0.4528, 0.0044$ *respectively.*

connected triples. Hence the clustering coefficient will be given by

$$C = \frac{3(k-1)}{2(2k-1)}\,. \tag{1.55}$$

From this starting point, Watts and Strogatz then rewire each edge independently at random with some probability p by taking one end of the edge and moving it to a new, uniformly random, location. The resulting graph may be seen [57] to have a clustering coefficient of

$$C = \frac{3(k-1)}{2(2k-1)}(1-p^3)\,. \tag{1.56}$$

Hence, while only a small amount of rewiring, and so a small increase in p, is seen to effectively reduce the average path length, the clustering coefficient is only affected by a factor of p^3 and so is relatively resilient to increases in p. This is shown in Figure 1-3 where we see a broad range of intermediate values for the rewiring probability give the desired properties of a large clustering coefficient and short average path length.

Scale-free networks

As we saw earlier, the Erdős-Rényi random graph has a Poisson degree distribution. However, this is often not representative of many observed networks. Figure 1-4 shows plots of observed degree distributions in a number of real world networks. It may be seen that, rather than following a Poisson distribution, in general they correlate strongly to a power law degree distribution where the probability, p_k, that a vertex would be connected to k is given by

$$p_k \propto k^{-\gamma}\,. \tag{1.57}$$

This type of structure is a mixed blessing. Pastor-Satorras et al. [62] observe a power law degree distribution in the network of the Internet and find that, while on one hand

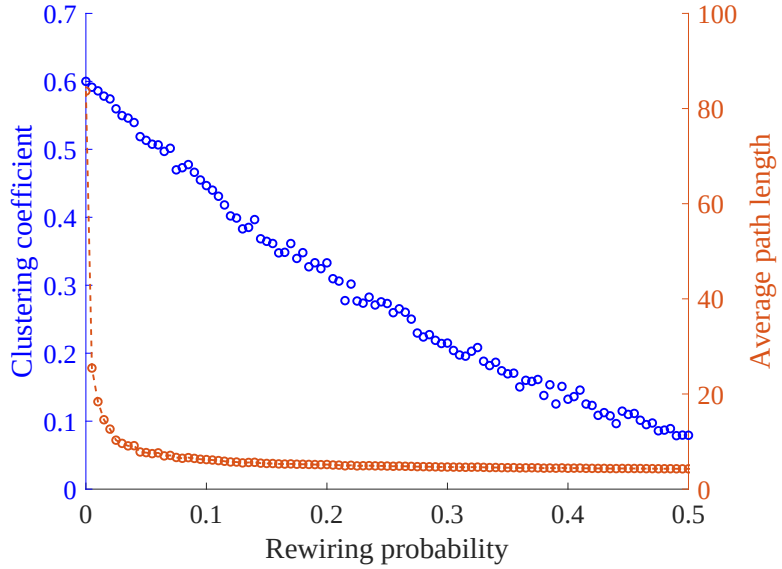

Figure 1-3: *Plot of measured clustering coefficients and average path lengths for a range of Watts-Strogatz graphs with differing rewiring probabilities.*

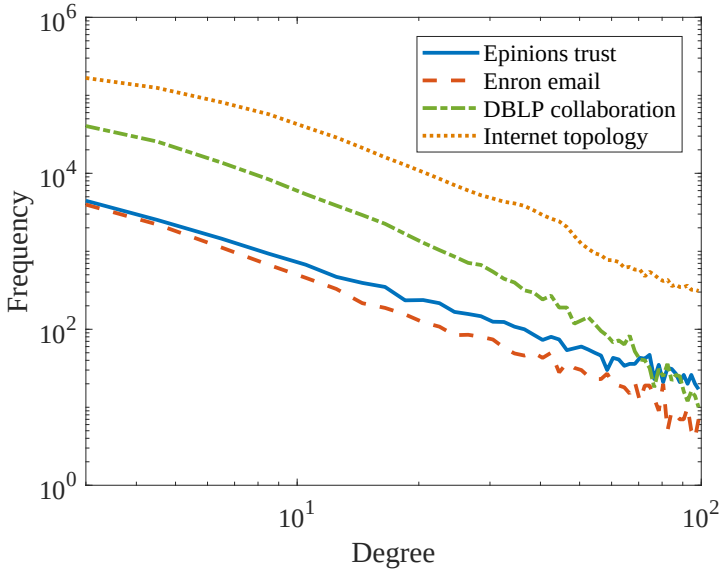

Figure 1-4: *Log-log plot of observed degree counts for a number of real networks: a "who trusts whom" social networks from the site Epinions.com [58], an email correspondence network within the company Enron [59], a collaboration network based on papers in the DBLP computer science bibliography [60] and an internet topology graph of traceroutes run daily in 2005 from several scattered sources [61].*

this is good for communication, on the other it also means that negative quantities such as viruses may rapidly proliferate– thus power law population structures must be carefully observed by the epidemiologist.

Power law networks were first studied by Barabási and Albert [63] who found such degree distributions, with the exponent γ typically about 3, whilst studying networks of the world wide Web, the movie actor database (a large network of actors connected by co-appearances in films) and academic citation networks. They put this down to the insight that, unlike all existing random graph models, many real world networks grow with time and even exhibit a degree of self organisation.

The mechanism by which this emerges in such diverse environments they propose to be a result of *preferential attachment* in the growth process. This is a phenomenon that is demonstrably present in the following discrete time model often referred to as the preferential attachment model, or by its name sakes, the Barabási-Albert model.

Starting from a small seed network with n_0 vertices, their model evolves by a new node with m attached edges being introduced at each time step. The free end of each of the m new edges is then connected at random to the existing nodes in the graph, but with probability proportional to vertex degree.

In their paper Barabási and Albert give the following heuristic argument as to how this construction gives rise to a network with power law degree distribution. Several more rigorous proofs of this have since been given, see for instance [64].

Taking k_i to be the degree of vertex i, then the probability, $Q(k_i)$, that a new edge will connect to vertex i will be given by

$$Q(k_i) = \frac{k_i}{\sum_j k_j}\,. \tag{1.58}$$

Now on average the degree of the vertex will increase at a rate proportional to that degree. So if we make the assumption that k_i always takes the mean value then its time evolution may be captured by

$$\frac{\mathrm{d}k_i}{\mathrm{d}t} = mQ(k_i)\,. \tag{1.59}$$

But since the total degree is simply twice the number of edges added, it follows that $\sum_j k_j = 2mt$, and thus

$$\frac{\mathrm{d}k_i}{\mathrm{d}t} = \frac{k_i}{2t}\,. \tag{1.60}$$

Then given the initial degree, m, of vertex i at the time, t_i, at which it is added, we may solve to find that

$$k_i(t) = m\left(\frac{t}{t_i}\right)^{1/2}\,. \tag{1.61}$$

The probability that the degree of vertex i is less than k is then given by

$$\begin{aligned}\mathbb{P}[k_i(t) < k] =& \mathbb{P}\left[t_i > \frac{m^2 t}{k^2}\right] \\ =& 1 - \mathbb{P}\left[t_i \leq \frac{m^2 t}{k^2}\right] \\ =& 1 - \frac{m^2 t}{k^2}(t + n_0)\,.\end{aligned} \tag{1.62}$$

From this the explicit probability that some chosen node is of degree k, p_k, may be found by considering

$$p_k = \frac{\partial \mathbb{P}\left[k_i(t) < k\right]}{\partial k} \tag{1.63}$$

which over long time periods leads to the stationary solution

$$p_k = \frac{2m^2}{k^3}\,. \tag{1.64}$$

Thus we conclude, the oft observed, power law degree distribution with exponent 3.

While both Barabási and Albert and Watts and Strogatz successfully create random graphs exhibiting observed real world properties, it is worth noting that the Watts-Strogatz graph is not itself scale free, nor does the Barabási-Albert model exhibit clustering. While efforts to tie these two concerns together have since been made [65], it is exemplative of one of the biggest remaining challenges in both network and epidemic modelling: the need to unify numerous successful methods to address problems considered in isolation.

1.1.4 The giant component for arbitrary degree distributions

Since its observation in Erdős and Rényi's inaugural paper, study of the giant component has received a lot of attention. It was not until much later however that this phase transition was discovered to be more than a peculiarity of the classic random graph model, but rather a much more general phenomenon. Molloy and Reed [42] show that in fact, given a graph with an arbitrary distribution of node degrees, the same phase transition may be observed. Using generating functions enables a simple proof of this threshold [56]:

If we take again p_k to be the probability that a randomly chosen vertex has degree k, then we may combine information about the whole distribution into the generating function defined as

$$G_0(x) = \sum_{k=0}^{\infty} p_k x^k\,. \tag{1.65}$$

From this function individual probabilities may be recovered as

$$p_k = \frac{1}{k!} \left. \frac{\mathrm{d}^k G_0}{\mathrm{d}x^k} \right|_{x=0} . \tag{1.66}$$

Moments may also be simply found, for instance the mean degree is then

$$\langle k \rangle = \sum_k k p_k = G_0'(1) . \tag{1.67}$$

Now suppose we start somewhere randomly in the graph and want to know how many other vertices are reachable. We know immediately from G_0 the expected size of the immediate neighbourhood, let us then consider where we would expect to end up if we follow a random edge? Since higher degree nodes connect to more edge ends, then the probability, q_k, that a randomly chosen edge ends at a node of degree k will be given by

$$q_k = \frac{k p_k}{\sum_k k p_k} = \frac{k p_k}{\langle k \rangle} , \tag{1.68}$$

and thus we have a generating function for this distribution of the form

$$G_1(x) = \frac{\sum_k k p_k x^k}{\langle k \rangle} = x \frac{G_0'(x)}{G_0'(1)} . \tag{1.69}$$

If we assume that the graph is large enough so that node degrees are approximately independent, then the probability that two randomly chosen edges end in nodes of degrees totalling m would be given by $\sum_{j+k=m} q_j q_k$. Thus it may be seen that the generating function for this distribution would be given by

$$\sum_{j,k} q_j q_k x^{j+k} = \left(\sum_k q_k x^k \right)^2 \tag{1.70}$$

$$= (G_1(x))^2 . \tag{1.71}$$

Similarly the distribution of the sums of the degrees at the end of l edges would be generated by $(G_1)^l$.

Supposing our graph doesn't contain any triangles (in probability, for a given degree distribution, this is again just a matter of choosing a large enough graph), if we take H_1 to be the generating function for the distribution of the number of nodes reachable by following a particular edge and r_k to be the probability that a node has k edges leading out of it (disregarding one it itself has been reached by), it follows that

$$H_1(x) = x r_0 + x r_1 H_1(x) + x r_2 (H_1(x))^2 + ... \tag{1.72}$$

$$= x G_1(H_1(x)) . \tag{1.73}$$

Thus, starting from a random vertex, the generating function for the size of the component

that vertex belongs to would equal

$$H_0(x) = xG_0(H_1(x))\,, \tag{1.74}$$

giving a mean component size of

$$H_0'(1) = 1 + G_0'(1)H_1'(1) \tag{1.75}$$

$$= 1 + \frac{G_0'(1)}{1 - G_1'(1)}\,. \tag{1.76}$$

The mean component size is then seen to blow up at the pole $G_1'(1) = 1$ and hence this marks the phase transition at which a giant component forms. Further, by equations (1.65) and (1.69), this may be alternatively written as

$$\sum_k k(k-2)p_k = 0\,. \tag{1.77}$$

Another way to reach this conclusion is again by comparison to a branching process in the following manner. As well as the immediate neighbourhood, we may also find the distribution of the number of second neighbours to be generated by

$$\sum_k p_k \left(G_1(x)\right)^k = G_0\left(G_1(x)\right)\,. \tag{1.78}$$

In a similar fashion, again given sufficient sparsity conditions so that m^{th} neighbours may be considered independent, the number of m^{th} neighbours may be shown to have generating function $G_0(\underbrace{G_1(G_1(...G_1(x)...))}_{m-1})$.

Disregarding the first, G_0, step, the distribution of number of m^{th} neighbours is generated by the same function as the size of the m^{th} generation in the appropriate branching process. More precisely, we are again returning to the observation, discussed in Section 1.1.2, that the structure of large random graphs may be locally approximated by a branching process with offspring distribution generated by G_1. Recall also that a large Erdős-Rényi graph matches a Poisson branching process. In the case of an Erdős-Rényi graph with mean degree λ, this may be seen by considering

$$G_1(x) = \frac{G_0'(x)}{\lambda} \tag{1.79}$$

$$= \frac{1}{\lambda}\sum_{k=1}^{\infty} k\frac{\lambda^k e^{-\lambda}}{k!}x^{k-1} \tag{1.80}$$

$$= \sum_{k=0}^{\infty} k\frac{\lambda^k e^{-\lambda}}{k!}x^{k} \tag{1.81}$$

$$= G_0(x)\,. \tag{1.82}$$

So the generating function for each successive node is identical, and by uniqueness of generating functions, the graph matches a Pois(λ) branching process.

Furthermore, a branching process has a positive probability of survival if and only if the mean of the offspring distribution is greater than 1 (see Section 1.1.1), it follows that our graph will only have a large connected component if

$$G_0'(1) > 1\,, \tag{1.83}$$

so this again is the threshold for the emergence of a giant component.

So now we have constructed an approximate network model and know something about the size of communities within it. However, when an infection spreads it will not necessarily get the opportunity, or successfully manage, to exploit every available connection, rather it will define some stochastic subgraph. Asking when this subgraph contains the giant component is the study of percolation. One of the main questions we shall be seeking to address in chapters 2 and 3 is: when does a large epidemic happen? or equivalently, what is the *percolation threshold*?

1.1.5 Percolation

The study of percolation is concerned with the proportion of a population that may be reached from any starting point given the probabilistic existence of a set of connections [66, 67, 68]. Various methods of determining edge (or equivalently vertex) inclusion have been studied, corresponding to different types of percolation. Most notable amongst these are:

- **Bond percolation.** Starting with an undirected network, assign each edge independently to be either *open* with probability q or *closed* with probability $1-q$. We are interested in the size of the percolation clusters, that is the sets of nodes connected by open edges. Bond percolation on a fully connected graph is then simply equivalent to the study of connected components in an Erdős-Rényi graph.

- **Site percolation.** Vertices are included independently with probability q, we then consider the induced subgraph on these included vertices (equivalently all the edges connected to a vertex are excluded with probability $1-q$). Component sizes are then determined as usual.

- **Bootstrap or k-core percolation.** The graph is pruned by removing all vertices and their associated edges of degree less than some chosen k. The process is then repeated iteratively until a stable state is reached with connected components of vertices with at least k connections [69, 70].

The main question of interest in the study of percolation is determining the existence of a *percolating cluster*. In an infinite graph this is simply an infinite connected component, so

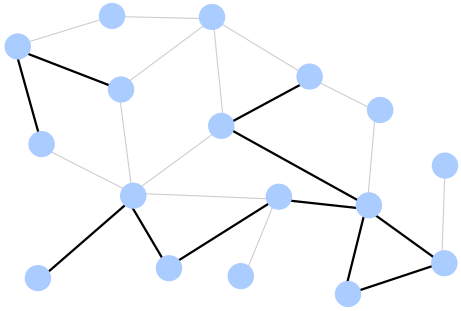

Figure 1-5: *An illustration of bond percolation on a network. Dark edges are classed as closed and light open. If the size of the largest darkly connected component is, with high probability of order n, we say it is a percolating cluster.*

providing you start at an appropriate vertex an infinite number of others may be reached. In a finite graph, however, this requires a rather more delicate definition– since every component is finite this is rather a cluster that reaches a non-vanishing proportion of population in its large-scale limit. The percolating cluster is thus equivalent to the giant component and so, by the results of the previous section, with high probability there is at most one *percolating cluster* which exists only for values of q above the *percolation threshold*, q_c.

Let us consider now perhaps the most natural and simple of these models, that of bond percolation. For a sparse, locally tree like, network it is observed in [71] that the probability of node i belonging to a small cluster of size s, $\pi_i(s)$, may be approximated by the sum of the number of nodes reachable through each of i's neighbours. That is, if we take $\pi_{i\to j}(s)$ to be the probability that s nodes may be reached through node j from node i, then

$$\pi_i(s) = \sum_{\substack{s_j\,:\,j\in\mathcal{N}_i \\ \sum s_j = s-1}} \left(\prod_{j\in\mathcal{N}_i} \pi_{i\to j}(s_j) \right) . \tag{1.84}$$

If we further define $H_{i\to j}(z) = \sum_{s=0}^{\infty} \pi_{i\to j}(s) z^s$ as the generating function for $\pi_{i\to j}(s)$, by noting that $\pi_{i\to j}(0) = 1 - q$, it follows that

$$H_{i\to j}(z) = 1 - q + qz \prod_{k\in\mathcal{N}_j\setminus i} H_{j\to k}(z)\,. \tag{1.85}$$

Evaluating these equations requires knowledge of the graph's topology so neighbourhoods may be evaluated. Alternatively for an infinite graph a mean field approach may instead be used [72].

To implement this, again consider the degree distribution of our graph to be given by p_k, the probability that a vertex chosen uniformly at random has degree k, the subsequent generating function for this distribution $G_0(x) = \sum_{k=0}^{\infty} p_k x^k$ and the related $G_1(x) =$

$G_0(x)/z$, where z denotes the average degree. We may then approximate

$$H_{i\to j} \approx H_0 \text{ for all } i, j \tag{1.86}$$

where H_0 is the generating function for the number of vertices reachable through a randomly chosen edge. Defining also H_0 as the generating function for the probability that a randomly chosen edge leads to the percolating cluster we may arrive at a mean field analogue of the previous equations by the relations:

$$H_1(x) = 1 - q + qxG_1[H_1(x)] \tag{1.87}$$

$$H_0(x) = xG_0[H_1(x)] \tag{1.88}$$

From these equations we may then find the mean cluster size $\langle s \rangle$ in the graph as

$$\langle s \rangle = H_0'(1) = G_0'(1)H_1'(1) \tag{1.89}$$

$$= \frac{qG_0'(1)}{1 - qG_1'(1)} \tag{1.90}$$

Hence it may be seen that $\langle s \rangle$ becomes infinite as $qG_1'(1) \to 1$, suggesting the formation of at least one infinite component, and thus this is the point at which a percolating cluster first forms. The percolation threshold is then given by

$$q_c = \frac{1}{G_1'(1)} \tag{1.91}$$

Let us consider this formula for different degree distributions. Since we have

$$G_1'(1) = \frac{\sum_k (k^2 - k)p_k}{\sum_k kp_k} \tag{1.92}$$

for Erdős-Rényi graphs with $p_k \sim \text{Pois}(\lambda)$ then $G_1'(1) = \lambda$ so the percolation threshold is $1/\lambda$. However for a scale free network with $p_k = k^{-\tau}$ we see that the series (1.92) is divergent for $\tau < 3$; this may be interpreted then to mean that the percolation threshold is 0 for such networks and so a percolating cluster always exists. Figure 1-6 shows the change in the size of the largest connected component with q for these two graph dynamics (albeit finite). We can see clearly here that the sudden emergence of a percolating cluster at the critical value of $1/\lambda$ on the Erdős-Rényi graph is not found in the scale free case, where it instead grows smoothly from zero.

Suppose now that the topology of the graph is known however. By this we mean that we explicitly know the neighbourhood of any chosen vertex (at the end of any chosen edge). This is the case for both finite graphs, where such information may be listed for instance in an adjacency matrix, and to a class of infinite graphs where we have a finite number of vertex types [73] (so given this information neighbourhoods are deterministic). More precisely, we require the graph to be *quasi-transitive*, meaning that there exists an

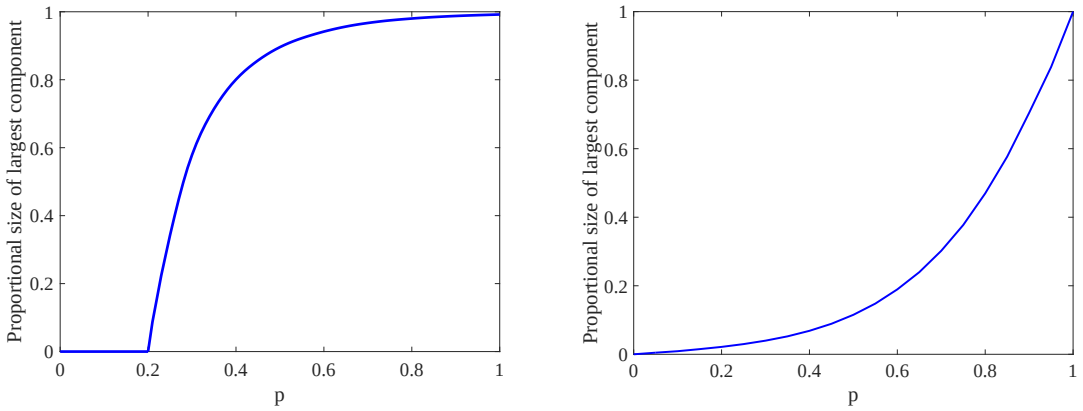

Figure 1-6: *Figure showing the change in the size of the percolating cluster against q, the probability each edge is open. The left panel shows an Erdős-Rényi graph with mean degree 5 and the right a scale free network generated by the Barabási-Albert algorithm. In each case a connected component of size 100000 is considered with the plots generated as the mean of 100 percolation simulations.*

automorphism that maps the set of vertices into a finite set of equivalence classes.

In such circumstances we may instead be able to solve (1.85) directly via iteration starting from random initial H values. Now $H_{i\to j}(1)$ is the probability that i belongs, through j, to a small cluster of any size, or equivalently the probability that i does not belong to an infinite cluster through j. Hence the trivial solution $H_{i\to j}(1) = 1$ for all i, j corresponds to the graph having no percolating cluster. Thus the q value at which $H_{i\to j}(1) = 1$ goes from being a stable to an unstable solution of (1.85) is precisely the percolation threshold.

To find this point we may take $H_{i\to j}(1) = 1 - \epsilon_{i\to j}$ and so linearize (1.85) to gain

$$\epsilon_{i\to j} = q \sum_{k\in\mathcal{N}_j\setminus i} \epsilon_{j\to k} \tag{1.93}$$

or equivalently $\boldsymbol{\epsilon} = q\mathbf{B}\boldsymbol{\epsilon}$ where $\boldsymbol{\epsilon}$ is the vector of $\epsilon_{j\to k}$ and $\mathbf{B}$ is the matrix over directed edges $i \to j$ with elements

$$B_{i\to j,k\to l} = \delta_{j,k}(1 - \delta_{i,l}\,. \tag{1.94}$$

We may conclude that $\boldsymbol{\epsilon}$ only tends to 0 if p times the leading eigenvalue of $\mathbf{B}$ is less than 1, and so the reciprocal of this eigenvalue is precisely the percolation threshold.

The matrix $\mathbf{B}$ is known as the *non-backtracking* or *Hashimoto* matrix, an object only recently introduced into the field of network science. As given explicitly by equation (1.94), it is constructed as an adjacency matrix over directed edges (each edge in a non-directed graph gives rise to two edges representing the traversal in both directions), where two edges are considered connected if one feeds into the other but doesn't backtrack. Thus it describes the possible traversals of the graph.

Alongside its use here as an estimator of the percolation threshold, the non-backtracking

matrix has also been used to measure other properties such as community structure and has motivated a new notion of centrality [74]. Centrality measures have recently been conjectured to correlate to infection arrival times on networks [75], in Chapter 4 we return to this notion to demonstrate that the infection arrival time may be well predicted by the non-backtracking centrality.

The direct approach to (1.85) is based on the assumption that our graph is a treelike, however if we suppose instead that this was not the case then we may instead gain a bound.

Recall that we are relying an the fact that, on a tree, the number of nodes reachable from i is the sum over the number of nodes reachable through each of i's neighbours. On an arbitrary graph however this may lead to overcounting since nodes may be reachable through more than one edge from i. In this way it follow that the equality in equation (1.85) becomes the inequality

$$H_{i\to j}(1) \geq 1 - q + q \prod_{k\in\mathcal{N}_j\setminus i} H_{j\to k}(1)$$

and hence the inverse leading eigenvalue, λ_B^{-1}, of the non-backtracking matrix (when it exists) provides only a lower bound on the percolation threshold. Furthermore, the inverse of the leading eigenvalue of the non-backtracking matrix is never less than that of the adjacency matrix, which has itself been shown to bound the percolation threshold [76], and thus forms a tighter bound [71].

This analysis has similarly been applied to a set of infinite quasi-transitive graphs. These are graphs whose vertices may be split into a finite number of sets within which all members are transitive. For such a class it is shown that [73] λ_B^{-1} exists, $0 < \lambda_B^{-1} \leq 1$ and bounds the percolation threshold from below.

Over the course of this section we have demonstrated how large complex networks, like population structures, may be approximated by random graphs. We have seen a phase transition at which connections across the bulk of such a population are made and considered, by way of percolation, when a random process such as an infection, may achieve this. With this framework in place then, let us introduce the mathematical modelling of infections.

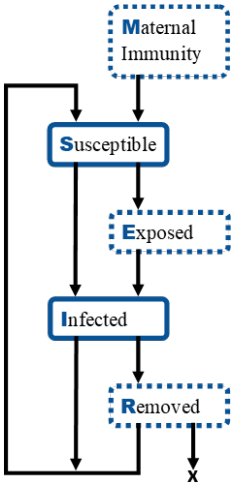

Figure 1-7: *Illustration of the possible states of infection that have been considered in epidemic models and the routes between them, most general of which being the MSEIRS model.*

1.2 Infections

To model an infection in a population we need to track, at the very least, two quantities: firstly those who are susceptible– the uninfected who are vulnerable to the infection, and secondly those who are infected– the infection carriers who may pass it on to others. Typically then, contagions spread through a population with the susceptibles becoming infected upon reaching some, often stochastic, exposure threshold. Of course in this simple system, if the exposure threshold is finite and no part of the population is isolated, the whole population will eventually become infected. Already this gives rise to some non-trivial questions: how long is *eventually* and in what way is it affected by both the exposure time distribution and the population structure? These are questions we shall return to in Chapter 4.

The trajectory of an epidemic is often more complex than this, however, and the success of an infection much less guaranteed; in reality hosts and disease do not often exist in harmony, rather fight to the destruction of one or other. Thus the infected state is rarely stable and it is necessary to include a third state of being recovered, or removed, from the system (perhaps by death), and thus no longer infected nor susceptible.

While the dynamics of this three state system is perhaps the most prevalent in epidemiology, many variations have been considered, including: an exposed period in which an infection reaches an individual but they are not yet able to infect others [77, 78], a period of immunity, typically as a result of anti-bodies inherited from a mother [79, 80], and a transition back to the susceptible state allowing possible reinfection [81, 82, 83]. The possible dynamics due to these various inclusions are shown in Figure 1-7.

We shall primarily restrict our attention to the three state Susceptible-Infected-Removed (SIR) dynamics in chapters 2 and 3, and, in Chapter 4, simply Susceptible-Infected without recovery. It is worth noting, however, that many of the techniques we have discussed may be augmented to model more complex systems with additional states.

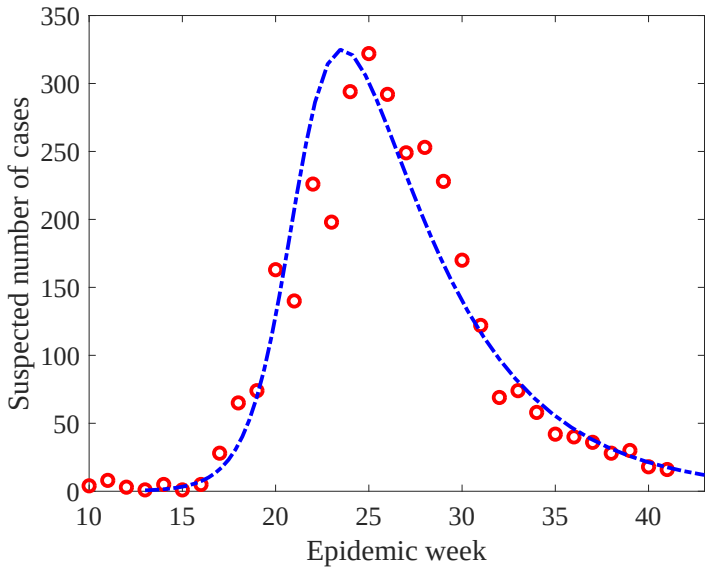

Figure 1-8: *Plot showing the typical bell shaped curve of an epidemic and its effective representation by the Kermack McKendrick equations. The circles show real data for the suspected number of individuals infected by the Zika virus per week in 2016– data collated by the Pan American Health Organisation (PAHO) [85] from surveys done by the Ecuador ministry of Public health [86]. The line shows the solution to the Kermack McKendrick equations for parameters reflecting a similar sized epidemic.*

1.2.1 Compartmental models

At the start of the twentieth century it was assumed that an epidemic would only die out if either the infection itself had become less aggressive, or there were no more susceptible people left [4]. No satisfactory explanation had been given however for the bell shaped curve (seen in Figure 1-8) that typically describes the number of infections during the course of an epidemic, nor any kind of appraisal made for the size and duration of a given outbreak. These were questions Kermack and McKendrick [3] sought to address with the introduction of the now exhaustively studied compartmental epidemic model [84].

In their paper Kermack and McKendrick assumed a well mixed population and tracked the number of individuals at various stages of infection; those who are still Susceptible, $X(t)$, those who are Infected, $Y(t)$, and those who have Recovered (or have died), $Z(t)$. Their interpretation of the SIR model then evolves according to a simple set of differential equations of the form:

$$\frac{\mathrm{d}X}{\mathrm{d}t} = -\beta XY \tag{1.95}$$

$$\frac{\mathrm{d}Y}{\mathrm{d}t} = \beta XY - \nu Y \tag{1.96}$$

$$\frac{\mathrm{d}Z}{\mathrm{d}t} = \nu Y \tag{1.97}$$

Where β and ν are parameters describing the infection and recovery rates respectively.

Examining these equations they observed that the number of infectives will only increase when $\beta X > \nu$, and so the infection peak may be characterised by the reaching of a critical proportion of susceptibles $X^c = \frac{\nu}{\beta}$. Thus, no epidemic can occur unless the initial susceptible population, N, exceeds X^c. If it does the outbreak size, that is then number of individuals ever reached by the infection, will be approximately

$$Z(\infty) = 2\left(N - X^c\right) . \tag{1.98}$$

To see the shape of the epidemic curve, a solution to these equations may be sought. Given the initial state of the population as $X(0) = X_0, Y(0) = n - X_0, Z(0) = 0$, then combining (1.95) and (1.97) and integrating we can obtain

$$\frac{\mathrm{dX}}{\mathrm{d}Z} = -\frac{\beta X}{\nu} \tag{1.99}$$

$$\Rightarrow \quad X = X_0 e^{-\frac{\beta}{\nu}Z} \tag{1.100}$$

and so

$$\frac{\mathrm{d}Z}{\mathrm{d}t} = \nu Y \tag{1.101}$$

$$= \nu(n - X - Z) \tag{1.102}$$

$$= \nu\left(n - Z - X_0 e^{-\frac{Z\beta}{\nu}}\right) . \tag{1.103}$$

Kermack and McKendrick analysed this by taking a Taylor approximation of the exponential term, then integrating to obtain

$$Y = C\mathrm{sech}^2(\alpha t - \phi) \tag{1.104}$$

for constants C, α, ϕ.

Kermack and McKendrick's differential equations very much dominated the epidemiology literature throughout the 20th century, however, while they proved informative their work was not without its problems. For instance, while the above approximate solution widely dominated for some 30 years, it actually often significantly underestimated the size of large epidemics [23]. Outbreaks exceeding X^c, for instance, will induce a negative infection rate, though simple numerical and even exact analytical solutions have since been given.

A less easily solvable problem arose from the absence of any consideration of population structure and heterogeneity. This was an issue that epidemiologists certainly appreciated, as early as 1945 Wilson and Worcester [87] introduced some heterogeneity into the model by sub dividing the population, an idea later taken to its full generality by Rushton and Mautner [88]. However, all such early attempts to deal with population structure comprised of increasingly complex versions of Kerrmack and McKendrick's equations [89] and it was not until the very end of the century when we see the shift to true network

epidemiology.

1.2.2 Structured populations

The premise on which network epidemiology was founded is the belief that considering heterogeneity is of great importance in epidemic modelling, the use of networks was not initially proposed as an answer to the question of how to this may best be done however.

The simplest measure of heterogeneity is perhaps the size of an individual's immediate neighbourhood. Consequently a natural question to ask is: given that a node has degree k, how will it respond to the infection? Vespignani and Pastor-Satorras [90, 62, 91] attempted to address this by creating a mean field model with subsets of vertices of equal degree.

To illustrate their approach, suppose a graph has a degree distribution given by p_k, the probability a node has degree k. We can then describe the time evolution of the proportion of nodes with degree k via a system of equations similar to those of Kermack and McKendrick. Take then $X_k(t), Y_k(t), Z_k(t)$ to be the proportion of degree k nodes that are susceptible, infected and removed at time t respectively, so $X_k(t) + Y_k(t) + Z_k(t) = 1$ and $\sum_k p_k X_k = X$. In order to study the time evolution of the average degree k node, we need to know the probable state of its neighbourhood. The probability that, at time t, a randomly chosen edge will lead to an infected node will be given by

$$\theta(t) = \frac{\sum_k p_k Y_k(t)}{\sum_k k p_k}, \tag{1.105}$$

so the probability that a node with degree k is connected to an infected node at time t is given by $k\theta(t)$

This then allows us to formulate the following system of equations

$$\frac{\mathrm{d}X}{\mathrm{d}t} = -\beta X_k k\theta(t) \tag{1.106}$$

$$\frac{\mathrm{d}Y}{\mathrm{d}t} = \beta X_k k\theta(t) - \nu Y_k \tag{1.107}$$

$$\frac{\mathrm{d}Z}{\mathrm{d}t} = \nu Y_k \tag{1.108}$$

$$\tag{1.109}$$

Some stability analysis allows Vespignani and Pastor-Satorras to find the *epidemic threshold* condition of

$$\lambda_c = \frac{\mathbb{E}[k]}{\mathbb{E}[k^2]} \tag{1.110}$$

a critical value for the ratio between infectivity and recovery, $\frac{\beta}{\nu}$, below which no outbreak will occur and above which the infection will attain a finite value.

This measure is ineffective in arbitrary graphs, however. As we saw in case of prefer-

ential attachment graphs for instance, node degrees are not always homogeneous and thus more detailed topological information is needed. A number of more recent modifications have sought to overcome this including the edge based compartmental model [92, 93] and the effective degree model [94].

The latter considers the evolution of classes Ω_{xy} where Ω is the individuals own state (in the space $\{X, Y, Z\}$), and x and y denote the number of susceptible and infected neighbours respectively. This model has proved successful in a prediction of an epidemic threshold in agreement to that found by the network epidemic models we shall consider [95], though while it may sometimes be more readily computable, has weaknesses in its evaluation of other heterogeneous measures.

A similar modification has been used by Keeling [96] to respect the impact of the large degree of clustering, as discussed in Section 1.1.3 and often found in population structures due to the existence of families and friendship groups. Keeling considers this by an adaptation of the Kermack-McKendrick model to study the time development of connected doubles rather than individuals. The state space is then of the form $\Sigma = \{[XX], [XY], [XZ], [YY], [YZ], [ZZ]\}$, where $[\Omega_1\Omega_2]$ denotes the number of connected pairs of types Ω_1 and Ω_2. The degree of clustering is then incorporated by a calculated approximate relationship between the number of connected triples and connected pairs. So the number of connected triples is given by

$$[\Omega_1\Omega_2\Omega_3] = f^{123}(\Sigma, C) \tag{1.111}$$

for f^{123} some deduced function and C the clustering coefficient of the graph. This enables them to express the system as a set of 5 differential equations:

$$\begin{aligned}
[\dot{XX}] =& -2\beta[XXY] \\
[\dot{XY}] =& \beta([XXY] - [XYX] - [XY]) - \nu[XY] \\
[\dot{XZ}] =& -\beta[ZXY] + \nu[XY] \\
[\dot{YY}] =& 2\beta([YXY] + [XY]) - 2\nu[YY] \\
[\dot{YZ}] =& \beta[ZXY] + \nu([YY] - [YZ])
\end{aligned} \tag{1.112}$$

By analysing these equations (and also later in [97] by other means) it is shown that increasing the level of clustering has the effect of increasing the epidemic threshold. The logic in this case being that each new infection may arise in an already infection saturated neighbourhood, limiting scope for continued proliferation.

The existence of families within a population, as well as introducing clustering effects, may present connections with much higher exposure, corresponding to high proximity. In modelling terms this is the existence of groups with heightened susceptibility, an effect studied by Ball et al. in [98]. What is really important about Ball et al.'s approach however is that they present the relationships between families as network based, and are as such notable in giving one of the first mathematically precise treatments of epidemic

spreading on a network– an area of study which exploded shortly after their publication [99].

1.2.3 Network epidemiology

Recent advances in epidemiology have abandoned the mean field approach entirely in favour of applying disease spread models directly to a network approximation of the population. An early example may be found in [100] where the spread of sexually transmitted diseases are simulated directly onto a network structure. Rather than every susceptible individual becoming infected at a rate dependent on the proportion of infectives in the whole population, it is instead dependent on only the proportion of infectives in each individual's neighbourhoods.

Chakrabati [101, 102] suggests this may otherwise be presented as a Markov chain with a state space comprised of every possible configuration of susceptibile, infected and recovered nodes. Possible transitions between states then depends on the network topology, with probabilities dependent on the disease dynamics. For SIS dynamics, by analysis of this chain they found that the chain may only move far from the fully susceptible absorbing state if the ratio of infectivity exceeds the top eigenvalue of the network's adjacency matrix, λ_A. Hence an epidemic threshold is found of

$$\frac{\beta}{\nu} = \lambda_A \tag{1.113}$$

which may be shown to hold similarly for SIR dynamics due to the rarity of reinfection in sub-critical epidemics.

The difficulty with respect to further analysis of this model, however, is due to the size of the state space. Some recent developments have achieved a reduction of this by lumping equivalent states [103, 104], that is states between which similar vertices may be matched via graph automorphism. However, while such methods can prove somewhat effective in assessing macroscopic dynamics based on a network's structural measures they are unsuitable for considering specific node vulnerability, and in practice little reduction is achieved as equivalence classes are limited.

In some respects network epidemiology was not actually such a new idea being, as it is, highly related to percolation– the chance of edge existence in this context reflecting the probability of a simple contagion being passed to a neighbour. Epidemic spread was in fact one of the main original motivations for studying percolation [105].

At any stage in the infection spread, the probability of including an edge between an infected individual and a susceptible neighbour is equal to the probability that the individual passes the infection down this edge before recovering. So for an infection with Markovian dynamics (eg. exponential rates), then the probability that an infected individual transmits to its neighbours is simply $\frac{\beta}{\beta+\nu}$ where, as before, β and ν are the rates of infection and recovery respectively.

Two specific cases are immediate. If, rather than exponentially distributed, we make

the time to recovery deterministic, equal to some value T, then the probability of infection is independent for every one of an infected individual's neighbours (rather than correlated by the lifetime of the shared neighbour). Specifically this probability will be given by

$$p = 1 - e^{-\beta T} . \tag{1.114}$$

Thus, by the independence of edges in this model, it is possible to see that the epidemic threshold problem is equivalent to that of finding the bond percolation threshold with an edge inclusion probability of p [106].

A similar infection model analogue may also be found for site percolation: here suppose instead that we still have exponential lifetimes and infection times, but if and when an infected individual passes on its infection it does so simultaneously to all of its neighbours. Thus, the model may be seen to be equivalent to that of site percolation with occupation probability

$$p = \frac{\beta}{\beta + \nu} . \tag{1.115}$$

Due to this duality the epidemic and percolation thresholds have both enjoyed similar treatment. We have already seen that the top eigenvalue of the adjacency matrix provides an upper bound for both the bond percolation and epidemic thresholds. More recently it has further been observed that the refined estimate we noted for percolation given by the top eigenvalue of the non-backtracking matrix is relevant for infection models also [107]– an estimate found dependent on the *message passing* equation discussed below.

We then have the three epidemic threshold estimates:

1. $\frac{\beta}{\nu} = \frac{\mathbb{E}[k]}{\mathbb{E}[k^2]}$
2. $\frac{\beta}{\nu} = \lambda_A$
3. $\frac{\beta}{\nu} = \lambda_B$

The effectiveness of each is compared for a variety of networks in Figure 1-9 where we see that their ranking is not straightforward and the "correct" modelling approach is highly dependent on the system being studied.

1.2.4 Message passing

So far we have only discussed infections with exponential distributions for infection and recovery times. Working with such Markovian dynamics clearly has a number of advantages for model simplicity; without having constant probabilities of infection and recovery per unit time, Kermack and McKendrick's equations will break down. Exponential rates, however, are often not biologically realistic and disease lifetimes may often be relatively deterministic – one might expect, for instance, a person to take about a week to recover

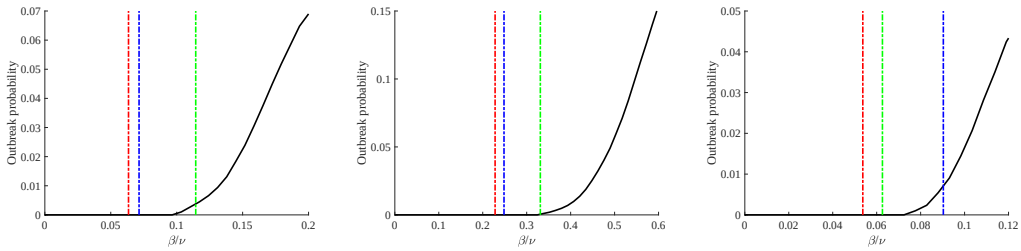

(a) **(b)** **(c)**

Figure 1-9: *Comparison of different epidemic threshold estimates on a variety of networks. The solid, black, line plots the probability of an outbreak that reaches more than* 1% *of the graph against the infectivity ratio,* $\frac{\beta}{\nu}$*, found as an estimate based on 1000 simulations from a single random starting node. In each the blue line corresponds to the value of infectivity equal to* $\frac{\mathbb{E}[k]}{\mathbb{E}[k^2]}$*, and the red and green lines to the reciprocals of the maximum eigenvalues of the graph's adjacency matrix and non-backtracking matrix respectively. Networks used are (a) a scale free graph on 10000 nodes created using the Barabási-Albert algorithm, (b) an Erdős-Rényi random graph on 10000 nodes with mean degree 3, and (c) a real social network of friendships from the Romanian version of the music streaming service Deezer [47]*

from measles. One way in which this may be addressed is by the modification to a form of integrodifferential equations [108, 91] as follows.

We let recovery time be described by a function $P(t)$, the probability that an individual remains infectious t time after receiving the infection. Now, however, the requirement for an exponential recovery time period is relaxed and we instead just require that $P(t)$ is a non increasing function with $P(0) = 1$ and $P(\infty) = 0$. Taking again $X(t), Y(t), Z(t)$ to be the number of infected, susceptible and recovered individuals at time t respectively with initial conditions $X(0) = n - Y_0$, $Y(0) = Y_0$, $Z(0) = 0$ and infection at exponential rate β, then we may write

$$X(t) = n - Y_0 - \int_0^t \beta X(s)Y(s)\mathrm{d}s \tag{1.116}$$

$$Y(t) = Y_0 P(t) + \int_0^t \beta X(s)Y(s)P(t-s)\mathrm{d}s \tag{1.117}$$

$$Z(t) = Y_0(1 - P(t)) + \int_0^t \beta X(s)Y(s)(1 - P(t-s))\mathrm{d}s\,, \tag{1.118}$$

with

$$X(t) + Y(t) + Z(t) = 1\,. \tag{1.119}$$

Such systems may yield solutions [109], and thresholds found via stability analysis similar to the that of the exponential case [108], and recently an attempt has also been made to incorporate the effects of heterogeneity into this model [110]. However, these models only produce limited approximations of network structure. To incorporate non-Markov infection dynamics in a structured population then necessitates a rather different approach as timings suddenly become of great importance– the disease may only spread when infectious

and susceptible periods align within the network.

A method to study this by tracking the time development of an infection has been suggested by Newman and Karrer [111]. Their work based on the *message passing* model, or *cavity method*, introduced in [112, 113]. Here a consideration is made as to how individual vulnerabilities evolve based on the state of their immediate environment. Further, by tracking time development, in Chapter 3 we are able to harness this approach to study instances of infection interaction, and in Chapter 4 to study the infection spread speed and arrival timings.

Suppose we take c to be the density function for the contact time required between an infected susceptible pair before the infection is passed on; so if the infection were to spread at exponential rate β then $c(t) = \beta e^{-\beta t}$. Take also r as the density for the recovery time, then the probability density function, $f(t)$, for the time after infection at which an individual transmits the infection to a given neighbour will be given by

$$f(t) = c(t) \int_t^\infty r(t) \tag{1.120}$$

since for an individual to pass on the infection t time after they become infected themselves, recovery must happen after this time.

The idea behind the algorithm is that in order for the infection message to reach an individual it must have first reached one of its neighbours, and prior to that, one of its neighbours neighbours and so on back to the infection source. The fundamental quantity we connect together in this chain is the probability $H^{i\leftarrow j}(t)$ that vertex i does not receive the infection message from vertex j by time t. For this to happen, then the sum of the transmission time after receiving the infection, as described by f, with the time at which j receives the infection must exceed t. Taking $H^j(t')$ to be the probability that vertex j does not receive the infection at all by time t', then it follows that

$$H^{i\leftarrow j}(t) = 1 - z \int_0^t f(t') \left(1 - H^j(t')\right) \mathrm{d}t' \,. \tag{1.121}$$

However, the probability that j does not receive the infection message by time t' is equal to the probability that all of its neighbours have not sent the message to j by this time, ie. $z \prod_{k\in\mathcal{N}(j)\setminus i} H^{j\leftarrow k}(t')$, recalling z is the probability that any given vertex does not start infected.

If the network in question is sparse, and so approximately tree-like, then it follows that we may treat $H^{j\leftarrow k}$ for $k \in \mathcal{N}(j)\setminus i$ as independent to $H^{i\leftarrow j}$. This means we may conclude that

$$H^{i\leftarrow j}(t) = 1 - \int_0^t f(t') \left(1 - z \prod_{k\in\mathcal{N}(j)\setminus i} H^{j\leftarrow k}(t')\right) \mathrm{d}t' \,. \tag{1.122}$$

In a tree-like network then, these equations may be used to describe the full time

evolution of the system, though direct solutions may not easily be found.

Considering just the end state statistics is somewhat more tractable. The probability that an individual will ever transmit the infection is given by

$$T = \int_0^\infty f(t)\mathrm{d}t\,, \tag{1.123}$$

so then defining the probability i will never receive the infection message from j, $H^{i\leftarrow j}(\infty) = h^{i\leftarrow j}$

$$h^{i\leftarrow j} = 1 - T\left(1 - z\prod_{k\in\mathcal{N}(j)\setminus i} h^{j\leftarrow k}\right)\,. \tag{1.124}$$

And so the probability that vertex i will never become infected (remain susceptible) will be given by

$$h^i = z\prod_{j\in\mathcal{N}(i)} h^{i\leftarrow j}(t)\,. \tag{1.125}$$

As well as allowing for non-exponential infection dynamics, this manner of epidemic modelling is also advantageous in its description of individual nodes. It can tell us not only how much of the network is likely to be reached by an outbreak but also who is most vulnerable, or even, by rewriting the system in reverse, who is most likely to start an epidemic [107, 114]. As such the model has proven useful in determining quantities such as optimal immunisation sets [115]. While the message passing approach is informative for the dynamics of infection spread in appropriate networks, however, as we have presented it the method is only applicable to a special case of a tree-like network.

The tree-like assumption is essential because otherwise there may be multiple paths to the infection source from i. Putting it another way, in a tree the infection source determines the direction down an edge which the infection may travel and thus, for two connected vertices i and j, the order in which they may become infected. Without this there is a possibility, when determining $H^{i\leftarrow j}$, that the infection may reach j after first going by i and thus $H^{i\leftarrow j} = 0$, since an individual may not receive the infection twice.

To determine the probability that i receives the infection from j, $H^{i\leftarrow j}$, then we need to know firstly the probability that an infected j passes the infection to i, determined by f as before, and secondly the probability that j itself will receive the infection in the network with i unable to transmit, $H^j_{(i)}$. Taking also $H_{(i,j)}$ to give infection probabilities in the network with i and j removed, we may write

$$H^{i\leftarrow j}_{(i)}(t) = 1 - \int_0^t f(t')\left(1 - z\prod_{k\in\mathcal{N}(j)\setminus i} H^{j\leftarrow k}_{(i,j)}(t')\right)\mathrm{d}t'\,. \tag{1.126}$$

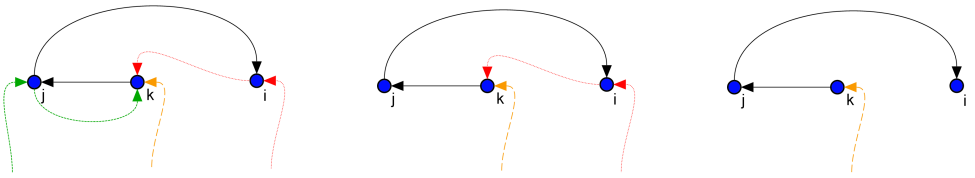

(a) $H^{j\leftarrow k}$ **(b)** $H^{j\leftarrow k}_{(j)}$ **(c)** $H^{j\leftarrow k}_{(i,j)}$

Figure 1-10: *Possible infection routes from k to j to i given transmission restrictions for arrival at j.*

Since removing i as a transmission source may only decrease the number of paths between the infection source and some vertex k, it follows that $H^{j\leftarrow k} \leq H^{j\leftarrow k}_{(j)} \leq H^{j\leftarrow k}_{(i,j)}$. This is demonstrated in figure 1-10, where we see how transmission restriction at each stage of spread leads to tree-like infection routes. We then find

$$H^{i\leftarrow j}_{(i)}(t) \geq 1 - \int_0^t f(t') \left(1 - z \prod_{k\in\mathcal{N}(j)\setminus i} H^{j\leftarrow k}_{(j)}(t') \right) \mathrm{d}t' \,. \tag{1.127}$$

Suppose we replace the inequality in (1.127) with the equality

$$\hat{H}^{i\leftarrow j}(t) = 1 - \int_0^t f(t') \left(1 - z \prod_{k\in\mathcal{N}(j)\setminus i} \hat{H}^{j\leftarrow k}(t') \right) \mathrm{d}t' \tag{1.128}$$

then it may be shown that the solution to this set of equations, which has been shown both to exist [116] and be unique [117] as a result of an iterative procedure, provides upper bounds of the form

$$\hat{H}^{i\leftarrow j} \geq H^{i\leftarrow j}_{(i)} \geq H^{i\leftarrow j} \,. \tag{1.129}$$

Finally, by observing that the form of the systems (1.128) and (1.122) are identical, we may conclude that the message passing equations, which are precise in a tree-like network, also provide an upper bound for an arbitrary network.

The effectiveness of sparse approximations

In the three papers that form the subsequent chapters of this thesis, sparse network assumptions are frequently made. In Chapter 2 the infection dynamics are coupled with a branching process and in chapters 3 and 4 we make extensive use of the message passing equations discussed above. Of course many networks, especially those reflecting community structure are not locally tree-like at all, but instead contain many short cycles. However, even here approximations based on sparsity have been shown to be rather more effective than one might expect.

A tree approximation, T_G, for a network, G, of size n can be formed by way of a multi-type branching process with offspring distributions designed to fix the between degree

edge probability. That is, if we take $P_k(k')$ to be the probability that a vertex of degree k is connected to a vertex of degree k', then grow a branching process in the following way:

1. Starting from a single individual branch to a number k of children sampled from the degree distribution of G.

2. For each individual in the new generation in turn branch to a subsequent number, k', of children chosen independently from the distribution P_k.

3. Repeat until the total size of the process first meets or exceeds n.

Considering the mean distance between vertices in both the original network and the tree approximation, if this differs by no more than 10% it is shown in [118] that dynamics on both networks will be very similar, regardless of the structure of the original network. For example, the percolation threshold for a network G may be well approximated by the percolation threshold of T_G provided the mean between vertex distance differs by no more than 10% between the two graphs. In Chapter 4 we shall see that, as a consequence of this, calculations based on sparse approximation often prove effective on a range of real network structures.

CHAPTER 2

A RE-ENTRANT PHASE TRANSITION IN THE SURVIVAL OF SECONDARY INFECTIONS ON NETWORKS

Infections can't always be considered in isolation. The Hepatitis D virus (HDV) is only able to complete its life cycle in the presence of HBV [119]. Thus a HDV outbreak may only occur alongside a larger HBV outbreak and its dynamics must be considered accordingly. A similar obligate relationship may be seen in the case of bacteriophage viruses which live in bacterial hosts so the virus's transmission is limited to the dynamic sub-population in whom the bacteria is currently active.

Modelling the dependent, secondary, infection is then rather complex as it acts in the temporal network defined by the carrying, primary, infection. Infections on temporal networks has been studied previously, see [120, 121, 121] for instance, however, not with any methodology matching network dynamics as defined by an infection. Perhaps the simplest approach would be to disregard the network structure entirely and consider instead just the proportions of the population affected, by way of a mean field model.

We may do this with an adaptation of the classic compartmental SIR process. The system is now more complicated, however, as we now have 6 possible states differentiated by the statuses of each of the two infections. We shall denote the number in each of these states as follows:

1. S_X, number susceptible to the primary infection.
2. I_S, number infected with the primary infection and susceptible to the secondary infection.
3. I_I, number infected with the primary infection and infected with the secondary infection.
4. I_R, number infected with the primary infection and recovered from the secondary infection.

5. R_X, number recovered from the primary infection and never had the secondary infection.

6. R_R, number recovered from the primary and secondary infections.

If β_i and ρ_i for $i \in \{1, 2\}$ denote the rates of infection spread and recovery respectively, then the rates at which individuals transfer between states may be given by the following diagram:

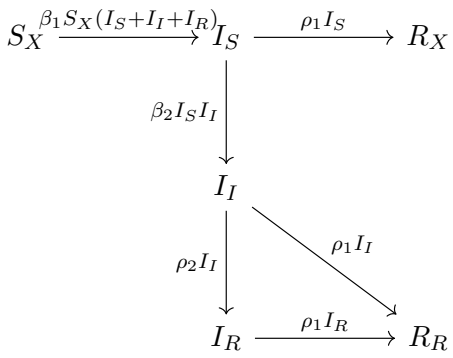

For the sake of simplicity we may re-parametrise to

$$\begin{aligned} X &= S_X \\ Y &= I_S + I_I + I_R \\ S &= I_S \\ I &= I_I \\ R &= I_R + R_R \,, \end{aligned}$$

then the time evolution of these states may be given by the following system of odes

$$\frac{\mathrm{d}X}{\mathrm{d}t} = -\beta_1 XY \tag{2.1}$$
$$\frac{\mathrm{d}Y}{\mathrm{d}t} = Y(\beta_1 X - \rho_1) \tag{2.2}$$
$$\frac{\mathrm{d}S}{\mathrm{d}t} = \beta_1 XY - (\beta_2 I + \rho_1)S \tag{2.3}$$
$$\frac{\mathrm{d}I}{\mathrm{d}t} = (\beta_2 S - \rho_1 - \rho_2)I \tag{2.4}$$
$$\frac{\mathrm{d}R}{\mathrm{d}t} = (\rho_1 + \rho_2)I \,. \tag{2.5}$$

Success of a simple infection depends on the relative rates of infectivity to recovery, that is the ratio $\frac{\beta}{\rho}$. The success of the secondary infection is somewhat more complex as, additionally to this ratio, it is also dependent on both the success of the primary infection

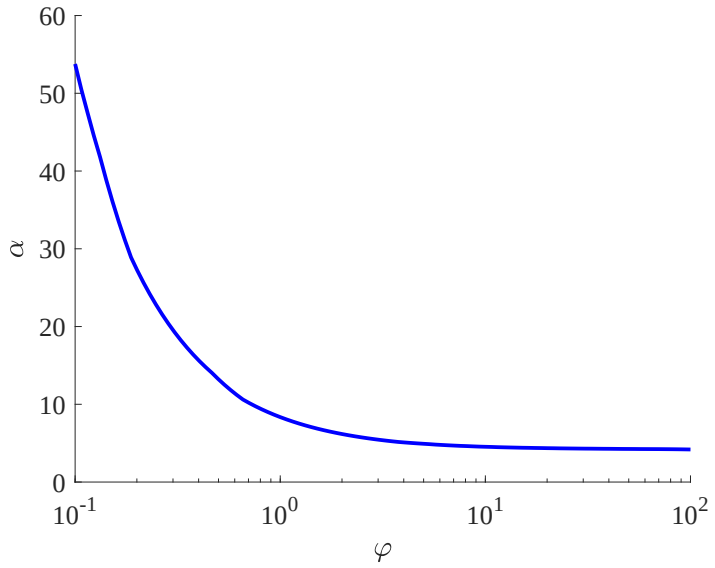

Figure 2-1: *Figure showing minimum parameters needed for a secondary infection outbreak as found by numerically solving the system of equations* (2.1)*. An outbreak is classed as the infection reaching at least* 1% *of the population.*

and the relative speed at which the two infections operate. To gain an understanding of the interaction between the two infections, we will concentrate on the latter of these, the relative speed $\frac{\beta_1}{\beta_2} = \varphi$. Suppose we then fix $\frac{\beta_1}{\rho_1} = \frac{\beta_2}{\rho_2} = \alpha$ and ask, for varying φ, how large must α be for there to be a secondary infection outbreak? Solving the system of equations numerically gives us the answer to this question shown in Figure 2-1.

It seems, therefore, that the mean field equations are telling us that the greater the relative speed, φ, the more successful the secondary infection will be. This makes some sense, as the recovery rate of the secondary infection is essentially equal to $\rho_1 + \rho_2$ so, unless φ is large, then the effective infectivity ratio is actually much less than α.

However, some important aspects of the interaction between the two infections is lost in this model. Moreover, both spatial structure and timings of the two infections are of importance– an individual may only pass on the secondary infection in the time period in which both the secondary infection is active in themselves, and the primary infection is active in their neighbours. Due to this relationship, we argue that an alternative model is necessary to consider these dynamics.

In the following paper we address this by proposing to map the secondary infection to a multi-type branching process of the type discussed in Section 1.1.1. Unlike in the mean field model, the branching process model is able to capture the dynamic that the number of neighbours successfully infected (number of offspring of the branching process) is dependent upon the duration the primary infection is active in that neighbourhood, not just the overall primary outbreak size. This reveals a re-entrant phase transition in the relative infection speed; while the secondary infection must indeed act relatively quickly in order to survive, as found by the mean field model, it must also not act too quickly and

instead limit itself to a window proportional to the primary infection speed.

A re-entrant phase transition in the survival of secondary infections on networks

Sam Moore[*] **Peter Mörters**[†] **Tim Rogers**[*]

[*] *Department of Mathematical Sciences, University of Bath, Bath, BA2 7AY, UK*

[†] *Mathematisches Institut, Universität zu Köln, Weyertal 86-90, 50931* Köln, Germany

Abstract

We study the dynamics of secondary infections on networks, in which only the individuals currently carrying a certain primary infection are susceptible to the secondary infection. In the limit of large sparse networks, the model is mapped to a branching process spreading in a random time-sensitive environment, determined by the dynamics of the underlying primary infection. When both epidemics follow the Susceptible-Infective-Recovered model, we show that in order to survive, it is necessary for the secondary infection to evolve on a timescale that is closely matched to that of the primary infection on which it depends.

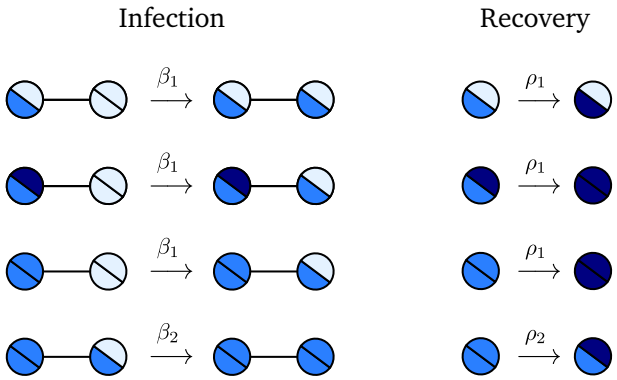

Figure 2-2: *Possible events and their rates in the network superinfection model. Circles represent nodes in the network, with the state of the primary (resp. secondary) infection shown by the colour of the lower-left (resp. top-right) sector; light denotes susceptible, midtone denotes infective, dark denotes recovered.*

Introduction

Superinfections are a major cause of global mortality and morbidity. For example, the WHO estimates 15 million cases worldwide of Hepatitis D, which spreads only amongst carriers of Hepatitis B and greatly worsens their prognosis [1]. There is a need, therefore, to develop a robust understanding of the conditions under which outbreaks of secondary infections are possible. Coevolving infections have been studied previously in the case of symbiotic/antagonistic relationships where infections mutually affect fitness [2, 3, 4], however, relatively little is known in the case that one infection has a strict obligate relationship with another.

In 2013, Court, Blythe and Allen [5] introduced a model of hierarchical infection referred to as the *stacked contact process*. Their model concerns the fate of a population of coevolving hosts, spreading as a contact process on a lattice, and parasites, spreading as a contact process restricted to sites currently occupied by hosts. In epidemiological language, the contact processes of [5] correspond to coupled Susceptible-Infective-Susceptible (SIS) epidemics; empty lattice sites are interpreted as susceptible individuals, who may be infected by the primary (host) and then secondary (parasite) infections. Simulations of this model system revealed a surprising feature: the success of the parasites depends non-monotonically on the turnover rate of the host population. Specifically, for the parasite to succeed, it is necessary for the dynamics of the host population to be neither too fast, nor too slow. Later in [6], Lanchier and Zhang rigorously established the main features of the phase diagram for the stacked contact process.

At around the same time, Newman and Ferrario [7] independently proposed a related model in the context of epidemic dynamics in social contact networks. They considered a pair of Susceptible-Infective-Recovered (SIR) epidemics with a strictly obligate relationship such that the secondary infection is only transmitted amongst those who have *recovered* from the primary. In this formulation, the dynamics of the two diseases are completely separated in time, allowing for analytical treatment of the model using

"cavity method" techniques which have been quite successful in the study of epidemics on networks (see, e.g. [8, 9]). The introduction of network structure to the population in [7] has the advantage of improving the relevance of the model for human epidemic dynamics. However, by separating the dynamics of the two diseases this model cannot display the curious interaction between infection timescales observed in [5, 6].

In this paper we study the dynamics of coevolving SIR superinfections in sparse contact networks. We consider a population of individuals occupying the vertices of an Erdős-Rényi (ER) random graph with mean degree c. A primary infection spreads through the population with infective individuals passing the disease on to their neighbours with rate β_1, and recovering from the disease with rate ρ_1. Individuals who are carrying a *live* primary infection may also play host to a secondary infection, which spreads and recovers with rates β_2, ρ_2 respectively. See Fig. 2-2 for an illustration of the possible state transitions. As in [7], our secondary infection is restricted to spread on the subgraph of hosts infected with the primary; however, differently from that paper we consider the more complex case in which this subgraph is evolving in time due to the recovery of primary infections.

As well as arguably improving the realism of the model, moving from lattice to network topologies allows us access to a rigorous branching process approximation — an approach that has previously enjoyed success in approximating SIR-type models in large populations, as seen for instance in [10, 11]. By coupling the dynamics of the secondary infection to those of a multi-type branching process, we will be able to characterise the phase diagram of the system. Note that, in the context of large finite networks, when we discuss *survival* of the infection we mean an asymptotically positive proportion of vertices become infected at some point in time.

The success of the primary infection is controlled by the connectivity (mean node degree) c of the network, and the ratio of the infection and recovery rates $\alpha := \beta_1/\rho_1$. This parameter is well understood as the basis of the classical single infection process; for fixed α there exists a critical value of c above which the infection survives with positive probability and at or below which we have certain extinction, see e.g. [12]. Note that simultaneously adjusting β_1 and ρ_1 by a multiplicative factor will change the timescale of the disease dynamics, but will not alter the probability of survival since α is unchanged.

Inspired by the results of [5, 6], we are interested here in the behaviour possible when the primary and secondary diseases are similarly virulent, but may differ in their timescales. To this end, we will mainly concentrate on the case that $\beta_2/\rho_2 = \alpha$ also. We have made this choice only for simplicity of presentation; the more general case is in fact covered by Lemma 2, and the results are not qualitatively different in other cases. Three parameters then describe success of secondary infection: the connectivity of the underlying graph, c; the ratio between rates of spread and recovery, α; and, crucially, the relative timescales of the two infections, $\varphi := \beta_1/\beta_2$. If $\varphi \gg 1$ then the dynamics of the primary infection are very much faster than those of the secondary; if $\varphi \ll 1$ then

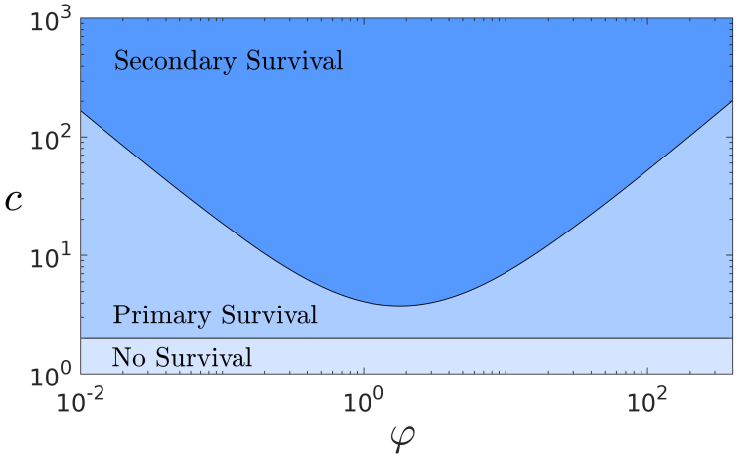

Figure 2-3: *Phase diagram of the superinfection network model for fixed $\beta_1/\rho_1 = \beta_2/\rho_2$, shown as a function of the relative timescale $\varphi = \beta_1/\beta_2$ of the infections and the connectivity c of the network. The secondary infection survives with positive probability only in a convex region whose boundary is characterised in our Theorem 2.1. In this log-log plot, the asymptotic slope of the boundary is -1 for small φ, and 1 for large φ, as implied by the scaling laws in* (2.2).

they are much slower.

In order for the secondary infection to survive it is perhaps intuitive that it must progress at a rate fast enough compared to the primary infection, else the primary infection will have itself recovered and subsequently ended the secondary infection before it has a chance to spread. Perhaps more surprisingly however we shall also show that the secondary infection should not act too quickly as this too compromises survival potential. Our characterisation of the survival of the secondary infection is illustrated in Fig. 2-3 and summarised by our main result:

Theorem 2.1. For all $\alpha, \varphi > 0$ there exists a critical connectivity $c^\star$ such that, in the limit of large network size, for $c < c^\star$ the secondary infection dies out with probability one, and for $c > c^\star$ it survives with positive probability.

Furthermore, the critical connectivity $c^\star$ is found to be the smallest positive solution of the implicit equation

$$c^\star = \frac{(1+\alpha+\alpha\varphi)(1+\varphi+2\alpha+\alpha\varphi)}{\varphi} \frac{{}_0F_1(2+\varphi+(1+\varphi)/\alpha; -c^\star\varphi/\alpha^2)}{{}_0F_1(3+\varphi+(1+\varphi)/\alpha; -c^\star\varphi/\alpha^2)}\,, \tag{2.1}$$

where ${}_0F_1(a;z) = \sum_k \frac{z^k}{k!(a)_k}$ is a hypergeometric function. In particular, for large and small φ we have the scaling behaviour

$$c^\star = \Theta(\varphi) \quad \text{for} \quad \varphi \to \infty\,, \quad c^\star = \Theta(1/\varphi) \quad \text{for} \quad \varphi \to 0\,. \tag{2.2}$$

Here we have made use of "big theta" notation, defined as follows: $f(x) = \Theta(g(x))$ as $x \to \infty$ (resp. $x \to 0$) if there exist positive constants L and U and X such that

$\forall x > X$ (resp. $x < X$) we have

$$Lg(x) < f(x) < Ug(x)\,.$$

The remainder of the article is organised as follows: in the next section we map the early dynamics of our network superinfection model to a certain multitype branching process; in Section 3 we compute the long-time behaviour of this process and thus give the proof of Theorem 2.1; Section 4 is for discussion, including illustrative numerical results.

Branching process description

Primary infection

We begin by recapping the standard branching process approximation to the dynamics of an infection spreading on an Erdős-Rényi random graph [13, 10]. Heuristically, the method relies on the fact that for fixed connectivity, short cycles become asymptotically rare in the limit of large graphs, meaning that during the crucial early dynamics of the infection, each susceptible node may have at most one infective neighbour.

Let us consider the infection spread as generational; the n^{th} generation being the individuals at graph distance n from the seed vertex that gain the infection at any point in time. In this way the primary infection is modelled as a simple Galton Watson process described by the quantity Z_n, giving the number of individuals in the n^{th} generation. The *offspring distribution* describes the probability p_i for an individual to pass the infection on to i others in the next generation. If the offspring distribution has mean μ, the expected number of infected individuals at distance n from the seed is then given by $\mathbb{E}Z_n = \mu^n$. If $\mu \leq 1$ then the branching process will almost surely go extinct after finitely many generations; if $\mu > 1$ then it may survive; survival of the branching model being simply characterised by the size of the n^{th} generation being non zero for all n.

In the network SIR model, the number of offspring is equated with the number of neighbours (other than the single infected 'parent') that an infective node succeeds in transmitting the disease to before it recovers. There are several sources of randomness: the number of neighbours to potentially infect, the recovery time, and times of infection. We note that whilst the fates of the neighbours of an infected node are not independent (they are jointly exposed to the random time to recovery of the parent) the mean of the offspring distribution can be found simply by multiplying the probability $\alpha/(1+\alpha)$ to infect any given neighbour before recovery, with the expected number of neighbours to infect, c. From standard branching process theory, we thus deduce that in the limit of large networks the primary infection will have a non-zero chance of survival if and only if $\mu > 1$, that is, if $c > 1 + 1/\alpha$.

For finite graphs, the coupling between the random graph and branching process

model is of course only local. Suppose in a population of size N, in generation n we have m infected individuals, so $Z_n = m$ in the branching model. We then have errors coming from the fact that each infective may only be connected to at most $N - m$ susceptibles (not constant for each generation) as well as the fact that each of these may not be unique (and so children in the subsequent generation of the branching process may not be unique). However when $m = o(\sqrt{n})$ the random graph may be coupled to the branching model with high probability; for a proof of this see [14].

Secondary infection

For the primary infection, to determine if the probability of survival is positive only requires knowledge of two quantities: the expected number of susceptible neighbours an individual has, and the chance any one of those will gain the infection. The difficulty with modelling the secondary infection is that the first of these is dynamic, since the subgraph composed of individuals currently carrying the primary infection changes with time. We account for this additional complexity by introducing a *type* parameter t, which specifies the time elapsed between the primary and secondary infections. Specifically, if an individual acquires the primary infection at time t_1 and the secondary at time t_2, then they are said to have type $t = t_2 - t_1$.

It is clear that at least this much information is required to predict the potential of an individual to transmit the secondary infection to new hosts; for example, the larger t, the more likely an individual is to pass on the primary infection long before it passes on the secondary, by which time the primary infection in the new host may have recovered. We will see in Section 3.1 that in fact knowledge of t is enough to completely characterise the distribution of the number and timing of new secondary infections arising from an individual. The progress of the secondary infection is then mapped to that of a multi-type branching process with type space $\mathbb{T} = [0, \infty)$.

Where previously survival was predicted by just the mean number of offspring, now the picture is more complicated, and we are required to compute the *intensity of production* of all types of offspring resulting from all types of parents. This information is captured in the kernel $\mu(t'|t)$, which is defined by the property that the expected number of offspring with types in the interval $[a, b]$ coming from a parent of type t is given by the integral of $\mu(t'|t)$ over $t' \in [a, b]$. This kernel defines a linear operator with the action

$$M[\psi](t') = \int \mu(t'|t)\psi(t)\mathrm{d}t\,, \tag{2.3}$$

We shall in particular be interested in functions $\psi : \mathbb{T} \to \{0, 1\}$, an indicator for the types present in the population. $M[\psi]$ then describes the expected size and composition of the population of offspring arising from a population of parents with types given by ψ.

We say that a kernel μ defined over an interval I is: strictly positive if $\forall t, t' \in I$ we have $\mu(t'|t) > 0$; uniformly positive if $\exists\, \varepsilon > 0$ such that $\forall t, t' \in I, \mu(t'|t) > \varepsilon$;

integrable if $\iint \mu(t'|t)\mathrm{d}t\,\mathrm{d}t' < \infty$. We assume that M can be defined as a linear operator $M\colon \mathcal{C}_\mathrm{b}(\bar{\mathbb{T}}) \to \mathcal{C}_\mathrm{b}(\bar{\mathbb{T}})$ over the space of continuous bounded functions on the compact interval $\bar{\mathbb{T}} = [0, \infty]$ equipped with the supremum norm, and in particular that μ has vanishing mass as t goes to infinity. One then has the following general result:

Lemma 2.2. Let $\{Z_n\}$ be a multi-type branching process on $\mathbb{T} = [0, \infty)$ with production operator M arising as above from a kernel μ that is strictly positive on $\mathbb{T}$, integrable, and continuous in both arguments. Then

1. There exists an eigenvalue $\lambda > 0$ equal to the spectral radius of M. Moreover, this is the only eigenvalue corresponding to a non-negative eigenfunction
2. If $\lambda < 1$ then the process goes extinct in finite time with probability one
3. If $\lambda > 1$ then the process survives with positive probability.

Proof.

1. For the first part let us first observe that the operator M is compact on $\mathcal{C}_\mathrm{b}(\bar{\mathbb{T}})$, which is the case if and only if the image of the ball, $M(B(0,\delta))$, is relatively compact where

$$B(0,\delta) := \{\psi \in \mathcal{C}_\mathrm{b}(\bar{\mathbb{T}}) \; s.t. \; \|\psi\| < \delta\}\,. \tag{2.4}$$

   Since is the kernel μ is strictly positive on $\mathbb{T}$, integrable, and continuous in both arguments, two properties follow:

   (a) For all $t \in \bar{\mathbb{T}}$

$$\sup_{\|\psi\|<\delta} \left| \int \mu(t'|t)\psi(t)\mathrm{d}t \right| < \infty\,. \tag{2.5}$$

   (b) For all $t'_0 \in \bar{\mathbb{T}}$, $\epsilon > 0$ there exists $\delta > 0$ such that for all $t' \in \bar{\mathbb{T}}$, $|t'_0 - t'| \leq \delta$ and for all $\psi \in \mathcal{C}_\mathrm{b}(\bar{\mathbb{T}})$

$$\left| \int (\mu(t'_0|t) - \mu(t'|t))\psi(t)\mathrm{d}t \right| < \epsilon\,. \tag{2.6}$$

   These two properties are the sufficient conditions for the Arzéla-Ascoli theorem [15, IV.6.7], which gives us that the image of the ball is relatively compact as required.

   Since the operator M is compact, the Krein-Rutman theorem [16, Th 1.3 §3.2] (an analogue of the Perron Frobenius theorem for compact operators) then gives that the spectral radius is a positive eigenvalue and by [17, Theorem 7.3] the only nonzero eigenvalue with a non-negative eigenfunction.

2. We simply observe that if $\lambda < 1$ then $\|M^n[\psi]\| \to 0$ for all ψ, hence we have convergence of the expected generation size to zero (i.e. $\mathbb{E}Z_n \to 0$), which implies extinction in finite time with probability one.

3. We make use of results of Harris [18, §3] who proved positive survival probability for multi-type branching processes with a uniformly positive kernel. Our kernel μ is not uniformly positive, but we are able to couple to such a process by restricting to a bounded type space $[0, T]$. Choosing T large enough forces close agreement in the maximum eigenvalues of the corresponding production operators.

   Let us start by considering the process $\{Z_n^{(T)}\}$ obtained from $\{Z_n\}$ by removing all individuals of type greater than T along with their descendants. The law of $\{Z_n^{(T)}\}$ is that of a multitype branching process on $[0, T]$ with operator $M^{(T)} : \mathcal{C}_\mathrm{b}[0, T] \to \mathcal{C}_\mathrm{b}[0, T]$ defined by

$$M^{(T)}[\psi](t') = \int_{[0,T]} \mu(t'|t)\psi(t)\mathrm{d}t\,. \tag{2.7}$$

   Note that $\inf_{t,t'\in[0,T]} \mu(t'|t) > 0$ and so the kernel is strictly positive and we refer to [18, §3] to prove both the existence of a positive top eigenvalue $\lambda^{(T)}$ of $M^{(T)}$ strictly greater in magnitude than all others and survival of the process $\{Z_n^{(T)}\}$ with positive probability if $\lambda^{(T)} > 1$.

   To show closeness of the eigenvalues $\lambda^{(T)}$ and λ we extend the operator $M^{(T)}$ to $\tilde{M}^{(T)} : \mathcal{C}_\mathrm{b}(\bar{\mathbb{T}}) \to \mathcal{C}_\mathrm{b}(\bar{\mathbb{T}})$ defined by

$$\tilde{M}^{(T)}[\psi](t') = \int_{[0,T]} \mu(t' \wedge T|t)\, \psi(t)\, \mathrm{d}t \tag{2.8}$$

   Note that the eigenvalues of $M^{(T)}$ are also eigenvalues of $\tilde{M}^{(T)}$, so the top eigenvalue $\tilde{\lambda}^{(T)}$ of $\tilde{M}^{(T)}$ forms the bound $\tilde{\lambda}^{(T)} \geq \lambda^{(T)}$. Since μ is continuous and integrable, for all $\varepsilon > 0$ there exists T such that

$$\left\|M - \tilde{M}^{(T)}\right\| < \varepsilon\,, \tag{2.9}$$

   where $\|\cdots\|$ is the operator norm induced by the infinity norm on $\mathcal{C}_\mathrm{b}(\bar{\mathbb{T}})$.

   We have already observed that the principal eigenvalue λ of M can be separated from the rest of the spectrum by a closed curve. Hence, by Kato [19, IV § 3.5], we have that $|\lambda - \lambda^{(T)}|$ goes to zero with $\|M - \tilde{M}^{(T)}\|$. In particular, if $\lambda > 1$ it follows from (2.9) that we can choose T such that

$$\left|\lambda^{(T)} - \lambda\right| < \lambda - 1, \tag{2.10}$$

   and hence $\lambda^{(T)} > 1$ and $\{Z_n^{(T)}\}$ survives with positive probability. The untrimmed process satisfies $Z_n \geq Z_n^{(T)}$ and hence also survives with positive probability. □

To prove our main result about the survival of the secondary infection, we must explicitly identify the operator M, analyse its spectrum, and compute the scaling behaviour when the timescales of the infections are well separated.

Survival of the secondary infection

Production kernel

The form of the kernel $\mu(t'|t)$ may be found by considering when a type t parent will have a type t' offspring. For this to happen, the parent must pass on the primary infection at some time s (measured from the moment they first acquired it), and then pass on the secondary infection at time $s+t'$. The primary and secondary infections in the parent, and the primary infection in the child, must all survive long enough for this process to complete. We find it useful to break the calculation into two cases, depending on whether the primary infection is transmitted before or after the parent acquires the secondary; that is, depending on the order of s and t.

The case $s < t$ is illustrated in Fig. 2-4(i). To achieve a type t' offspring in this case: the transmission time $s > 0$ of the primary must occur before t but after $t - t'$ (which may be negative); the secondary must be transmitted $s + t' - t$ time units after it was acquired in the parent at time t; the primary infection in the parent must not recover in the time between s and t; and none of the three active infections may recover in the window of time between t and $s + t'$. Putting these contributions together, we reach

$$\mu(t'|t, s < t) = c \int_{(t-t')_+}^{t} \left[\beta_1 e^{-\beta_1 s}\right] \left[\beta_2 e^{-\beta_2 (t'-t+s)}\right] \left[e^{-\rho_1 (t-s)}\right] \left[e^{-(2\rho_1+\rho_2)(t'-t+s)}\right] \mathrm{d}s,$$

where $(\cdots)_+$ denotes the positive part, and the prefactor of c comes from the expected number of neighbours to which the infection may be transmitted.

Similarly, the case $s \geq t$ is illustrated Fig. 2-4(ii). Here transmission of the primary may occur any time after t, with the secondary being transmitted t' time units later. Both infections in the parent must survive until time s, after which all three infections must survive for at least t' time units. The resulting expression is

$$\mu(t'|t, s \geq t) = c \int_{t}^{\infty} \left[\beta_1 e^{-\beta_1 s}\right] \left[\beta_2 e^{-\beta_2 t'}\right] \left[e^{-(\rho_1+\rho_2)(s-t)}\right] \left[e^{-(2\rho_1+\rho_2)t'}\right] \mathrm{d}s\,.$$

Combining the two cases and evaluating the integral gives

$$\mu(t'|t) = \begin{cases} \frac{c\beta_1\beta_2(\beta_2 e^{-\beta_1 t-(\beta_2+2\rho_1+\rho_2)t'}+(\beta_1+\rho_1+\rho_2)e^{-\beta_1 t-(\rho_1-\beta_1)t'})}{(\beta_1+\rho_1+\rho_2)(\beta_1+\beta_2+\rho_1+\rho_2)} & \text{if } t' \leq t \\ \frac{c\beta_1\beta_2(\beta_2 e^{-\beta_1 t-(\beta_2+2\rho_1+\rho_2)t'}+(\beta_1+\rho_1+\rho_2)e^{(\beta_2+\rho_1+\rho_2)t-(\beta_2+2\rho_1+\rho_2)t'})}{(\beta_1+\rho_1+\rho_2)(\beta_1+\beta_2+\rho_1+\rho_2)} & \text{if } t' > t\,. \end{cases} \tag{2.11}$$

We are now ready to state our result about the spectrum of the production operator

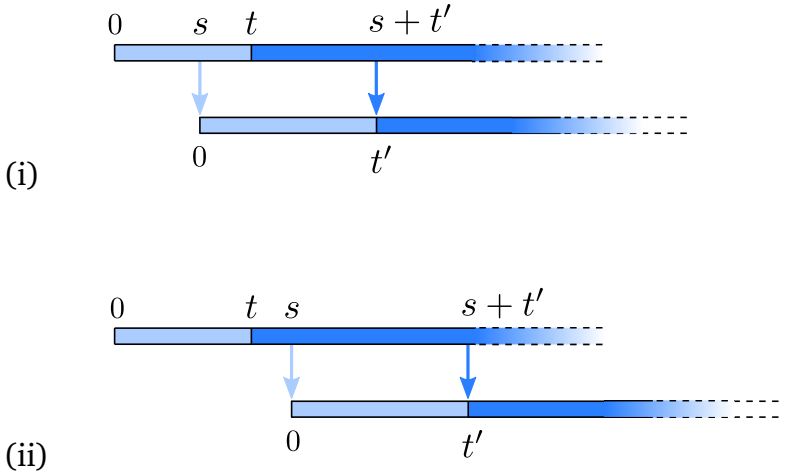

Figure 2-4: *Illustration of the timing of the necessary events for the secondary infection to successfully create a type t' offspring from a type t parent; in each case the top line represents the life of the parent and the bottom line that of the offspring. Pale lines denote the transmission of the primary and dark lines denote the transmission of the secondary, similarly, pale/dark regions denote the corresponding status of the nodes. We split into two cases depending on whether the time s of transmission of the primary infection (measured from when it is acquired by the parent) is (i) before, or (ii) after, the time t that parent acquires the secondary infection.*

resulting from this kernel.

Lemma 2.3. For the integral operator M defined in (2.3) with kernel μ given in (2.11), the top eigenvalue λ solves the implicit equation

$$\frac{c\beta_1\beta_2\, {}_0F_1\left(\frac{\beta_1+\beta_2+3\rho_1+\rho_2}{\rho_1}; -\frac{\beta_1\beta_2}{(\lambda/c)\rho_1^2}\right)}{\lambda(\beta_1+\rho_1+\rho_2)(\beta_1+\beta_2+2\rho_1+\rho_2)} = {}_0F_1\left(\frac{\beta_1+\beta_2+2\rho_1+\rho_2}{\rho_1}; -\frac{\beta_1\beta_2}{(\lambda/c)\rho_1^2}\right) \tag{2.12}$$

where ${}_0F_1(a;z) = \sum_k \frac{z^k}{k!(a)_k}$ is a hypergeometric function.

Proof. From part 1 of Lemma 2.2, to determine that λ is the top eigenvalue of M, it is sufficient to exhibit a non-negative function ψ such that $\lambda\psi = M\psi$. We begin a search for such a function by considering the successive action of M starting from the initial state $\psi_0(t) = \delta_0(t)$, corresponding to a single seed infected individual who acquires the primary and secondary infections at the same instant. Defining the series

$$\psi_{n+1} = M[\psi_n]\,, \tag{2.13}$$

we observe that each iterate ψ_n is a member of a family, Ψ, of functions that can be written as a certain positive sum of exponentials:

$$\Psi = \left\{ \psi(t) = e^{-(\beta_2+\rho_1+\rho_2)t} \sum_{k\geq 1} a_k e^{-k\rho_1 t} \;:\; a_k \geq 0 \right\}. \tag{2.14}$$

We look for an eigenfunction of M that lies in Ψ. The eigenvalue equation $\lambda\psi = M[\psi]$

is thus reduced to a statement about the coefficients $\{a_k\}$. Specifically, we find

$$\begin{aligned}\lambda\psi(t) &= \int_{\mathbb{T}} \mu(t|t')\psi(t')\mathrm{d}t' \\ &\Downarrow \\ \lambda e^{-(\beta_2+\rho_1+\rho_2)t}\sum_{k\geq 1} a_k e^{-k\rho_1 t} &= ce^{-(\beta_2+\rho_1+\rho_2)t}\sum_{k\geq 1} a_k(b_k e^{-\rho_1 t} - d_k e^{-(k+1)\rho_1 t})\,, \end{aligned} \tag{2.15}$$

where

$$\begin{aligned} b_k =& \frac{\beta_1\beta_2(\beta_1+(k+1)\rho_1+\rho_2)}{k\rho_1(\beta_1+\rho_1+\rho_2)(\beta_1+\beta_2+(k+1)\rho_1+\rho_2)} \\ d_k =& \frac{\beta_1\beta_2}{k\rho_1(\beta_1+\beta_2+(k+1)\rho_1+\rho_2)}\,. \end{aligned}$$

Equating coefficients in (2.15) determines

$$\lambda = c\sum_{k\geq 1} a_k b_k \tag{2.16}$$

where the $\{a_k\}$ are found to satisfy

$$a_{k+1} = -\frac{ca_k d_k}{\lambda}\,. \tag{2.17}$$

This recursive equation specifies a solution up to a multiplicative constant:

$$a_k = \left(-\frac{\beta_1\beta_2}{(\lambda/c)\rho_1^2}\right)^{(k-1)} \frac{a_1}{(k-1)!((\beta_1+\beta_2+2\rho_1+\rho_2)/\rho_1)_{k-1}}\,, \tag{2.18}$$

where $(\cdots)_k$ denotes the Pochhammer symbol. Combining this result with (2.16), yields the implicit equation (2.12) for λ given in the statement.

□

Bounds on the ratio of hypergeometric functions

Recall that the survival of the primary infection is dependent only on its birth-death ratio α and the connectivity of the underlying graph c, while the secondary infection additionally depends on its relative speed when compared primary, $\varphi := \beta_1/\beta_2$. As per the discussion in Section , we specialise to the case that $\beta_1/\rho_1 = \beta_2/\rho_2 = \alpha$. Then the implicit eigenvalue equation (2.12) can be rewritten in terms of the parameters α and φ to give

$$\frac{c}{\lambda} = \frac{(1+\alpha+\alpha\varphi)(1+\varphi+2\alpha+\alpha\varphi)}{\varphi}\frac{1}{\Phi_\gamma(c\varphi/\lambda\alpha^2)}\,, \tag{2.19}$$

where $\gamma = (1+\varphi)(1+1/\alpha)$ and Φ denotes the hypergeometric ratio

$$\Phi_a(z) := \frac{{}_0F_1(a+2;-z)}{{}_0F_1(a+1;-z)}\,. \tag{2.20}$$

Our strategy to prove the scaling relations claimed in Theorem 2.1, will be to replace this function by suitably simple upper and lower bounds with the same asymptotic behaviour. Fortunately, there is a substantial literature on topic that we may draw on.

Lemma 2.4. For $a > 0$ write j_a for the smallest positive root of J_a, the Bessel function of the first kind. Then

$$a(a+2) < j_a^2 < 4(a+1)(a+2)\,, \tag{2.21}$$

and for all $z \in (0, j_a)$ we have

$$1 < \Phi_a(z) < 1 + \frac{4z}{j_a^2 - 4z}\,. \tag{2.22}$$

Proof. Ismail and Muldoon [20] list many different bounds on j_a, including those in (2.21) coming from formulas (6.7) and (6.22) in that article. For the second part, it is well-known [21] that the Bessel functions of the first kind may be expressed as

$$J_a(x) = \frac{(x/2)^a}{\Gamma(a+1)}\, {}_0F_1(a+1; -x^2/4)\,,$$

hence, introducing $x = 2\sqrt{z}$, we obtain

$$\Phi_a(z) = \frac{2(a+1)}{x}\frac{J_{a+1}(x)}{J_a(x)}\,. \tag{2.23}$$

This function has previously been studied by Ifantis and Siafarikas [22], who proved various inequalities including their formulas (1.2) and (2.17) which imply the lower and upper bounds of (2.22).

□

Proof of Theorem 1

Proof. As argued previously, in the limit of large Erdős-Rényi random graphs with mean degree c, the survival probability of the secondary infection coincides with that of a multi-type branching process $\{Z_n\}$ with production kernel given by equation (2.11). From Lemma 2.3 and Theorem 2.2 we establish that Z_n has non-zero probability to survive indefinitely if and only if $\lambda^\star > 1$, where $\lambda^\star$ is the largest real number satisfying

$$\frac{\beta_1\beta_2\, {}_0F_1\left(\frac{\beta_1+\beta_2+3\rho_1+\rho_2}{\rho_1}; -\frac{\beta_1\beta_2}{(\lambda^\star/c)\rho_1^2}\right)}{(\lambda^\star/c)(\beta_1+\rho_1+\rho_2)(\beta_1+\beta_2+2\rho_1+\rho_2)} = {}_0F_1\left(\frac{\beta_1+\beta_2+2\rho_1+\rho_2}{\rho_1}; -\frac{\beta_1\beta_2}{(\lambda^\star/c)\rho_1^2}\right)\,. \tag{2.24}$$

Noticing that $\lambda^\star$ appears only in ratio with c, it follows that the condition for the possibility of survival may be rewritten in terms of the critical connectivity $c^\star$ such that for $c > c^\star$ we have $\lambda^\star > 1$. Rearranging equation (2.24) we straightforwardly find that

$c^\star$ is the smallest positive solution to

$$c^\star = \frac{(1+\alpha+\alpha\varphi)(1+\varphi+2\alpha+\alpha\varphi)}{\varphi}\frac{1}{\Phi_\gamma(c^\star\varphi/\alpha^2)}\,, \tag{2.25}$$

which is precisely equation (2.1), as required.

To quantify the scaling behaviour of $c^\star$ for large and small φ, we recall the definition of "big theta" notation: $f(x) = \Theta(g(x))$ as $x \to \infty$ (resp. $x \to 0$) if there exist positive constants L and U and X such that $\forall x > X$ (resp. $x < X$) we have

$$Lg(x) < f(x) < Ug(x)\,.$$

Two sufficient conditions are easy to check: $f(x) = \Theta(g(x))$ if either

(i) $f(x)/g(x)$ has a positive finite limit, or

(ii) there exist functions $l(x), u(x) = \Theta(g(x))$ such that $l(x) < f(x) < u(x)$.

We will use the bounds in Lemma 2.4 to exhibit functions with appropriate finite limits that sandwich $c^\star$. Specifically, recalling $\gamma = (1+\varphi)(1+1/\alpha)$, let

$$u(\varphi) = \frac{1}{\varphi}(1+\alpha+\alpha\varphi)(1+\varphi+2\alpha+\alpha\varphi)\,, \tag{2.26}$$

$$l(\varphi) = u(\varphi)\left(1 - \frac{4\varphi u(\varphi)}{\gamma(\gamma+2)\alpha^2 + 4\varphi u(\varphi)}\right)\,. \tag{2.27}$$

First we check the upper bound. From (2.25) and the lower bound of unity in equation (2.22) of Lemma 2.4, we have that

$$c^\star = \frac{u(\varphi)}{\Phi_\gamma(c^\star\varphi/\alpha^2)} < u(\varphi)\,. \tag{2.28}$$

For the lower bound, we note that the upper bound on Φ given in Lemma 2.4 implies a lower bound on $c^\star$ as the smallest positive $l^\star$ satisfying the equation

$$l^\star = u(\varphi)\left(1 + \frac{4l^\star\varphi/\alpha^2}{j_\gamma^2 - 4l^\star\varphi/\alpha^2}\right)^{-1}\,. \tag{2.29}$$

In fact there is only one solution:

$$l^\star = u(\varphi)\left(1 - \frac{4\varphi u(\varphi)}{j_\gamma^2\alpha^2 + 4\varphi u(\varphi)}\right)\,. \tag{2.30}$$

The lower bound $l(\varphi) < c^\star$ given in (2.27) follows immediately from this and the lower bound on j_γ^2 given in equation (2.21) of Lemma 2.4.

It remains to check that the upper and lower bounds both have the desired scaling

in large and small φ. We begin with $u(\varphi)$, which has easily determined limits

$$\lim_{\varphi\to 0} \varphi\, u(\varphi) = (1+\alpha)(1+2\alpha)\,, \quad \lim_{\varphi\to\infty} \frac{u(\varphi)}{\varphi} = \alpha(1+\alpha)\,, \tag{2.31}$$

both of which are finite and positive, implying $u(\varphi) = \Theta(\varphi)$ for large φ and $u(\varphi) = \Theta(1/\varphi)$ for small φ. For the lower bound we use these results to obtain

$$1 - \frac{4\varphi u(\varphi)}{\gamma(\gamma+2)\alpha^2 + 4\varphi u(\varphi)} \to \frac{1+3\alpha}{1+\alpha(8\alpha^2+4\alpha+3)} \in (0,\infty) \quad \text{as} \quad \varphi \to 0\,, \tag{2.32}$$

and

$$1 - \frac{4\varphi u(\varphi)}{\gamma(\gamma+2)\alpha^2 + 4\varphi u(\varphi)} \to \frac{1+\alpha}{1+\alpha+4\alpha^3} \in (0,\infty) \quad \text{as} \quad \varphi \to \infty\,. \tag{2.33}$$

It follows from the defintion of $l(\varphi)$ and finiteness of these limits that $l(\varphi)$ has the same scaling form as $u(\varphi)$ for both large and small arguments. Since u and l sandwich $c^\star$, the desired scaling is confirmed.

□

Discussion

Theorem 1 provides an exact but implicit formula for the region in which survival of the secondary infection is possible (in the limit of infinitely large graphs), and establishes the scaling behaviour of the boundary of this region for large and small values of the parameter $\varphi = \beta_1/\beta_2$ which controls the relative timescales of the two infections. Knowledge of this scaling behaviour is enough to prove that, for fixed α and c, the survival of the secondary infection is confined to a bounded region of φ values — this is the reentrant phase transition of our title. Figure 2-5 shows the results of numerical simulations of both the branching process and the network model to illustrate this phenomenon.

It is interesting to note that the simulations of the network process and the limiting branching process are not in perfect agreement. Viewing the mean outbreak size over 1000 runs of the model we see in Figure 2-5 that, while we have agreement with the branching process for small values of φ, large outbreaks still seem to be possible beyond the point predicted by the branching process. Moreover, considering the individual simulation results it seems that this unexpected tail is comprised of a few very large outbreaks; while outbreaks of any size are rare for large values of φ, when they do happen they reach most of the graph. By considering the infection spread in a closed connected community we start to encounter finite size effects. Recall that the branching approximation is only valid when the number of infected is relatively small compared to the size of the graph. As the outbreak becomes large the approximation breaks down, a problem exacerbated by the two levels of infection we study. Furthermore in a more

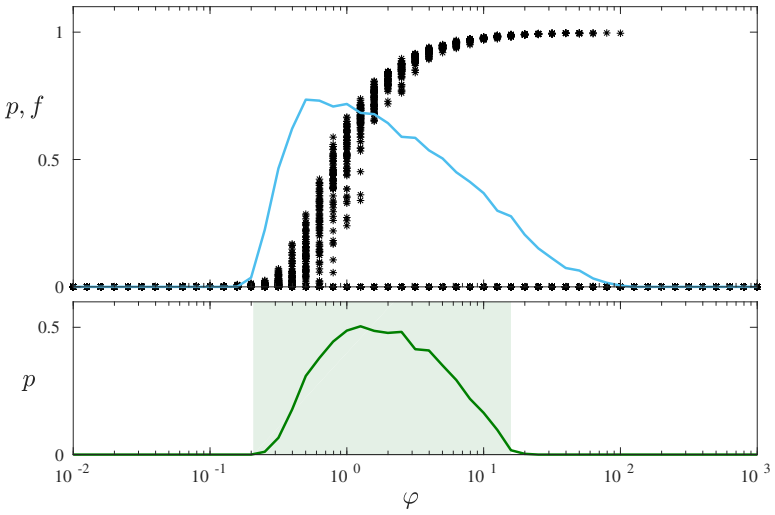

Figure 2-5: *The top panel shows the fractional size of outbreaks (f, stars) and the probability of an outbreak of size* > 100 *(p, blue curve) of the secondary infection, measured from 1000 simulations with random starting nodes on ER networks with mean degree c=10 and N=10000 nodes. The bottom panel shows on the same scale the theoretical survival region of the branching process (pale green box) and the probability of the branching process to reach size* > 100 *(p, green curve), measured from 1000 simulations of the branching process.*

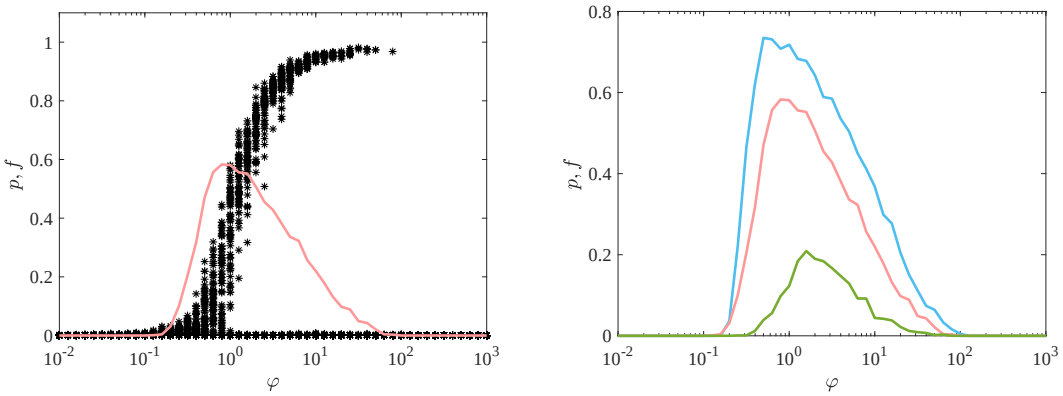

Figure 2-6: *The left plot shows a repeat of the top panel in figure 2-5, though now on ER networks with mean degree c=6. The right hand plot shows the probability of an outbreak of size* > 100 *measured from 1000 simulations with random starting nodes on ER networks with N=10000 nodes and varying mean degrees: the blue curve for c=10, the pink curve for c=6, and the green curve for c=3.*

highly connected environment we may have the existence of transmission routes for the secondary infection to primary infected cousins as well as direct descendants allowing opportunity for the secondary infection to progress before direct primary progression. Similar finite size scaling effects have been observed in other coevolving infection models; see [4] for example.

Figure demonstrates how this is an effect seen equally in sparser graphs also as multiple infection pathways may become realised equally here as the graph becomes relatively saturated. It is seen that a sparser network structure instead simply restricts

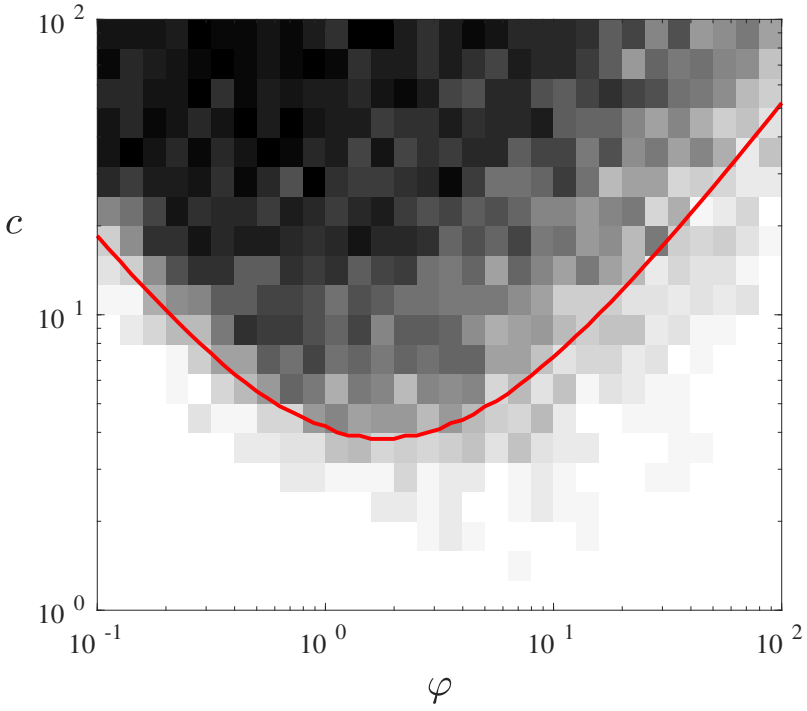

Figure 2-7: *The density plot shows the probability (estimated as a fraction of 25 simulations per pixel) of a secondary infection outbreak of size* > 100*, starting from a single infected node, in an ER network of 10000 nodes and c=10. The red line is the boundary of the region where* $\lambda > 1$.

the survival region.

Comparing the average outbreak size with individual realisations demonstrates an interesting choice of risk vs reward in the strategy of a secondary infection, due to the different locations of the maxima of the curves shown in the top panel of Figure 4. The values of φ for which outbreaks are most likely to occur (blue curve) are in the lower end of the survival window, corresponding to smaller total outbreak sizes (black stars). Conversely, larger values of φ have potential for much larger outbreaks, but come with a higher risk of rapid extinction. Looking at this another way, in nature we should expect survival probability to be a strongly selected characteristic, and hence to find that the majority of secondary infections reach only a minority of primary hosts.

The work presented here could easily be extended to a host of other random graph models, for example by building on techniques of [23, 24, 25]. It may also be interesting to explore the application of the model (or variants) to other areas, including: the successive invasions of different species necessary to rebuild a diverse ecosystem in a damaged habitat; the evolution of hyperparasitism (that is, parasites that live on other parasites); radicalisation, and the incremental spread of increasingly extreme political views through social media.

REFERENCES

[1] "WHO — Hepatitis D," *WHO*, 2017.

[2] P. Grassberger, L. Chen, F. Ghanbarnejad, and W. Cai, "Phase transitions in cooperative coinfections: Simulation results for networks and lattices," *Physical Review E*, vol. 93, p. 042316, apr 2016.

[3] L. Chen, F. Ghanbarnejad, W. Cai, and P. Grassberger, "Outbreaks of coinfections: The critical role of cooperativity," *Europhysics Letters*, vol. 104, no. 5, p. 50001, 2013.

[4] W. Cai, L. Chen, F. Ghanbarnejad, and P. Grassberger, "Avalanche outbreaks emerging in cooperative contagions," *Nature physics*, vol. 11, no. 11, pp. 936–940, 2015.

[5] R. A. Blythe, R. J. Allen, *et al.*, "Parasites on parasites: Coupled fluctuations in stacked contact processes," *Europhysics Letters*, vol. 101, no. 5, p. 50001, 2013.

[6] N. Lanchier and Y. Zhang, "Some rigorous results for the stacked contact process," *Latin American Journal of Probability ALEA*, vol. 13, pp. 193–222, 2014.

[7] M. E. Newman and C. R. Ferrario, "Interacting epidemics and coinfection on contact networks," *PloS one*, vol. 8, no. 8, p. e71321, 2013.

[8] M. E. Newman, "Spread of epidemic disease on networks," *Physical review E*, vol. 66, no. 1, p. 016128, 2002.

[9] T. Rogers, "Assessing node risk and vulnerability in epidemics on networks," *Europhysics Letters*, vol. 109, no. 2, p. 28005, 2015.

[10] R. Bartoszynski, "Branching processes and the theory of epidemics," in *Proceedings of the Fifth Berkeley symposium on Mathematical Statistics and Probability*, pp. 259–69, 1967.

[11] S. Singh, *Branching processes in disease epidemics*. Cornell University, 2014.

[12] M. M. Henkel, H. Hinrichsen, S. Lubeck, and M. Pleimling, *Non-equilibrium phase transitions.* Springer, 2008.

[13] D. G. Kendall, "Deterministic and stochastic epidemics in closed populations," in *Proceedings of the Third Berkeley Symposium on Mathematical Statistics and Probability*, vol. 4, pp. 149–165, 1956.

[14] R. Durrett, *Random graph dynamics*, vol. 200. Cambridge university press Cambridge, 2007.

[15] N. Dunford and J. T. Schwartz, *Linear operators. Part I.* Wiley Classics Library, John Wiley & Sons, Inc., New York, 1988. General theory, With the assistance of William G. Bade and Robert G. Bartle, Reprint of the 1958 original, A Wiley-Interscience Publication.

[16] R. G. Pinsky, *Positive harmonic functions and diffusion*, vol. 45. Cambridge university press, 1995.

[17] P. M. Anselone and J. W. Lee, "Spectral properties of integral operators with nonnegative kernels," *Linear Algebra and its Applications*, vol. 9, pp. 67–87, 1974.

[18] T. E. Harris, *The theory of branching processes.* Dover, 1989.

[19] T. Kato, *Perturbation theory for linear operators*, vol. 132. Springer Science & Business Media, 2013.

[20] M. E. Ismail and M. E. Muldoon, "On the variation with respect to a parameter of zeros of Bessel and q-Bessel functions," *Journal of Mathematical Analysis and Applications*, vol. 135, pp. 187–207, oct 1988.

[21] M. Abramowitz and I. A. Stegun, *Handbook of mathematical functions : with formulas, graphs, and mathematical tables.* Dover Publications, 1970.

[22] E. Ifantis and P. Siafarikas, "Inequalities involving Bessel and modified Bessel functions," *Journal of Mathematical Analysis and Applications*, vol. 147, pp. 214–227, mar 1990.

[23] T. Kurtz, *Approximation of Population Processes.* Society for Industrial and Applied Mathematics, 1981.

[24] S. Bhamidi, R. van der Hofstad, and G. Hooghiemstra, "Universality for first passage percolation on sparse random graphs," *The Annals of Probability*, vol. 45, pp. 2568–2630, 07 2017.

[25] H. Andersson, "Limit theorems for a random graph epidemic model," *The Annals of Applied Probability*, vol. 8, no. 4, pp. 1331–1349, 1998.

CHAPTER 3

HETEROGENEOUS NODE RESPONSES TO MULTI-TYPE EPIDEMICS ON NETWORKS

The multi-type branching process that was discussed in the previous section also lends itself very naturally to modelling a different form of complex infection model, that with multiple mutations. More specifically, consider a finite number of co-evolving infection strains of types in $\mathcal{T}$ that may mutate into each other with given probabilities. That is, some type α may mutate into a type β infection with probability $m_{\alpha\beta}$, leaving the probability of no mutation to be given by $m_{\alpha\alpha} = 1 - \sum_{\beta\neq\alpha} m_{\alpha\beta}$. Further, if the α strain infects with exponential rate b_α and recovers at rate ρ, then its probability of passing a β infection to a given neighbour will be $\frac{b_\alpha}{\rho} m_{\alpha\beta}$.

Suppose these infections spread on a random graph with mean degree c. Recall, from Section 1.1.2, that the exploration of such a graph may be effectively approximated by a simple branching process with a Pois(c) offspring distribution. Suppose we say the individual at the root of this branching process has a type α infection. This individual will then have Pois(c) children, of which Pois $\left(\frac{b_\alpha}{\rho} c\right)$ will become infected. Further, assuming individuals may not be multiply infected (if this is not the case we may simply add in additional types corresponding to multiple strains), Pois $\left(\frac{b_\alpha}{\rho} m_{\alpha\beta} c\right)$ will be infected with strain β. In this way then the infection may be approximated by a multi-type branching process with an offspring distribution defined by

$$P_\alpha^\beta(k) = \frac{1}{k!} \left(\frac{b_\alpha}{\rho} m_{\alpha\beta} c\right)^k e^{-\frac{b_\alpha}{\rho} m_{\alpha\beta} c}, \tag{3.1}$$

where $P_\alpha^\beta(k)$ denotes the probability that a type α parent has k type β children.

To assess the survival probability of the infection as a whole (the probability not all types go extinct) we may find the mean matrix, M, with entries

$$M_{\alpha\beta} = c \frac{b_\alpha}{\rho} m_{\alpha\beta} \,. \tag{3.2}$$

As discussed in Section 1.1.1, by the theory of multi-type branching processes, if we start with some number of each type given by the vector v, then the expected composition of n^{th} generation will be given by vM^n. The infection then has a positive survival probability if and only if the maximum eigenvalue of the mean matrix, λ_M, is not less than 1.

Evaluating the mean matrix with t types, two cases may be considered most immediately:

1. If there is no mutation, so $m_\alpha = 0$ for every type α, then the eigenvalues are all of the form $c\frac{b_\alpha}{\rho}$ for every type α. Thus, we have a positive survival probability iff at least one type has a positive survival probability when acting independently.

2. If there is no type preferences, so we have equal chances of mutation, $m_\alpha = 1/t$ for every type α, then the maximum eigenvalue is given by $\frac{c}{\rho t}\left(\sum_{\mathcal{T}} b_\alpha\right)$. Thus, we have a positive probability of survival iff the mean birth rate is greater than $\frac{\rho}{c}$.

For strictly positive mutation probabilities any single type survival equates to the survival of all infection strains, however, if some mutations never happen this may not be so. To calculate the probability of some strain, α, surviving in general then, we need to know which strains may at some point cause an α type infection.

In the language of Markov chains we say α is *accessible* from β if there exists some chain of strictly positive mutations between β and α, $m_{\beta 1}m_{12}...m_{(n-1)n}m_{n\alpha}$. We then define the *accessibility class* of state α to be the set of states from which α is accessible. Taking M^α to be the matrix of just the rows and columns from the mean matrix of types in the accessibility class of α, then with a little thought it may be seen that the maximum eigenvalue, λ^α of M^α, corresponds to the survival probability of the type α strain.

In the case of multiple surviving types, it may be of interest to assess which become dominant. Branching processes have in fact been used previously to model competitive contagions in the context of meme propagation [122]. Since the expected number of each type in the n^{th} generation is given by vM^n, and the total expected size of the n^{th} generation is approximately $s\lambda^n$ where s gives the number of initially infected, then it follows that the expected type proportions in the n^{th} generation are approximately $\frac{vM^n}{s\lambda^n}$ and dominance may be assessed by taking $n \to \infty$.

The detriments of such a model are in its regard for network structure and respect for heterogeneity– is type susceptibility uniform or are some individuals more likely to get certain types than others? And, how uniform is infection susceptibility in general? As discussed in Section 1.2.4 such questions of heterogeneity have successfully been answered in a simple SIR model using a system of message passing equations [107, 114]. In the following paper we study an adaptation of these equations for the multi-type model described above. Evaluating these enables us to successfully calculate the individual node vulnerabilities to multiple different strains of infection.

Heterogeneous node responses to multi-type epidemics on networks

Sam Moore
s.moore@bath.ac.uk

Tim Rogers
t.c.rogers@bath.ac.uk

Department of Mathematical Sciences, University of Bath, Bath, BA2 7AY, UK

Abstract

Having knowledge of the contact network over which an infection is spreading opens the possibility of making individualised predictions for the likelihood of different nodes to become infected. When multiple infective strains attempt to spread simultaneously we may further ask which strain, or strains, are most likely to infect a particular node. In this article we investigate the heterogeneity in likely outcomes for different nodes in two models of multi-type epidemic spreading processes. For models allowing co-infection we derive message-passing equations whose solution captures how the likelihood of a given node receiving a particular infection depends on both the position of the node in the network and the interaction between the infection types. For models of competing epidemics in which co-infection is impossible, a more complicated analysis leads to the simpler result that node vulnerability factorises into a contribution from the network topology and a contribution from the infection parameters.

Introduction

The networks present everywhere in today's world are very busy. People travel rapidly across the globe carrying goods, ideas and diseases; inboxes are constantly bombarded with work and personal correspondence; social media facilitates the exchange of diverse ideas. Thus, when a contagion process of any kind breaks out it rarely acts in isolation; when ideas spread they may often inspire innovation, alternatives or opposing reactions. A curious example is given by trends in diet. In the United States in 2014 there was a sudden and massive increase, of up to 686%[1, 2], in the consumption of a variety of alternative grains including Quinoa, Teff, Amaranth, Freekeh, Spelt and Kamut. This rapid change in consumer behaviour was driven in a large part by activity on social media networks. Crucially, there was a cooperative effect: individuals who had already received and propagated positive messages about one type of alternative grain are more likely to do the same for another, making the spread of excitement about these products inter-reinforcing. Contagious diseases can be similarly complex in their relationships. For example, the common cold may be attributed to some 200 different viruses and multiple bacterial infections most common amongst which, the Rhinovirus, is itself comprised of three different species and some 160 different types [3]. To understand a cold outbreak, one really needs to study a host of different interacting, mutating and competing pathogens.

Following its introduction by Kermark and McKendrick [4] in the context of modelling spread of infectious diseases in humans, the Susceptible–Infected–Recovered (SIR) epidemic model has been adapted to fit a host of different spreading dynamics, including viruses across computer networks, ideas through social media, and even traffic flow [5, 6, 7]. Furthermore, several multi-type infection models have also been considered with variants exhibiting cooperation [8], dependence [9, 10] and competition [11].

The above cited works all consider the the bulk behaviour of the propagating contagions. Looking in closer detail, knowledge of the underlying network structure over which a contagion spreads should enable us to make individualised predictions for the likely outcomes for particular nodes [12]. Machinery to study heterogeneity in infection models has been in development for several years. An appreciation of the importance of network structure in disease spread, unseen by original mean field approaches [13], has inspired the emergence of network epidemiology [14, 15, 16]. One such approach is message passing, also known as the "cavity method", introduced in [17, 18] for statistical physics models. The idea is to understand the vulnerability of, or conversely threat posed by, a single individual in the network by considering similar statistics of those in their immediate neighbourhood. This approach has been used, for example, by Newman and Karrer in [19] to describe the time development of an epidemic on a network, and in [12, 20] to assess the heterogeneous responses of individual nodes.

In this article we adapt the message passing approach to study the heterogeneous node responses in a generalised multi-type infection model that may exhibit both co-

operative characteristics and competitive ones. In particular, this enables us to determine a formula for node vulnerability in terms of the between-type infection probability matrix, T, and show that large outbreaks may only occur, in both competitive and non-competitive multi-type infection models, if the maximum eigenvalue of T is greater than the inverse of the largest eigenvalue of the network's Hashimoto matrix [21, 22]. Furthermore, in the case of competitive infections we also show that node vulernability to different infections factorises into a contribution from the network architecture, and a contribution from the infection dynamics (specifically, the dominant eigenvector of T).

The remainder of the article is organised as follows. In the next section we introduce a multi-type infection model with both competitive and non-competitive variants. Beginning with the most trivial single type instance of this model, we start by considering the dependency of edge infection time on local topology, first when a neighbourhood's state is known deterministically and then in distribution in order to recap the formulation of the time dependent message passing equations as introduced previously by Karrer and Newman. We then move on to generalise this same approach to considering first non-competitive then competitive multi-type cases. Finally, a toy example of multi-type infection model where timings play a critical role to node vulnerabilities is considered. Here it is seen that careful choice of parameters leads to a change in type prevalence with infection speed; a phenomenon however which is dependent upon graph sparsity.

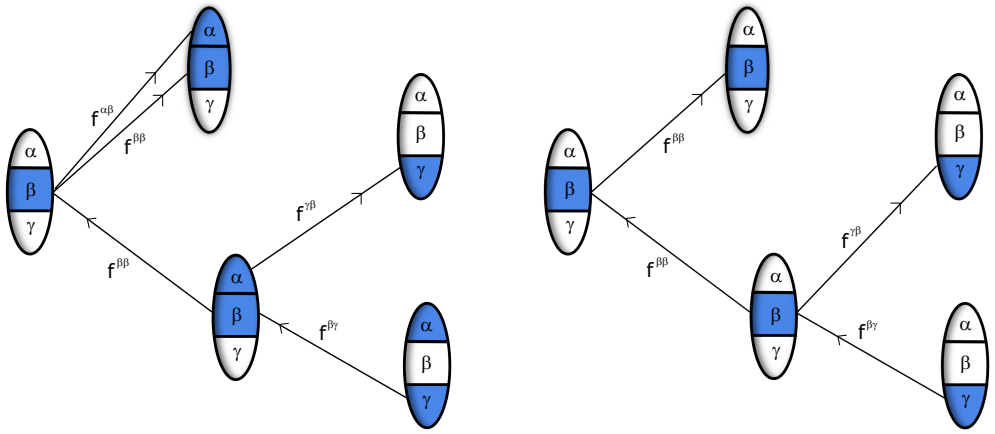

(a) *Co-infection* **(b)** *Competition*

Figure 3-2: *Illustration of possible infection pathways on a network in each of the two cases considered. Greek letters α, β, γ, denote different strains of the infection, with, for example, $f^{\alpha\beta}$ giving the rate with which an individual carrying strain β induces an infection of type α in a neighnour.*

Preliminaries

Multi-type infection model

We present a general model for the spread of an infection with multiple types on a network, based on the well-known SIR process for simple infections, but with allowance for multiple different infection dynamics. We shall consider two cases: one allowing co-infection, where a single individual may be infected by more that one disease type, and another in which infection with one type excludes infection with any other.

Our simple disease model is constructed as follows. We work with a static population of individuals with potential infectious contacts described by some fixed network. With respect to each of some number of different diesease strains (or *types*), every individual node is in one of three possible states: susceptible, infected, or recovered. The model evolves in time with each individual infected with a strain α either recovering from that strain with rate r^α, or transmitting an infection to a neighbour. Importantly, rather than the separate types being treatable as separate infections, we take a more general approach in which each strain may in principle pass on any other strain. An individual carrying infection type α will attempt to induce an infection of type β in a neighbour with rate $f^{\beta\alpha}$. Whether or not this infection attempt succeeds is dependent on the target's own infection history. We consider two cases: co-infection, and competitive exclusion illustrated in Fig.3-2.

If co-infection is allowed, each individual node may contract multiple strains of the epidemic, potentially from multiple infected neighbours. In the exclusive case an individual may only be able to contract a maximum of one infection strain which adds an element of competition to the model, making it possible for a virulent infection to

crowd-out a weaker strain. This creates the complication that in order to determine whether an individual is infected by a particular strain, we the need to know not just whether an individual is reached by that infection type, but also which type reaches them first. This makes it cruicial to consider the full time development of the multi-type epidemic in order to determine the end state.

Message-passing

To analyse the node-dependent outcomes of the multi-type epidemic model introduced above, we will employ a variant of the message-passing approach formulated by Newman and Karer [19]. Let us begin by recapping here the derivation of the method for the case of a single infection type.

For a single-type infection we may consider the time $t_{i\leftarrow j}$ at which node j attempts to pass the infection to i, a quantity which is infinite if either j never receives the infection themselves or recovers before attempting to pass it on. This quantity is equal to the first time at which one of j's other neighbours attempts to pass it the infection, plus an additional time period, S_{ij}, before j will itself transmit to i (note $S_{ij} = \infty$ if j recovers before it can propagate the infection). That is

$$t_{i\leftarrow j} = \min_{k\in\mathcal{N}(j)\setminus i} [t_{j\leftarrow k}] + S_{ij}\,. \tag{3.1}$$

The time until infection of node i can then be deduced by computing the first time at which one of i's neighbours attempts to pass on the infection to it, that is,

$$t_i = \min_{j\in\mathcal{N}(i)} [t_{i\leftarrow j}]\,. \tag{3.2}$$

From these definitions we can formulate equations for the distribution of $t_{i\leftarrow j}$. More specifically, we shall consider the probability, $H_{i\leftarrow j}(t)$, that i does not receive the infection from j before time t. In order to make progress here we shall introduce a sparse tree-like network approximation. If the graph is tree-like then the probable infection times of i's neighbours are approximately independent; using equation (3.2) we compute that the probability i doesn't receive the infection before time t is given by

$$H_i(t) = \prod_{j\in\mathcal{N}(i)} H_{i\leftarrow j}(t)\,. \tag{3.3}$$

To find an expression for $H_{i\leftarrow j}(t)$ we must integrate over the possible values of the delay S_{ij}. Write p for the density function of the i.i.d random variables S_{ij}. In a single type infection with recovery rate r and transmission rate f, we have $p(s) = fe^{-(r+f)s}$.

Equation (3.1) then gives

$$H_{i\leftarrow j}(t) = 1 - \int_0^t \left(1 - \prod_{l\in\mathcal{N}(j)\setminus i} H_{j\leftarrow l}(t-s)\right) p(s)\,\mathrm{d}s\,. \tag{3.4}$$

This expression is substantially simplified in the long-time limit. Taking $t \to \infty$, we may use this system to assess how likely each node is to ever be reached by the infection. To this end, write $T = \int_0^\infty p(s)\mathrm{d}s = f/(f+r)$ to be the probability that an infected individual will never attempt to pass on the infection to a given neighbour. Then we may consider the probability, $h_{i\leftarrow j} = H_{i\leftarrow j}(\infty)$, that j will never attempt to infect i by taking $t \to \infty$ in (3.4) to give

$$h_{i\leftarrow j} = 1 - T\left(1 - \prod_{k\in\mathcal{N}(j)\setminus i} h_{j\leftarrow k}\right)\,. \tag{3.5}$$

We define the *vulnerability* of node i, v_i, to be the probability it becomes infected eventually. From equations (3.3) and (3.5), we deduce:

$$v_i = 1 - \prod_{j\in\mathcal{N}(i)} h_{i\leftarrow j}\,. \tag{3.6}$$

To summarise, by first formulating an expression for t_{ij} given complete knowledge of the time progression of j's neighbourhood, then considering this in probability to find $H_{ij}(t)$ and finally sending t to infinity to find h_{ij} we are able to calculate h_i, the probability that i will never be reached by an infection. This is a powerful method for analysing the node response to epidemics on networks, the question we now wish to address is how it might be applied to more complex models.

Co-infection

For a co-infecting multi-type model, where a single individual may be able to gain any number of types, we seek to investigate the heterogeneous node responses for each type, as described by the probability v_i^α that individual i becomes infected by some specific strain α at any point during the outbreak. We refer to this as the vulnerability of node i to strain α.

Our analysis proceeds in a generalisation of the message passing approach. The time at which a node j will attempt to send the α strain to i will be equal to the minimum times at which any of j's other neighbours pass on any strain β to j, plus the delay $S^{\beta\alpha}$ between j aquiring strain β and passing on strain α. This logic encodes the statement:

$$t^\alpha_{i\leftarrow j} = \min_\beta \left[\min_{k\in\mathcal{N}(j)\setminus i}\left[t^\beta_{j\leftarrow k}\right] + S^{\beta\alpha}_{i\leftarrow j}\right]\,. \tag{3.7}$$

Note that $t^{\alpha}_{i\leftarrow j} = \infty$ if no strain that succeeded in infecting j then goes on to pass strain α to i.

An approximate form of the complementary cumulative distribution function $H^{\alpha}_{i\leftarrow j}(t)$ of $t^{\alpha}_{i\leftarrow j}$ may be obtained from (3.7) in a straightforward generalisation of (3.4). Specifically,

$$H^{\alpha}_{i\leftarrow j}(t) \approx 1 - \int_0^t \sum_{\beta} \left(1 - \prod_{l\in\mathcal{N}(j)\setminus i} H^{\beta}_{j\leftarrow l}(t-s)\right) p^{\beta\alpha}(s)\,\mathrm{d}s\,, \tag{3.8}$$

where $p^{\beta\alpha}$ is the density function of $S^{\beta\alpha}$. In writing (3.8) we make the assumption that contributions to the infection pressure at a given node from strains of different types are approximately additive. This holds in various circumstances including when t is small, when the outbreak is near critical, when mutations between types are relatively rare, or when one type spreads faster than the others. In the long term, the probability $h^{\alpha}_{i\leftarrow j}$ that i will never be infected with strain α by j is given by:

$$h^{\alpha}_{i\leftarrow j} \approx 1 - \sum_{\beta} T^{\beta\alpha} \left(1 - \prod_{k\in\mathcal{N}(j)\setminus i} h^{\beta}_{j\leftarrow k}\right)\,, \tag{3.9}$$

where

$$T^{\beta\alpha} = \int_0^{\infty} p^{\beta\alpha}(t)\,\mathrm{d}t = \frac{f^{\beta\alpha}}{r^{\beta} + \sum_{\gamma} f^{\beta\gamma}}\,.$$

This quantity defines the chance of a type β individual ever attempting to send a infection α to a neighbour. We will refer to the matrix of all these values for different α, β as the *transmission matrix*. Finally, the vulnerability v^{α}_i of node i to strain α will be given by

$$v^{\alpha}_i = 1 - \prod_{j\in\mathcal{N}(i)} h^{\alpha}_{i\leftarrow j}\,. \tag{3.10}$$

To numerically compute node vulnerabilities, it is first necessary to solve the system (3.9). In doing this it is convenient to examine the network of relationships between variables $h^{\alpha}_{i\leftarrow j}$. This is information that may be efficiently given by use of the non-backtracking, or *Hashimoto graph*.

The *Hashimoto graph* is formed of two nodes for each of the graph's edges traversed in both directions. The node $e = (i \to j)$ is then connected to $e' = (k \to \ell)$ if $k = j$ but $\ell \neq i$ [23]. On this graph the system (3.9) then equivalently becomes

$$h^{\alpha}_{e} = 1 - \sum_{\beta} T^{\beta\alpha} \left(1 - \prod_{e'\in\mathcal{N}(e)} h^{\beta}_{e'}\right)\,, \tag{3.11}$$

where $\mathcal{N}(e)$ refers to the neighbourhood of the node in the Hashimoto graph corresponding to edge e. Let us write B for the adjacency matrix of the Hashimoto graph, known as the *non-backtracking matrix*.

Solutions to the system of equations (3.11) may be found by iteration to give the probabilities over directed edges which can be used to find the node vulnerabilities, h_i^α, by equation (3.10). There is a trivial solution $h_e^\alpha \equiv 1$, corresponding to all nodes never receiving any infection. Depending on the values of $T^{\beta\alpha}$, there may or may not be a non-trivial solution set.

The boundary of the region of parameter space in which a non-trivial solution exists (and hence where a large-scale outbreak is possible) is known as the percolation threshold, which we now compute. We proceed by analysing the linear stability of the no-infection state $\mathbf{h} = 1$. To this end taking derivatives from (3.11) gives us

$$\frac{\partial h_e^\alpha}{\partial h_{e'}^\beta} = \mathbf{1}_{e' \in \mathcal{N}(e)} T^{\beta\alpha} \prod_{e'' \in \mathcal{N}(e) \setminus e'} h_{e''}^\beta \,, \tag{3.12}$$

and therefore the Jacobian matrix of the message-passing system at the trivial state is given by

$$J_{e,e'}^{\beta,\alpha} = \left. \frac{\partial h_e^\alpha}{\partial h_{e'}^\beta} \right|_{\mathbf{h}=1} = B_{e,e'} T^{\beta\alpha} \,. \tag{3.13}$$

If J has an eigenvalue with real part larger than one, then the dynamical system described by iteration of the message-passing equations is unstable around the state $\mathbf{h} = 1$, and an outbreak is possible. According to (3.13), J is the Kronecker product of the matrices B and T. More specifically, that is to say

$$J = B \otimes T = \begin{pmatrix} b_{1,1}T & \dots & b_{1,2|E|}T \\ \vdots & \ddots & \vdots \\ b_{2|E|,1}T & \dots & b_{2|E|,2|E|}T \end{pmatrix} , \tag{3.14}$$

where $b_{i,j}$ denotes the entry i, j of B. Since it follows that the eigenvalues of J are equal to the product of the eigenvalues of B and T [24] and both B and T have non-negative entries and hence real maximum eigenvalues, say λ_B and λ_T respectively, we deduce that a multi-type infection defined by transmission matrix T spreading on a network with non-backtracking matrix B has a non-zero probability to result in a large outbreak if and only if

$$\lambda_T \lambda_B > 1. \tag{3.15}$$

Around the neighbourhood of percolation, the factorisation we find in equation (3.13) implies that the node vulernabilities will be proportional to their *non-backtracking centrality* [25], as expounded in [20]. That is to say the vulnerability of node i is proportional

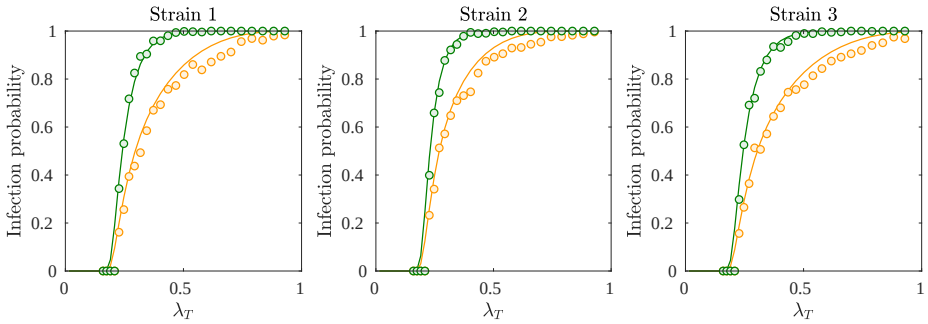

Figure 3-3: *Vulnerabilities to an infection with three types, computed for two separate nodes in an Erdős-Rényi random graph on 1000 nodes with mean degree 5. Solid lines show the theoretical prediction of equations (3.11) and (3.10); circles show the result of simulations averaged over 1500 samples, including only those samples in which an outbreak of at least 50 nodes was observed. The chosen nodes have degree 3 (orange, lower) and degree 9 (green, higher), and show a strong differential in outcome.*

to the centrality measure

$$x_i = \sum_j A_{ij} v_{i\to j} \tag{3.16}$$

where A is the graph's adjacency matrix and $v_{i\to j}$ denotes the eigenvector of B that corresponds to edge $i \to j$. For the case that λ_T is significantly larger than λ_B the relationship is more complex, and full solution of the system (3.11) is necessary.

Example: three types

Let us consider a co-infection model with infection dynamics of the form

$$f^{\beta\alpha} = b^\beta m^{\beta\alpha}\,, \tag{3.17}$$

where b^β decribes the overall transmission rate for type β, and $m^{\beta\alpha}$ the probability of mutation from type β to type α during transmission (with the rule $\sum_\gamma m^{\beta\gamma} = 1$). For simplicity we fix all recovery rates as equal, so $r^\beta \equiv r$. This gives the transmission matrix

$$T^{\beta\alpha} = \frac{b^\beta}{r + b^\beta} m^{\beta\alpha}\,. \tag{3.18}$$

Figure, 3-3 shows example results of such an infection. Here we have used the mutation matrix

$$m = \begin{pmatrix} 0.8 & 0.1 & 0.1 \\ 0.2 & 0.6 & 0.2 \\ 0.33 & 0.33 & 0.33 \end{pmatrix}\,, \tag{3.19}$$

and infection rates $b^1 = 0.1x$, $b^2 = 1x$, $b^3 = 10x$, where x is a parameter we vary in order to achieve different values of λ_T for plotting.

Exclusive infections

Many contagion processes spread at the expense of excluding others. In our model, if we do not permit co-infection, then the time at which j attempts to send the α strain to i depends strongly on which strain has suceeded in infecting j. Specifically,

$$t^{\alpha}_{i\leftarrow j} = \min_{\gamma,k}\left[t^{\gamma}_{j\leftarrow k}\right] + S_{\alpha\beta^\star} \tag{3.20}$$

where $\beta^\star = \arg\min_\gamma\left[\min_k\left[t^{\gamma}_{j\leftarrow k}\right]\right]$ is the strain infecting j. From here, to calculate $H^{\alpha}_{i\leftarrow j}(t)$ given the equivalent distributions for neighbouring nodes as before, we take the approach of first calculating how likely any infection is to be transmitted down the edge in question before then assessing the strain transmitted conditioned on this value.

Take now $q^{\alpha}_{i\leftarrow j}(t)$ to be the density function for the distribution describing the likelihood of j passing on α to i, so

$$H^{\alpha}_{i\leftarrow j}(t) = 1 - \int_0^t q^{\alpha}_{i\leftarrow j}(s)\mathrm{d}s\,. \tag{3.21}$$

Now if we consider the equivalent distribution for j passing on anything to i, with probability density function $q_{i\leftarrow j}(t)$, since types are exclusive it follows that

$$q_{i\leftarrow j} = \sum_{\alpha} q^{\alpha}_{i\leftarrow j} \tag{3.22}$$

and further there exists weights $\omega^{\alpha}_{i\leftarrow j}$ so that

$$q^{\alpha}_{i\leftarrow j} = \omega^{\alpha}_{i\leftarrow j} q_{i\leftarrow j}\,. \tag{3.23}$$

Thus

$$\begin{aligned} H^{\alpha}_{i\leftarrow j}(t) =& 1 - \omega^{\alpha}_{i\leftarrow j}\int_0^t q_{i\leftarrow j}(s)\mathrm{d}s & (3.24)\\ =& 1 - \omega^{\alpha}_{i\leftarrow j}\left(1 - H_{i\leftarrow j}(t)\right) & (3.25)\end{aligned}$$

Now for i to pass on α to j at time t, some other neighbour of j, say k, must pass on an infection of some given type, say β, at some prior time $t-\tau$ and then we must have a successful α infection from this after the remaining time period τ, this being described by the density $p^{\alpha\beta}$. To additionally observe exclusivity j must not gain an infection via another node before k, this happens with probability $\prod_{l\in\mathcal{N}(j)\setminus k} H_{i\leftarrow j}(t-\tau)$. Combining all this we see that

$$q^{\alpha}_{i\leftarrow j}(t) = \int_0^t \sum_{k\in\mathcal{N}(j)}^{\alpha} q^{\beta}_{j\leftarrow k}(t-\tau) \prod_{l\in\mathcal{N}(j)\setminus k} H_{i\leftarrow j}(t-\tau)p^{\alpha\beta}(\tau)\,\mathrm{d}\tau \tag{3.26}$$

and further by (3.21) it follows that

$$H^{\alpha}_{i\leftarrow j}(t) = 1 - \int_0^t \int_0^s \sum_{\substack{\alpha \\ k\in\mathcal{N}(j)}} q^{\beta}_{j\leftarrow k}(s-\tau) \prod_{l\in\mathcal{N}(j)\setminus k} H_{i\leftarrow j}(s-\tau) p_{\alpha\beta}(\tau)\,\mathrm{d}\tau\mathrm{d}s\,. \tag{3.27}$$

Then by (3.23) and substituting $u = s - \tau$

$$H^{\alpha}_{i\leftarrow j}(t) = 1 - \int_0^t \sum_{\substack{\alpha \\ k\in\mathcal{N}(j)}} p^{\alpha\beta}(\tau)\omega^{\beta}_{j\leftarrow k} \int_0^{t-\tau} q_{j\leftarrow k}(u) \prod_{l\in\mathcal{N}(j)\setminus k} H_{i\leftarrow j}(u)\,\mathrm{d}u\mathrm{d}\tau\,. \tag{3.28}$$

Now by summing over all the neighbours of j the inner integral here gives the probability that j gains any infection from any neighbour before time $t-\tau$, that is

$$\sum_{k\in\mathcal{N}(j)} \int_0^{t-\tau} q_{j\leftarrow k}(u) \prod_{l\in\mathcal{N}(j)\setminus k} H_{i\leftarrow j}(u)\,\mathrm{d}u = 1 - \prod_{k\in\mathcal{N}(j)} H_{j\leftarrow k}(t-\tau) \tag{3.29}$$

and thus

$$H^{\alpha}_{i\leftarrow j}(t) = 1 - \int_0^t \sum_{\beta} p^{\alpha\beta}(\tau)\omega^{\beta} \left(1 - \prod_{k\in\mathcal{N}(j)\setminus i} H_{j\leftarrow k}(t-\tau)\right) \mathrm{d}\tau\,. \tag{3.30}$$

We now have a similar expression to (3.20), the equivalent formulation for non-exclusive types, the difference here being due to the fact that the only infection that i may be infected by is the first to reach j.

In this way we see the perhaps surprising result that the probability of an individual gaining a specific type of infection may be broken down into two independent parts describing the probability of gaining any type of infection together with the probability that the infection if gained is of a certain type.

This decomposition is useful in computing probability $h^{\alpha}_{i\leftarrow j}$ that i will never get infected by strain α from j. The probability that j will send an α message to i having itself received a β message is given by

$$T_{\alpha\beta}\omega^{\beta}\left(1 - \prod_{k\in\mathcal{N}(j)} h_{j\leftarrow k}\right) \tag{3.31}$$

and so the probability of i ever receiving an α infection from j will be given by

$$\omega^{\alpha}(1 - h_{i\leftarrow j}) = \sum_{\beta} T_{\alpha\beta}\omega^{\beta}\left(1 - \prod_{k\in\mathcal{N}(j)\setminus i} h_{j\leftarrow k}\right)\,. \tag{3.32}$$

Writing $\boldsymbol{\omega}$ for the vector with entries ω_α we can deduce the eigenvector equation

$$T\boldsymbol{\omega} = \lambda_T \boldsymbol{\omega}\,, \tag{3.33}$$

where it must hold that

$$\lambda_T = \frac{1 - h_{i\leftarrow j}}{1 - \prod_{k\in\mathcal{N}(j)\setminus i} h_{j\leftarrow k}}\,. \tag{3.34}$$

That is, $\boldsymbol{\omega}$ is an eigenvector of the matrix T with eigenvector λ_T, and we may rearrange (3.34) to obtain the message-passing equations

$$h_{i\leftarrow j} = 1 - \lambda_T \left(1 - \prod_{k\in\mathcal{N}(j)\setminus i} h_{j\leftarrow k}\right)\,, \tag{3.35}$$

with the rule

$$h^\alpha_{i\leftarrow j} = \omega^\alpha h_{i\leftarrow j}\,. \tag{3.36}$$

Note that the system (3.35) is precisely the same as the well studied case of equation (3.5), with the substitution $T \mapsto \lambda_T$.

We have thus mapped the analysis of the initially more complex exculsive infection model onto the previous case, allowing one to immediately translate existing results. For example, we find that the percolation threshold is once again given by the condition $\lambda_T\lambda_B > 1$; the same as for the co-infection case. This result is perhaps to be expected as at the limit of infection survival each individual will become exposed to at most one infection.

Example: speed vs reliability

In a contagion with competing strains it may be interesting to know what characteristics will become dominant. Here we consider a trade-off between the speed and reliability with which an infection may spread. Both these quantities may be expected to have a bearing on whether a particular strain becomes dominant in a population. Using our formulated message passing equations we can then seek to answer the question of what makes for a more successful contagion type; that which is slow but reliable or fast but unreliable

Consider a model with two competing strains, α and β, with dyanmics specifed by infection and mutation rates as used in Section . The case we are interested in is when $b^\alpha < b^\beta$, but $m^{\beta\alpha} > m^{\alpha\beta}$; that is, β spreads faser, but is also more likely to mutate. In the two-type case, the matrix T has the form

$$T = \begin{pmatrix} \frac{m^{\alpha\alpha}}{1+d/b^\alpha} & \frac{m^{\alpha\beta}}{1+d/b^\alpha} \\ \frac{m^{\beta\alpha}}{1+d/b^\beta} & \frac{m^{\beta\beta}}{1+d/b^\beta} \end{pmatrix} \tag{3.37}$$

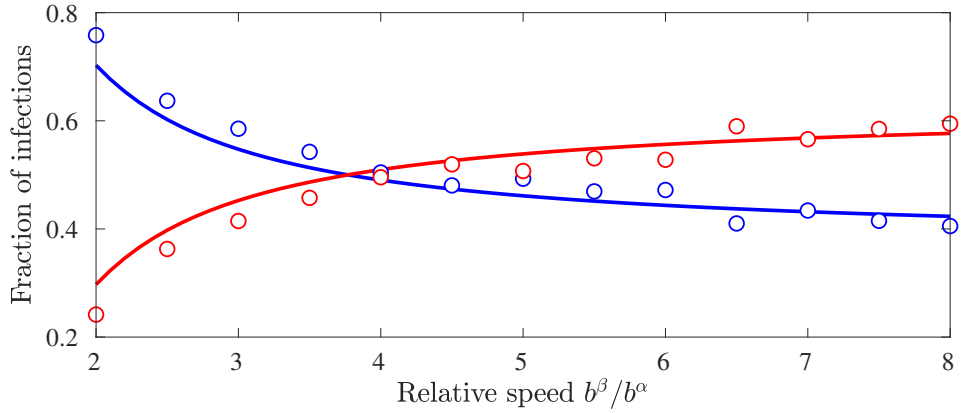

Figure 3-4: *Fraction of nodes infected with strain α (blue) or β (red) in theory (lines) compared to simulations (circles) of an exclusive infection model on an Erdős-Rényi random graph with $N = 1000$ and $c = 3$. Other parameters are: $m^{\alpha\beta} = 0.01$ and $m^{\beta\alpha} = 0.25$, $d = 2$.*

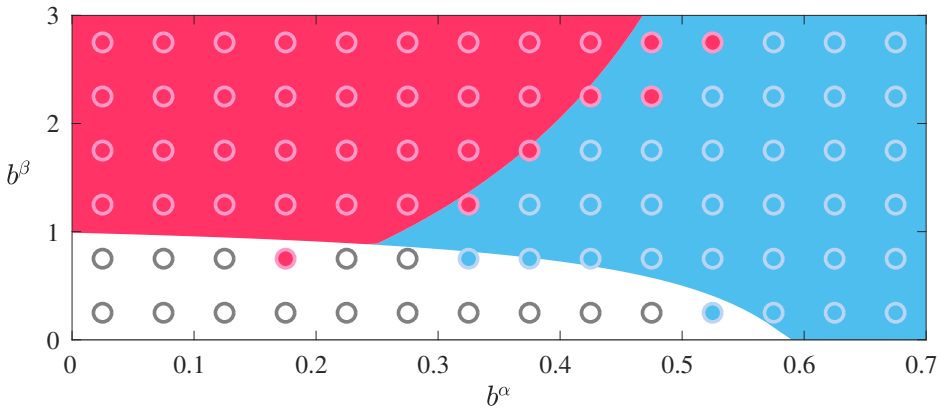

Figure 3-5: *Phase diagram showing parameter regions in which there is no outbreak (white), or where an outbreak occurs and is dominated by either strain α (blue) or β (red). Coloured circles show the modal result of 100 simulated outbreaks on an Erdős-Rényi random graph with $N = 1000$ and $c = 3$. Other parameters are: $m^{\alpha\beta} = 0.0$ and $m^{\beta\alpha} = 0.33$, $d = 1$.*

The top eigenpair $(\lambda_T, \boldsymbol{\omega})$ of T can be computed directly, then respectively used in equation (3.35) to compute node vulnerabilities and the overall probability of an outbreak, and in equation (3.36) to determine which infection type is dominant.

In Figure. 3-4 we plot the fraction of infections achieved by each strain in an Erdős-Rényi random graph. The plot shows how this quantity varies as a function of relative speed of infections b^β/b^α, with mutation probabilities are fixed at $m^{\alpha\beta} = 0.01$ and $m^{\beta\alpha} = 0.25$, and death rate $d = 2$. As is clearly visible from the figure, an infection which reproduces less reliably can come to dominate a more reliable one, provided it spreads fast enough. This relationship is considered in more detail in Figure. 3-5, shows a phase diagram of outcomes (no outbreak, α dominates, β dominates) as both strain infection rates are varied. In that figure we use $m^{\alpha\beta} = 0.1$ and $m^{\beta\alpha} = 0.33$.

Conclusion

In this article we have constructed systems of equations capturing the time development node states during a complex multi-type infection outbreak, dependent upon the local network topology. Furthermore, we have shown that this is an effective method for ranking nodes by their eventual susceptibility to a complex infection outbreak. This makes for a framework to be applied to evaluate heterogeneity of individual node outcomes in many complex contagion models.

Application of our co-infection model is, for instance, of potential interest in understanding the dynamics of cooperative contagions. These have been studied for example in [8] to model phenomena such as the co-epidemic of pneumonia and the 1918 Spanish flu. Alternatively, on might apply our approach to help understand individual strategy in models for human, Web based, cooperation as studied in [26]. Meanwhile, the framework for exclusive (i.e. competitive) contagions may be applied to study individual strain vulnerability in infection models with cross immunity, as studied in [27, 28].

Several promising areas of development for our theory are open to investigation. We have restricted attention here to models in which (i) recovery times are independent between co-infecting strains, and (ii) both recovery and infection times are memoryless (i.e. exponential) random variables specified by a rate parameter. Extensions to our theory that relax both of these assumptions are possible. Message passing equations can also be formulated for models of bootstrap percolation [29]. These models corrsepond to contagions dynamics whereby the infection may only spread to individuals once they have reached a critical number of infected neighbours. This concept is relevant for instance in the modeling of opinion dynamics.

What is useful in the potential application of our approach to the models mentioned above, beyond the existing techniques, is the way in which it is centred on network topology. As we have observed such information is perhaps most succinctly captured by the non-backtracking matrix which we are able to employ to great effect. This is worthy of mention as further evidence for the effectiveness of a powerful tool, only recently introduced into the field of network science, but already proven highly effective in measuring relevant structural properties, such as percolation threshold [22] and community structure [30].

In the course of our approach we potentially also gain much more information about the dynamics of an outbreak than just the end state. For instance we might see how a node's infection probability changes in time. However, in order to assess such quantities directly it would be desirable to be able to solve systems like (3.4) in an iterative manner similar to that done for (3.5). Attempting this, one quickly encounters the problem of being able to understand time-lag between successive infections and how this depends on the network structure. Progress in this direction would be a valuable step towards providing greater insight into the spread of contagious processes on networks.

REFERENCES

[1] W. G. Council, "Dollar sales growth of gluten-containing ancient grains in the united states in 2014 by category." `www.statista.com/statistics/509704/dollar-sales-growth-gluten-containing-ancient-grains-us-by-category/`.

[2] W. G. Council, "Dollar sales growth of gluten-free ancient grains in the united states in 2014 by category." `www.statista.com/statistics/509695/dollar-sales-growth-gluten-free-ancient-grains-us-by-category/`.

[3] M. J. Mäkelä, T. Puhakka, O. Ruuskanen, M. Leinonen, P. Saikku, M. Kimpimäki, S. Blomqvist, T. Hyypiä, and P. Arstila, "Viruses and bacteria in the etiology of the common cold," *Journal of clinical microbiology*, vol. 36, no. 2, pp. 539–542, 1998.

[4] M. Kermark and A. Mckendrick, "Contributions to the mathematical theory of epidemics. part i," *Proc. r. soc. a*, vol. 115, no. 5, pp. 700–721, 1927.

[5] A. Barrat, M. Barthelemy, and A. Vespignani, *Dynamical processes on complex networks*. Cambridge university press, 2008.

[6] D. Li, B. Fu, Y. Wang, G. Lu, Y. Berezin, H. E. Stanley, and S. Havlin, "Percolation transition in dynamical traffic network with evolving critical bottlenecks," *Proceedings of the National Academy of Sciences*, vol. 112, no. 3, pp. 669–672, 2015.

[7] P. Wang, M. C. González, C. A. Hidalgo, and A.-L. Barabási, "Understanding the spreading patterns of mobile phone viruses," *Science*, vol. 324, no. 5930, pp. 1071–1076, 2009.

[8] W. Cai, L. Chen, F. Ghanbarnejad, and P. Grassberger, "Avalanche outbreaks emerging in cooperative contagions," *Nature physics*, vol. 11, no. 11, p. 936, 2015.

[9] R. A. Blythe, R. J. Allen, *et al.*, "Parasites on parasites: Coupled fluctuations in stacked contact processes," *EPL (Europhysics Letters)*, vol. 101, no. 5, p. 50001, 2013.

[10] S. Moore, P. Mörters, and T. Rogers, "A re-entrant phase transition in the survival of secondary infections on networks," *Journal of Statistical Physics*, pp. 1–14, 2018.

[11] C. Neuhauser, "Ergodic theorems for the multitype contact process," *Probability Theory and Related Fields*, vol. 91, no. 3-4, pp. 467–506, 1992.

[12] T. Rogers, "Assessing node risk and vulnerability in epidemics on networks," *EPL (Europhysics Letters)*, vol. 109, no. 2, p. 28005, 2015.

[13] H. W. Hethcote, "The mathematics of infectious diseases," *SIAM review*, vol. 42, no. 4, pp. 599–653, 2000.

[14] M. J. Keeling and K. T. Eames, "Networks and epidemic models," *Journal of the Royal Society Interface*, vol. 2, no. 4, pp. 295–307, 2005.

[15] J. O. Lloyd-Smith, S. J. Schreiber, P. E. Kopp, and W. M. Getz, "Superspreading and the effect of individual variation on disease emergence," *Nature*, vol. 438, no. 7066, p. 355, 2005.

[16] S. Bansal, B. T. Grenfell, and L. A. Meyers, "When individual behaviour matters: homogeneous and network models in epidemiology," *Journal of the Royal Society Interface*, vol. 4, no. 16, pp. 879–891, 2007.

[17] J. Pearl, *Reverend Bayes on inference engines: A distributed hierarchical approach*. Cognitive Systems Laboratory, School of Engineering and Applied Science, University of California, Los Angeles, 1982.

[18] M. Mezard, G. Parisi, M. A. Virasoro, and D. J. Thouless, "Spin glass theory and beyond," *Physics Today*, vol. 41, p. 109, 1988.

[19] B. Karrer and M. E. Newman, "Message passing approach for general epidemic models," *Physical Review E*, vol. 82, no. 1, p. 016101, 2010.

[20] R. Kühn and T. Rogers, "Heterogeneous micro-structure of percolation in sparse networks," *EPL (Europhysics Letters)*, vol. 118, no. 6, p. 68003, 2017.

[21] K. E. Hamilton and L. P. Pryadko, "Tight lower bound for percolation threshold on an infinite graph," *Physical review letters*, vol. 113, no. 20, p. 208701, 2014.

[22] B. Karrer, M. E. Newman, and L. Zdeborová, "Percolation on sparse networks," *Physical review letters*, vol. 113, no. 20, p. 208702, 2014.

[23] K.-i. Hashimoto, "Zeta functions of finite graphs and representations of p-adic groups," in *Automorphic forms and geometry of arithmetic varieties*, pp. 211–280, Elsevier, 1989.

[24] A. Graham, *Kronecker products and matrix calculus with applications*. Courier Dover Publications, 2018.

[25] T. Martin, X. Zhang, and M. E. Newman, "Localization and centrality in networks," *Physical review E*, vol. 90, no. 5, p. 052808, 2014.

[26] S. Suri and D. J. Watts, "Cooperation and contagion in web-based, networked public goods experiments," *PloS one*, vol. 6, no. 3, p. e16836, 2011.

[27] J. R. Gog and B. T. Grenfell, "Dynamics and selection of many-strain pathogens," *Proceedings of the National Academy of Sciences*, vol. 99, no. 26, pp. 17209–17214, 2002.

[28] J. Gog and J. Swinton, "A status-based approach to multiple strain dynamics," *Journal of mathematical biology*, vol. 44, no. 2, pp. 169–184, 2002.

[29] M. Shrestha and C. Moore, "Message-passing approach for threshold models of behavior in networks," *Physical Review E*, vol. 89, no. 2, p. 022805, 2014.

[30] F. Krzakala, C. Moore, E. Mossel, J. Neeman, A. Sly, L. Zdeborová, and P. Zhang, "Spectral redemption in clustering sparse networks," *Proceedings of the National Academy of Sciences*, vol. 110, no. 52, pp. 20935–20940, 2013.

CHAPTER 4

PREDICTING THE SPEED OF EPIDEMICS SPREADING ON NETWORKS

In the previous chapter we made extensive use of message passing equations which are built upon distributions for time dependent vulnerabilities. However, as alluded to in the conclusion of the previous paper, there is no clear means to effectively evaluate such time dependent probabilities directly. More specifically, we would like to be able to know the probability that some vertex i does not receive the infection before time t, $H_i(t)$. Now we have the relations that

$$H_i(t) = \prod_{j \in \mathcal{N}(i)} H_{i \leftarrow j}(t) \tag{4.1}$$

and

$$H_{i \leftarrow j}(t) = 1 - \int_0^t \left(1 - \prod_{l \in \mathcal{N}(j) \setminus i} H_{j \leftarrow l}(t-s) \right) p(s) \, \mathrm{d}s \,, \tag{4.2}$$

where $p(s) = be^{-(r+b)s}$ for an infection with exponential infection and recovery rates given by b and r respectively. However, this system is not readily solvable. The situation is rather simpler when we take $t \to \infty$ to give $h_{i \leftarrow j} = H_{i \leftarrow j}(\infty)$, the probability the infection is never passed between two given nodes. We then find

$$h_{i \leftarrow j} = 1 - T \left(1 - \prod_{k \in \mathcal{N}(j) \setminus i} h_{j \leftarrow k} \right) \,, \tag{4.3}$$

where

$$T = \int_0^\infty p(s) \mathrm{d}s = \frac{b}{b+r} \,. \tag{4.4}$$

This is a system of equations we may be able to evaluate iteratively with $h_{\iota \leftarrow j}$ fixed, where ι the location of the infection seed.

While we may not be able to evaluate the time dependent probabilities, $H_{i \leftarrow j}(t)$, in this manner, we may make progress by considering a related distribution.

Let us assume for simplicity that the infection will never recover (so $r = \infty$). It is immediate that $H_{\iota \leftarrow j}(t) = e^{-bt}$ for ι the seed node and j in its neighbourhood. Now consider all nodes at distance n from the source and the probability, $H^n(t)$, that the infection does not reach one of these by time t. We then discover that, for moderately large n,

$$H^{n-1}(t) \approx H^n(t+\tau) \approx H^{n+1}(t+2\tau) \approx ... \approx H^{n+m}(t+m\tau) \tag{4.5}$$

where τ is the expected time lag for the infection to reach subsequent graph distances away from the source. The calculation of this time lag, which is the reciprocal of some form of infection speed parameter, turns out to be rather non-trivial, however, and forms the basis of the final paper presented below.

Predicting the speed of epidemics spreading on networks

Sam Moore
s.moore@bath.ac.uk

Tim Rogers
t.c.rogers@bath.ac.uk

Department of Mathematical Sciences, University of Bath, Bath, BA2 7AY, UK

Abstract

Global transport and communication networks enable information, ideas and infectious diseases now to spread at speeds far beyond what has historically been possible. To effectively monitor, design, or intervene in such epidemic-like processes, there is a need to predict the speed of a particular contagion in a particular network, and to distinguish between nodes that are more likely to become infected sooner or later during an outbreak. Here, we study these quantities using a message-passing approach to derive simple and effective predictions which are validated against epidemic simulations on a variety of real-world networks with good agreement. In addition to individualized predictions for different nodes, we find an overall sudden transition from low density to almost full network saturation as the contagion develops in time. Our theory is developed and explained in the setting of simple contagions on tree-like networks, but we are also able to show how the method extends remarkably well to complex contagions and highly clustered networks.

Introduction

It took more than nine years for the Black Death to spread across Europe. Progress of this devastating outbreak of bubonic plague was limited by 14^{th} century travel networks to an average daily dispersion of approximately 1.5km [1]. In frightening contrast, the recent Zika outbreak in South America was found to spread with an average daily dispersion of 42km, rising as high as 634km in the most densely populated parts of Brazil [2]. This extraordinary difference is indicative of a mobile society that is no longer rigidly bound by spatial structure, making the relevant notion of distance network-based rather than geographic. Similarly, in the highly connected domain of social media, the spread of concepts, memes and hashtags can be explosive. One recent empirical study of the dynamics of online rumour cascades — often reaching tens of thousands of users in a matter of days — made the worrying finding that false information spreads faster then true [3]. It takes little imagination to see how an understanding of propagation speeds in modern networks would have, in the digital case, great commercial and political benefit, and in the physical case be invaluable in planning outbreak prevention, monitoring and response.

The field of network epidemiology [4, 5, 6] has developed a wide spectrum of techniques for the analysis of spreading processes. One approach to the problem of spreading speed is through numerical simulations (see e.g. [7]), which yield useful results on small scales, but for increasingly large complex networks may prove slow and impractical. Alternative approximations have been made by considering only the most probable path between a given target node and the source [8]. It is known that this shortest-path approach can significantly overestimate the infection arrival times [9], but to take into account all possible paths would soon be infeasible as their number typically grows exponentially with the number of vertices in the network. One promising idea is a conjectured connection between centrality measures and infection arrival time [10], which so far has only been tested numerically.

While global networks of interest are highly connected, they are also typically sparse in the sense that individuals usually interact with a number of others that is very small relative to the total population size. Exploitation of this sparse network structure has been a key tool in network epidemiology, in particular via the message-passing approach pioneered in [11]. This technique has allowed for efficient characterization of the epidemic (percolation) threshold [12, 13], and gave rise to the new notion of *non-backtracking centrality* [14]. In [15, 16] a message-passing approach was used to make individualized predictions for node responses to spreading processes, giving a physical interpretation of non-backtracking centrality as the probability for a node to appear in the percolating cluster. None of these works has yet addressed the important questions of how fast an epidemic will spread in a given network, and which nodes may fall victim first.

Here, we seek to assess the full time-dependence of an epidemic outbreak in order

to characterize the speed of spread in a given network by calculating the mean delay in infection between nodes at different graph distances from the source. Technically, we achieve this through a saddle-point analysis of the left tail of the distribution of time to infection, expressed via the message-passing equations. This method enables us to find the overall speed of an infection in a network, and to show that the arrival time at a node is accurately predicted by the logarithm of its non-backtracking centrality.

Our theoretical predictions for both spreading speed and arrival times show excellent agreement with numerical simulations performed on real-world networks, even in the case of highly clustered contact networks with heavy tailed degree distributions. Remarkably, we show that the method can also be extended to complex threshold models of contagions in which a node must be exposed to multiple infective neighbours before acquiring the contagion itself. We finish by observing that the time for the infection to spread through the bulk of the network is independent of network size, implying an almost instantaneous jump from low to high density of infection when time is properly scaled; a property which we show to be common to time-ordered percolation in general.

Speed of spread

We begin by considering a simple SI infection spreading on a sparse network starting from a single infected node (details on the extension to other models, inlcuding SIR and complex contagions, are found in the supplement). When node i becomes infectious, it transmits the infection to a neighbour j after a delay $X_{i\to j}$; a random variable drawn from a distribution with density $f(x)$, independently from any other event. The choice of an exponential distribution for f would correspond to Markov disease dynamics, although it has been shown that real-world contagion dynamics differ substantially from this simple case [17, 18, 19, 20], and hence we study general distributions of transmission time.

Write T_i^n for the length of the shortest (temporal) path to a node at distance n from i, and $T_{i\to j}^n$ for the shortest such path whose first step is to node j. It follows that $T_i^n = \min_{j\in\partial i} T_{i\to j}^n$, where ∂i denotes the set of neighbours of i. More generally, $T_{i\to j}^n$ decomposes as

$$T_{i\to j}^n = X_{i\to j} + \min_{k\in\partial j\setminus i} T_{j\to k}^{n-1}\,. \tag{4.1}$$

Writing $F_{i\to j}^n(t)$ for the probability that $T_{i\to j}^n$ is less than t, we arrive at the message passing equation

$$F_{i\to j}^n(t) = \int_0^t f(x)\left(1 - \prod_{k\in\partial j\setminus i}\left[1 - F_{j\to k}^{n-1}(t-x)\right]\right)\mathrm{d}x\,. \tag{4.2}$$

In writing the above we have assumed independence between the variables $\{T_{j\to k}^{n-1}\}$; although this technically only holds for tree graphs, we will see that the approximation is effective for a broad class of real-world networks.

Equation (4.2) represents a nested hierarchy of expressions which could in principle be solved numerically for a given network, infection and source node. However, this process is computationally intensive and the results are not generalisable. We will pursue a different path and investigate the structure of the dynamics described by (4.2) to reveal useful general insights.

At first glance, it appears that the spreading process depends in a complicated way on the precise layout of the network, however, we find that the system possesses a regularity which emerges after a few iterations. In a network of $N \gg 1$ nodes, for $1 \ll n \ll N$ we observe the convergence $T_i^n/n \to \tau$ for some constant τ, describing the delay between spreading $n-1$ steps from the source to n. In this sense $1/\tau$ can be interpreted as the *speed* of spreading in the network. This effect is illustrated in the left panels of Fig. 4-1, showing the convergence and reduction of variance in simulated histograms of T_i^n/n for different source nodes i as n grows.

To compute the characteristic delay τ, we examine the left tails of $F_{i\to j}^n$ for large n. Our rationale for this approach is that, as illustrated in Fig. 4-1, the offset is the same across the whole distribution, and we will show that the left tails are amenable to a

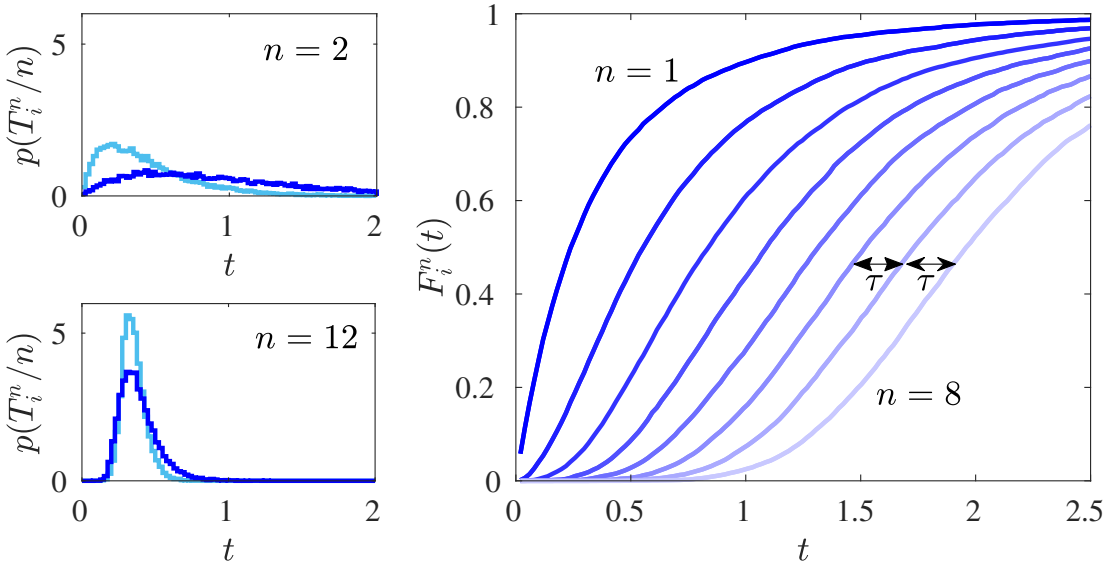

Figure 4-1: *Left panels: simulation of the distribution of the scaled time T_i^n/n for an epidemic to reach distance n from a source node i chosen to have degree 1 (dark) or degree 3 (pale); as $n \to \infty$ these distributions will converge to delta functions at some value τ. Right: simulation of the CDF $F_i^n(t)$ for time to reach distance n from a source node i chosen to have degree 1, showing convergence to a standard form with a fixed offset τ. In both cases node-to-node transmission times are standard exponentials and the network is an Erdős-Rényi graph with mean degree 3 on $N = 10^4$ nodes.*

linear analysis. For $t \ll n\tau$, we linearize (4.2) to obtain

$$F^n_{i\to j}(t) \approx \int_0^t f(x) \sum_{l\in\partial j\setminus i} F^{n-1}_{j\to l}(t-x)\,\mathrm{d}x\,. \tag{4.3}$$

This problem is mathematically analogous to that of front propagation and we therefore follow the standard method described in [21]. The trivial solution $F^0(t) \equiv 0$ is linearly unstable with increasing n, and the dominant rate of growth will determine τ. The two sided Laplace transform of Eq. (4.3) reads

$$\tilde{F}^n_{i\to j}(k) = \tilde{f}(k) \sum_{l\in\partial j\setminus i} \tilde{F}^{n-1}_{j\to l}(k)\,, \tag{4.4}$$

where $\tilde{f}(k) = \int e^{-kx} f(x)\mathrm{d}x$ is the Laplace transform of f. Viewing $\tilde{F}$ as a vector with entries indexed by directed edges, Eq. (4.4) describes an iterative process of multiplying by a matrix that encodes the entries of the sum, and then by the scalar $\tilde{f}(k)$. Thus, for large n we can expect

$$\tilde{F}^n_{i\to j}(k) \propto v_{i\to j}\, e^{-\omega(k)n}, \tag{4.5}$$

where the coefficient $v_{i\to j}$ contains the edge-specific information, and the function $\omega(k)$ determines the overall exponential growth rate. Substituting this ansatz into (4.4), we find $\boldsymbol{v} = \tilde{f}(k)e^{\omega(k)}B\boldsymbol{v}$, where B is the non-backtracking matrix [14]. This is an

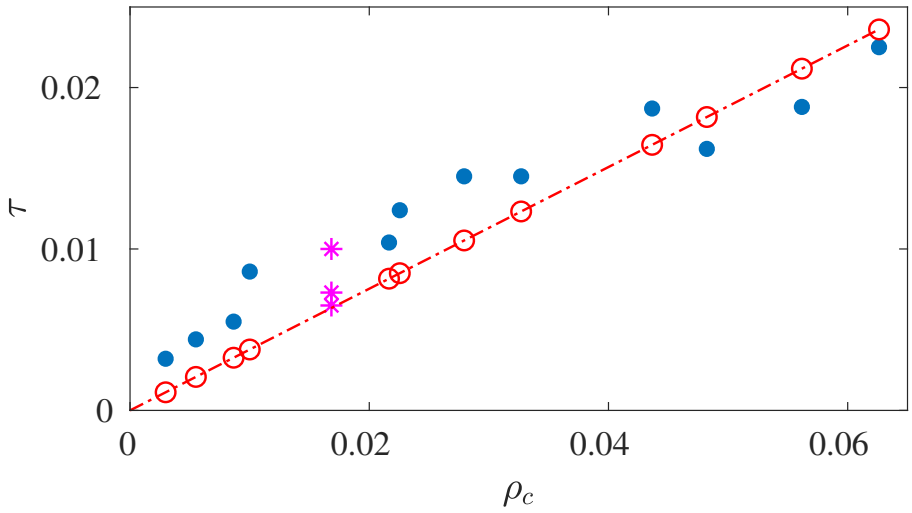

Figure 4-2: *Predicted and observed values of the spreading delay τ for a unit rate exponential infection spreading on a variety of social and communication networks with different percolation thresholds ρ_c. Predicted values (red circles) are calculated using Eq.* (4.6)*. Observed values (blue dots) show the average over 10^3 simulations with random source nodes. Stars show results for Watts-Strogatz random graphs on 10^4 nodes with degree 30 and rewiring probabilities of 0.1, 0.5 and 1. Full details of all simulations are given in the suplement.*

eigenvalue equation for B with a non-negative eigenvector $\boldsymbol{v}$; according to the Perron-Frobenius theorem, for a connected network there is a unique maximum eigenvalue λ, which is real and positive. Thus the growth rate is found as $\omega(k) = -\log(\lambda \tilde{f}(k))$. Note that $1/\lambda = \rho_c$ is the percolation threshold of the network [12, 15, 16].

Examining the inverse transform at time $t + n\tau$, one finds (full details are in the supplement) physically meaningful results in the limit of large n only when

$$\tau = \max_k \left\{ \frac{1}{k} \big(\log \rho_c - \log \tilde{f}(k) \big) \right\}. \tag{4.6}$$

This is our first main result, showing how the speed of spread is determined by the network via its percolation threshold ρ_c, and by the infection itself via the Laplace transform of its transmission time distribution. It is important to note that this result is derived from making a tree-like assumption for the underlying network, and our calculation holds in the limit of large distance from the source. In this sense it describes the fastest spreading regime; the mid-outbreak phase of exponential growth.

In practical applications, however, most networks of interest are not tree-like, and finite size effects mean the infection is unlikely to be able fully accelerate to the stable regime we have calculated. Nonetheless, our result still provides high-quality predictions. Fig. 4-2 demonstrates the effectiveness of this measure on a variety of real world networks from the Stanford Large Network Dataset Collection (SNAP) [22], many with heavy-tailed degree distributions and high clustering; Table S.I in the suplement gives full details. To further test the reliance of our method on the tree-like assumption

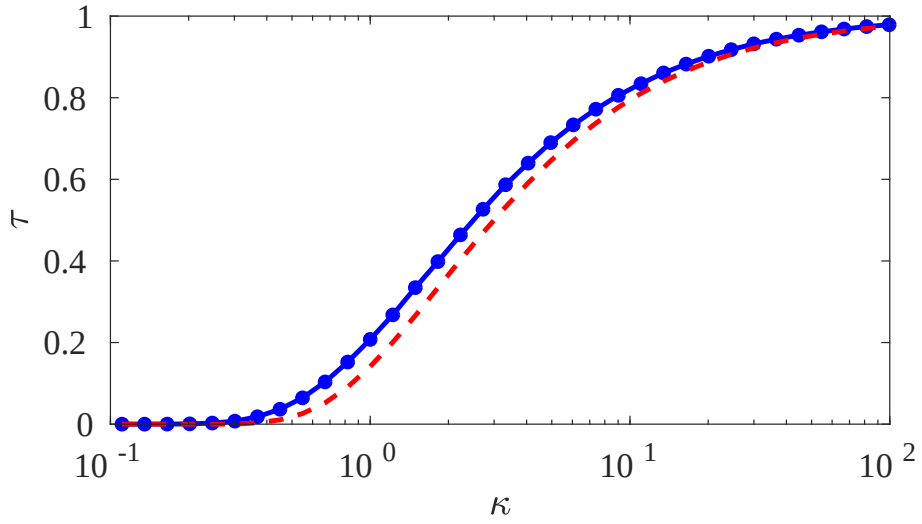

Figure 4-3: *Simulated (blue marked line) and predicted (red dashed line) spreading delay τ for infections with Weibull delay times with varying shape parameter κ and fixed mean 1 (example delay distributions shown in insets). Simulations follow the same method as Fig. 4-2, averaged over 100 samples on an Erdős-Rényi graph of 10^4 nodes and mean degree 3.*

made in writing (4.2), we have simulated spreading processes in Watts-Strogatz random graphs with varying rewiring probabilities. Included in Fig. 4-2, the results for these networks show that our method performs better for higher rewiring probability, but is still very successful for highly clustered networks with low rewiring.

As well as the network, our measure of speed also depends on properties of the infection. One might expect the time delay τ to be scaled by the mean delay time, but beyond this it is difficult to discern from (4.6) how the shape of the distribution should affect the global speed of spread. To explore this aspect we show in Fig. 4-3 the observed and predicted spreading speed for Weibull distributed delays, interpolating between heavy-tailed and Dirac distributed. Crucially, we find that the shape of the distribution of transmission time has a substantial effect on the speed of spread in a network. If there is mass near zero then delays are minimal due to the presence of extremely fast transmission routes. Conversely, if transmission time is close to deterministic then spreading is determined entirely by graph distance, meaning $\tau \approx 1$. In the supplement we prove that τ is always less than the mean delay time, with equality only for Dirac-delta distributions.

The time taken to receive the infection

As well as predicting the overall spreading speed, our approach also allows us to rank nodes in the network by their expected time to become infected. Write Δ_{ij} for the offset in infection time between nodes i and j, which for large n should satisfy $F_i^n(n\tau) = F_j^n(n\tau + \Delta_{ij})$. Inverting the transform in Eq. (4.5) for large n by steepest descent and

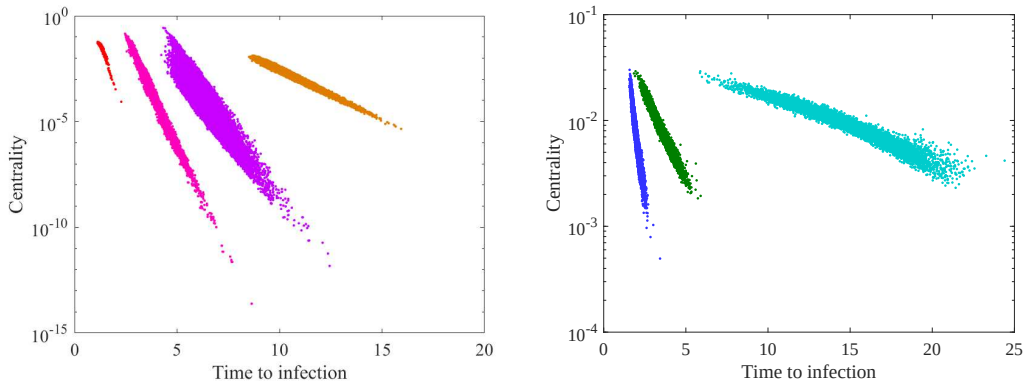

Figure 4-4: *Non-backtracking centrality predicts time to infection. Left: scatter plot of centrality and average arrival time for nodes in a selection of networks using a contagion with Weibull ($\kappa = 10$) infection times. Right: results for simulations of complex contagions with threshold θ in an Erdős-Rényi graph with 10^4 nodes and mean degree 6. Key: (a) an inter-personal contact network in an American high school [23], (b) 'Epinions' social media, (c) 'Deezer' Romanian social network [24], (d) an Erdős-Rényi graph with $N = 10^5$ nodes, (e) $\theta = 1$, (f) $\theta = 2$, (g) $\theta = 3$.*

	Exponential			**Weibull** ($\kappa = 10$)	
Network name	**Simple**	**2-core**	**3-core**	**Simple**	**2-core**
Erdős-Rényi	-0.9487	-0.9693	-0.9502	-0.9721	-0.9691
Epinions [25]	-0.8765	-0.7769	-0.7428	-0.9946	-0.8661
Deezer Croatia [24]	-0.8265	-0.8094	-0.8088	-0.9049	-0.8697
Facebook Artists [24]	-0.7943	-0.7481	-0.7322	-0.9586	-0.8778
Arxiv Cond. Mat.[26]	-0.8712	-0.7999	-0.7939	-0.9513	-0.8296
Facebook Companies [24]	-0.8439	-0.7203	-0.6685	-0.9138	-0.7606
School contact [23]	-0.7667	-0.7532	-0.7199	-0.9661	-0.9371

Table 4.1: *Correlation coefficient between contagion arrival time (measured from 10^3 simulated spreading processes with random sources) and the logarithm of non-backtracking centrality, for various networks. Values close to the theoretical limit -1 correlation imply strong prediction quality.*

comparing with the above (details in the supplement) we find that

$$\Delta_{ij} = \frac{1}{k^\star} \log\left(\frac{c_i}{c_j}\right) + \mathcal{O}(1/n)\,, \tag{4.7}$$

where $k^\star = \text{argmax}_k\{\omega(k)/k\}$ and $c_i = \sum_{j\in\partial i} v_{i\to j}$ is the non-backtracking centrality of node i. This log-linear relationship is demonstrated numerically in Fig. 4-4 for nodes in a selection of networks from SNAP. This result is important as it resolves the open question of exactly how network centrality measures may be used to estimate epidemic arrival time, and provides a robust theoretical justification for the use of non-backtracking centrality (see supplement for a comparison to other centrality measures).

Going further, many realistic models of network contagion require the number of infected neighbours of a node to reach some threshold $\theta \geq 1$ before the infection is

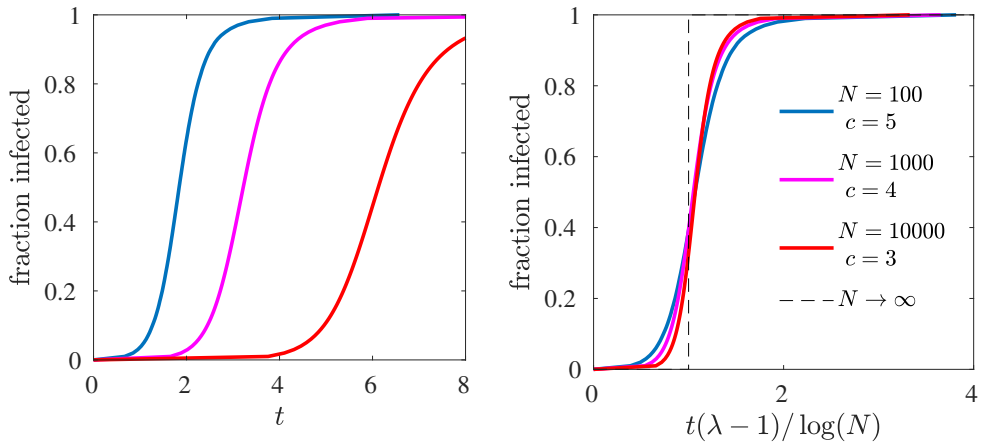

Figure 4-5: *Fractional size of the cluster of infected node as a function of time in various Erdős-Rényi graphs of different sizes N and mean degree c, averaged over 100 simulations from random seed nodes, with standard exponential infection times. The left panel shows real time, the right has rescaled time showing convergence to a step function in the limit $N \to \infty$ implying 'instantaneous' spread to the bulk of the network.*

passed on. In the supplement, we show how a variation of our theoretical formalism extends to these complex contagion models by considering the θ-shortest temporal paths from a node. Remarkably, the log-linear relationship derived above continues to hold in this more complex setting, as illustrated in Fig. 4-4. In addition to this visual demonstration, we present in Table 4.1 the Pearson correlation coefficients between log-non-backtracking centrality and infection arrival time for various disease dynamics in various networks. These results show that our theory, which is physically justified and cheap to compute, provides excellent predictions of the relative delay between nodes in a wide variety of spreading processes.

Since the non-backtracking centrality of a node is mainly a property of its local environment, the result (4.7) means that we should expect the vast majority infections to occur during a time window whose duration is independent of the total size of the network. However, it can be shown that in a network of size N the time needed for an infection to take hold grows like $\log(N)/(\lambda-1)$. Taken together these results imply that, on the timescale of the spreading contagion in a large network, one will observe an almost instantaneous jump between a vanishing fraction of nodes infected to almost complete infection. We illustrate this result in Fig. 4-5 for Erdős-Rényi graphs of increasing size, and provide precise theoretical derivations in the supplement, where we show that this property holds for models of temporal percolation in both sparse and dense networks.

Discussion

We have presented here a theoretical framework for determining the speed of contagion processes in large networks. Analysing the spreading front of contagion probability we derived Eq (4.6), showing how network topology and infection dynamics affect speed

via, respectively, the network percolation threshold and the Laplace transform of the transmission time law. Our theory also reveals in Eq. (4.7) a surprisingly simple relationship between contagion arrival times and the non-backtracking centrality of nodes. Finally, we have observed that these results imply that spreading process in large networks undergo an almost instantaneous expansion in their reach when time is properly scaled.

The setting for our theoretical derivation has been that of simple epidemics spreading on large tree-like networks. However, we have shown that the key results hold remarkably well for a broad class of networks, including those with high clustering, and for contagion models including non-Markov dynamics and complex threshold models. Further development of rigorous mathematical results for these models is a challenging problem worthy of considerable future efforts. Excitingly, our results suggest possible routes for the development of monitoring and intervention protocols for real-world contagions using message-passing methods. Progress in this direction may require the consideration of even more detailed models including temporally varying and multilayered networks; both promising avenues for future research.

REFERENCES

[1] C. McEvedy, "The bubonic plague," *Scientific American*, vol. 258, no. 2, pp. 118–123, 1988.

[2] K. Zinszer, K. Morrison, J. S. Brownstein, F. Marinho, S. F. Alexandre, and E. O. Nsoesie, "Zika virus speed and direction: reconstructing zika introduction in brazil," *Online journal of public health informatics*, vol. 9, no. 1, 2017.

[3] S. Vosoughi, D. Roy, and S. Aral, "The spread of true and false news online," *Science*, vol. 359, no. 6380, pp. 1146–1151, 2018.

[4] M. J. Keeling and K. T. Eames, "Networks and epidemic models," *Journal of the Royal Society Interface*, vol. 2, no. 4, pp. 295–307, 2005.

[5] L. Danon, A. P. Ford, T. House, C. P. Jewell, M. J. Keeling, G. O. Roberts, J. V. Ross, and M. C. Vernon, "Networks and the epidemiology of infectious disease," *Interdisciplinary perspectives on infectious diseases*, vol. 2011, 2011.

[6] R. Pastor-Satorras, C. Castellano, P. V. Mieghem, and A. Vespignani, "Epidemic Processes in Complex Networks," *Rev. Mod. Phys.*, vol. 87, pp. 925 – 979, 2015.

[7] W. Van den Broeck, C. Gioannini, B. Gonçalves, M. Quaggiotto, V. Colizza, and A. Vespignani, "The gleamviz computational tool, a publicly available software to explore realistic epidemic spreading scenarios at the global scale," *BMC infectious diseases*, vol. 11, no. 1, p. 37, 2011.

[8] A. Gautreau, A. Barrat, and M. Barthelemy, "Global disease spread: statistics and estimation of arrival times," *Journal of theoretical biology*, vol. 251, no. 3, pp. 509–522, 2008.

[9] A. Gautreau, A. Barrat, and M. Barthélemy, "Arrival time statistics in global disease spread," *Journal of Statistical Mechanics: Theory and Experiment*, vol. 2007, no. 09, p. L09001, 2007.

[10] S. P. Borgatti, "Centrality and network flow," *Social networks*, vol. 27, no. 1, pp. 55–71, 2005.

[11] B. Karrer and M. E. Newman, "Message passing approach for general epidemic models," *Physical Review E*, vol. 82, no. 1, p. 016101, 2010.

[12] K. E. Hamilton and L. P. Pryadko, "Tight lower bound for percolation threshold on an infinite graph," *Phys. Rev. Lett.*, vol. 113, p. 208701, 2014.

[13] B. Karrer, M. E. J. Newman, and L. Zdeborová, "Percolation on sparse networks," *Phys. Rev. Lett.*, vol. 113, p. 208702, 2014.

[14] T. Martin, X. Zhang, and M. E. Newman, "Localization and centrality in networks," *Physical review E*, vol. 90, no. 5, p. 052808, 2014.

[15] T. Rogers, "Assessing node risk and vulnerability in epidemics on networks," *EPL (Europhysics Letters)*, vol. 109, no. 2, p. 28005, 2015.

[16] R. Kühn and T. Rogers, "Heterogeneous micro-structure of percolation in sparse networks," *EPL (Europhysics Letters)*, vol. 118, no. 6, p. 68003, 2017.

[17] K. Gough, "The estimation of latent and infectious periods," *Biometrika*, vol. 64, no. 3, pp. 559–565, 1977.

[18] D. Anderson and R. Watson, "On the spread of a disease with gamma distributed latent and infectious periods," *Biometrika*, vol. 67, no. 1, pp. 191–198, 1980.

[19] A. L. Lloyd, "Realistic distributions of infectious periods in epidemic models: changing patterns of persistence and dynamics," *Theoretical population biology*, vol. 60, no. 1, pp. 59–71, 2001.

[20] M. Eichner and K. Dietz, "Transmission potential of smallpox: estimates based on detailed data from an outbreak," *American Journal of Epidemiology*, vol. 158, no. 2, pp. 110–117, 2003.

[21] W. Van Saarloos, "Front propagation into unstable states," *Physics reports*, vol. 386, no. 2-6, pp. 29–222, 2003.

[22] J. Leskovec and A. Krevl, "SNAP Datasets: Stanford large network dataset collection." `http://snap.stanford.edu/data`, June 2014.

[23] M. Salathé, M. Kazandjieva, J. W. Lee, P. Levis, M. W. Feldman, and J. H. Jones, "A high-resolution human contact network for infectious disease transmission," *Proceedings of the National Academy of Sciences*, vol. 107, no. 51, pp. 22020–22025, 2010.

[24] B. Rozemberczki, R. Davies, R. Sarkar, and C. Sutton, "Gemsec: graph embedding with self clustering," *arXiv preprint arXiv:1802.03997*, 2018.

[25] M. Richardson, R. Agrawal, and P. Domingos, "Trust management for the semantic web," in *International semantic Web conference*, pp. 351–368, Springer, 2003.

[26] J. Leskovec, J. Kleinberg, and C. Faloutsos, "Graph evolution: Densification and shrinking diameters," *ACM Transactions on Knowledge Discovery from Data (TKDD)*, vol. 1, no. 1, p. 2, 2007.

Supplemental Material: Predicting the speed of epidemics spreading on networks

In this supplemental material we provide additional details for the calculation of the asymptotic infection time delay, τ, the maximum of this value in terms of infection distribution, and the offset in infection arrival time, δ.

We show how the simple dynamics considered in our construction are still relevant when considering more complex infection dynamics and show infection time ranking using the non-backtracking centrality measure performs better than other such measures.

We also give full details of the calculation of time rescaling for configuration model networks and dense graphs, revealing the explosive transition for the fraction of infected nodes as a function of rescaled time.

Finally, we provide additional supporting figures and a table of the data used to demonstrate the effectiveness of our approach in a variety of real networks.

Calculation of time delay

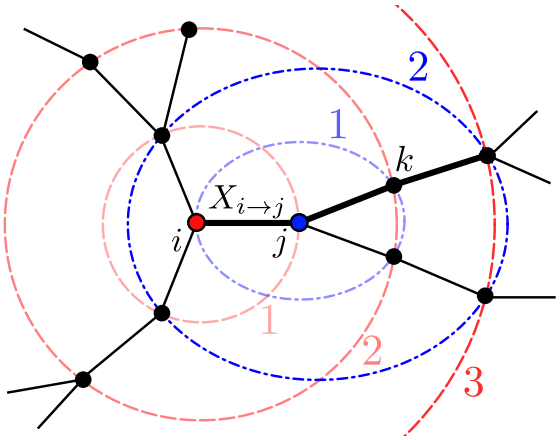

Figure 4-6: *The shortest temporal path (bold) from node i to reach distance n ($= 3$ here) going via j has length given by the delay $X_{i\to j}$, plus the minimum length of a path reaching distance $n-1$ from j that does not go via i.*

Recall that we write T_i^n for the shortest (temporal) path to a node at distance n from i, and $T_{i\to j}^n$ for the shortest such path whose first step is to node j. As illustrated in Fig. 4-6, we can decompse these quantities as follows:

$$T_i^n = \min_{j\in\partial i} T_{i\to j}^n\,, \quad T_{i\to j}^n = X_{i\to j} + \min_{k\in\partial j\setminus i} T_{j\to k}^{n-1}\,, \tag{4.1}$$

where ∂i denotes the set of neighbours of i. Writing $F_{i\to j}^n(t)$ for the cumulative distribution function of $T_{i\to j}^n$, Eq. (4.1) implies the message passing equation

$$F_{i\to j}^n(t) = \int_0^t f(x)\left[1 - \prod_{k\in\partial j\setminus i}\Big(1 - F_{j\to k}^{n-1}(t-x)\Big)\right]\mathrm{d}x\,. \tag{4.2}$$

For $t \ll n\tau$, we linearize (4.2) to obtain

$$F_{i\to j}^n(t) \approx \int_0^t f(x)\sum_{k\in\partial j\setminus i} F_{j\to k}^{n-1}(t-x)\,\mathrm{d}x\,. \tag{4.3}$$

The two sided Laplace transform of Eq. (4.3) reads

$$\tilde{F}_{i\to j}^n(k) = \tilde{f}(k)\sum_{k\in\partial j\setminus i}\tilde{F}_{j\to k}^{n-1}(k)\,, \tag{4.4}$$

where $\tilde{f}(k) = \int e^{-kx}f(x)\mathrm{d}x$ is the Laplace transform of f. For large n we can expect

$$\tilde{F}_{i\to j}^n(k) \propto v_{i\to j}\, e^{-\omega(k)n}. \tag{4.5}$$

Here v is identified as the top eigenvector of the non-backtracking matrix B with entries

$$B_{i\to j,k\to\ell} = \begin{cases} 1 & \text{if } k = j \text{ and } \ell \neq i \\ 0 & \text{else.} \end{cases} \tag{4.6}$$

Using the ansatz (4.5), the inverse transform reads

$$F_{i\to j}^n(t) = \frac{v_{i\to j}}{2\pi\mathrm{i}}\int_{c-i\infty}^{c+i\infty}\varphi(k)e^{kt-\omega(k)n}\,\mathrm{d}k\,, \tag{4.7}$$

where c is chosen freely in the region of convergence of $\tilde{F}_{i\to j}^n$.

To have convergence of time delay to a constant τ, setting $t = t + n\tau$ to get

$$F_{i\to j}^n(t+n\tau) = \frac{v_{i\to j}}{2\pi\mathrm{i}}\int_{c-i\infty}^{c+i\infty}\varphi(k)e^{kt-(\omega(k)-\tau k)n}\,\mathrm{d}k\,, \tag{4.8}$$

we should expect not to see either exponential growth or decay in F. Now for large n the integral (4.8) will be dominated by the saddlepoint $k^\star = c+iz^\star$. So then the requirement for F exhibiting neither exponential growth nor decay means that the modulus of the

exponential factor in (4.8) must vanish at this point.

That is for $k^\star$ such that

$$\left.\frac{\mathrm{d}(\omega(k)-\tau k)}{\mathrm{d}k}\right|_{k^\star} = 0 \tag{4.9}$$

then we require that

$$\Re[\omega(k^\star)] - \tau c = 0\,. \tag{4.10}$$

Combining these we get

$$\tau = \omega'(k^\star) = \frac{\Re[\omega(k^\star)]}{c}\,, \tag{4.11}$$

implying $\Im[\omega'(k^\star)] = 0$. Further since

$$\omega'(k^\star) = \frac{\Re[\omega(k^\star)]}{c} \iff \left.\frac{\mathrm{d}(\omega(k)/k)}{\mathrm{d}k}\right|_{k^\star} = 0 \tag{4.12}$$

then the possible $k^\star$ are the stationary points of $\frac{\omega(k)}{k}$ with τ the value at these points. Hence choosing $k^\star$ to maximize τ finds the asymptotic time delay we are seeking.

An upper bound on delay time

We claim that $\tau \leq \mathbb{E}X$ where $X \sim f$, the random variable for transmission time. The proof of this follows from considering our expression for $\tau = \min_k \left[\frac{-\log(\lambda\tilde{f}(k))}{k}\right]$. The Laplace transform of f is

$$\tilde{f}(k) = \mathbb{E}(e^{-kX}) \text{ where } X \sim f\,, \tag{4.13}$$

then by Jensen's inequality, since e^{-x} is convex,

$$\mathbb{E}(e^{-kX}) \geq e^{-k\mathbb{E}(X)} \tag{4.14}$$

with equality if f is the Dirac delta distribution. Then

$$-\frac{1}{k}\log(\lambda\tilde{f}(k)) \leq -\frac{1}{k}\log(\lambda e^{-k\mathbb{E}(X)}) = \mathbb{E}(X) - \frac{1}{k}\log(\lambda) \tag{4.15}$$

and

$$\tau \leq \max_k \left[\mathbb{E}(X) - \frac{1}{k}\log(\lambda)\right] = \mathbb{E}(X) \tag{4.16}$$

which is attained for Dirac delta f. Therefore, as noted in the main text, we expect time delay to be minimal for heavy tailed f and maximal, going to $\mathbb{E}(X)$, for Dirac

delta f.

Infection time offset

To quantify the heterogeneity in infection recieval we take advantage of the symmetry of the infection process to write

$$F_i^n(n\tau) = F_j^n(n\tau + \Delta_{ij})\,. \tag{4.17}$$

Thus an approximation of the offset, Δ, may be found by first approximating the c.d.f

$$F_i^n(t) = 1 - \prod_{j\in\partial i}\left(1 - F_{i\to j}^n(t)\right)\,. \tag{4.18}$$

Now using (4.9) and (4.10) it follows that

$$\omega(k) - \tau(k) \approx (\Im[\omega(k^\star)] - \tau z^\star)i - \frac{1}{2}\omega''(k^\star)(k-k^\star)^2 \tag{4.19}$$

and thus taking $\Delta k = k - k^\star$ equation (4.8) gives us that

$$F_{i\to j}^n(t+n\tau) \approx \frac{v_{i\to j}}{2\pi i}\int_{c-i\infty}^{c+i\infty}\varphi(k)e^{\phi}\,\mathrm{d}k \tag{4.20}$$

where

$$\phi = (k^\star + \Delta k)t - (\Im[\omega(k^\star)] - \tau z^\star)in - \frac{1}{2}\omega''(k^\star)\Delta k^2 n\,. \tag{4.21}$$

Further taking $\frac{1}{2}\omega''(k^\star) = D$, then

$$F_{i\to j}^n(t+n\tau) \approx \frac{v_{i\to j}}{2\pi i}e^{-(\Im[\omega(k^\star)]-\tau z^\star)in + k^\star t}\int_{c-i\infty}^{c+i\infty}\varphi(k)e^{-Dn(\Delta k - \frac{t}{2Dn})^2 + \frac{t^2}{4Dn}}\,\mathrm{d}k\,. \tag{4.22}$$

As n becomes large then the integrand becomes dominated by the contribution at $k^\star$ and we may approximate to a Gaussian integral to find

$$F_{i\to j}^n(t+n\tau) \underset{n\to\infty}{\approx} -\frac{v_{i\to j}\varphi(k^\star)}{2\sqrt{\pi Dn}}e^{-(\Im[\omega(k^\star)]-\tau z^\star)in + k^\star t + \frac{t^2}{4Dn}} \tag{4.23}$$

Going back to equation (4.1) we then have, for $t \ll n\tau$,

$$\begin{aligned} F_i^n(n\tau) =& 1 - \prod_{j\in\partial i}\left(1 - F_{i\to j}^n(n\tau)\right) \approx \sum_{j\in\partial i}\left(F_{i\to j}^n(n\tau)\right) \\ \approx& -\frac{\varphi(k^\star)}{2\sqrt{\pi Dn}}e^{-(\Im[\omega(k^\star)]-\tau z^\star)in}\sum_{j\in\partial i}v_{i\to j}\,. \end{aligned} \tag{4.24}$$

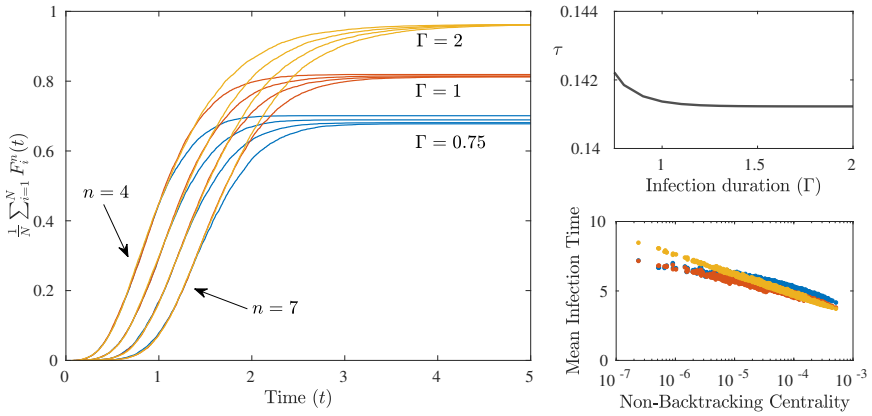

Figure 4-7: *Spreading speed of the SIR model with fixed infectious period* Γ *and unit rate (i.e.* $\beta = 1$*) infection. Left: simulation results on the cumulative distribution function of time to reach a given distance* n*, averaged over all starting points, for different durations of infection. The uncertain transmission affects the final fraction of contagions reaching a given distance, but does not appreciably affect the speed. Right upper: analytical calculation of the delay* τ *as a function of* Γ*, showing very little variation. Right lower: scatter plots of the correlation between node non-backtracking centrality and mean time to infection (excluding contagions that do not reach the node). We used an Erdős-Rényi random graph of* $N = 10^4$ *and mean degree* $c = 3$*.*

Thus, substituting this approximation into (4.17) and solving gives

$$\Delta_{ij} = \frac{1}{k^\star} \log\left(\frac{c_i}{c_j}\right) + \mathcal{O}(1/n)\,, \tag{4.25}$$

where $k^\star = \text{argmax}_k \omega(k)/k$ and $c_i = \sum_{j\in\partial i} v_{i\to j}$ is the non-backtracking centrality of node i

Different disease dynamics.

It is straightforward to adapt our set-up to include SIR models by adding a time R_i to recovery, so that transmission from i to j only occurs if $X_{i\to j} < R_i$. This presents the interesting complication that there is generally a difference between the time to transmit an infection up to a certain distance from a source, versus the time to recieve an infection that starts a certain distance away. This effect was explored in detail in [1]. However, for the asymptotic study of the fastest infection routes (obtained by considering the linearisation of the message passing equations), this distinction is not important. Similarly, SIS and SIRS dynamics do not behave substantially differently in this regard, since only the fastest passage time is relevant, not the subsequent recovery and reinfection dynamics.

In general, uncertain transmission is incorporated to our settting simply by allowing $X_{i\to j} = \infty$ with some probability, so that $\int_0^\infty f(x)\mathrm{d}x = \rho < 1$. Here ρ corresponds to the edge occupation probability in the bond percolation model induced by the epidemic [2]. In Figure 4-7 we show example results for the SIR model in which individuals remain

infected for a fixed duration Γ, during which they infect their neighbours at constant rate β. For this example, the transmission time density function is $f(x) = \beta e^{-\beta x}\mathbb{I}_{x<\Gamma}$. The corresponding edge occupation probability is $\rho = 1-e^{-\beta\Gamma}$ and Laplace transformed density is $\tilde{f}(k) = \frac{\beta}{\beta+k}(1 - e^{-(k+\beta)\Gamma})$. As expected, varying the infectious period Γ has almost no effect on the speed of propagation of the contagion, which is determined by the fastest transmission route and hence unaffected if slower routes are trimmed.

More interestingly, many popular models of contagion on networks require the number of infected neighbours of a node to reach some threshold $\theta \geq 1$ before the infection is passed on. Our formalism extends to these complex contagion models by considering the θ-shortest temporal paths from a node to the bulk of the network.

Specifically, the time that node i becomes infected in a complex contagion on a large network with threshold θ maps to the large n limit of T_i^n defined by

$$T_i^n = \theta\text{-min}\{\, T_{i\to j}^n \,|\, j \in \partial i\}\,, \tag{4.26}$$

where "θ-min" denotes the θ-smallest element of the specified set, and

$$T_{i\to j}^n = X_{i\to j} + \theta\text{-min}\{T_{j\to k}^{n-1} \,|\, k \in \partial j \setminus i\}\,. \tag{4.27}$$

As detailed in [3], the corresponding equations for the cumulative density functions are

$$F_{i\to j}(t) = \int_0^t f(x)\left[1 - \sum_{\substack{M\subseteq\partial j\setminus i\\ |M|<\theta}} \prod_{k\notin M}(1 - F_{j\to k}(t-x)) \prod_{m\in M} F_{j\to m}(t-x)\right] \mathrm{d}x\,. \tag{4.28}$$

Note that the special case $\theta = 1$ corresponds to the simple contagion model previously considered, and indeed the inner sum in Eq. (4.28) contains only the element $M = \emptyset$, and hence reduces to Eq. (2).

Our strategy for analysis in the $\theta = 1$ case was to consider the left tails of F, in which the recursion equation can be linearised. The simple physical intuition for this linear theory is that for a node to receive the infection unusually early, it is only necessary (and indeed likely) for one neighbour to be infected. Unfortunately, for the case of $\theta \geq 2$, such a linear theory is not possible as early infection of a node requires θ of its neigbours to be infected early. Mathematically, this rule is manifested in the fact that the small F expansion of the right hand side of (4.28) has order θ.

An alternative approach is to consider the recursion map $\mathcal{G}$ defined by the action

$$\mathcal{G}[\boldsymbol{F}^n](t) = \boldsymbol{F}^{n+1}(t-\tau)\,, \tag{4.29}$$

that is, $\mathcal{G}$ maps the collection of functions $\{F_{i\to j}^n\}$ to their updated versions according to equation (4.28), offest by the (as yet unknown) spreading delay τ. In the limit of

many applications of $\mathcal{G}$ we have convergence

$$\mathcal{G}^n[\boldsymbol{F}] \overset{n\to\infty}{\longrightarrow} \boldsymbol{F}^\star\,, \tag{4.30}$$

where $\boldsymbol{F}^\star$ is a non-trival limiting profile function (i.e. not identically one or zero). Let us consider the asymptotic stability of $\mathcal{G}$ around $\boldsymbol{F}^\star$. Let e be a directed edge in the network, then

$$\begin{aligned}\frac{\partial \mathcal{G}[\boldsymbol{F}]_e(t)}{\partial F_{e'}(t')} &= -\int_0^{t-\tau} f(x) \sum_{\substack{E\subseteq\partial e\\ |E|<\theta}} \frac{\partial}{\partial F_{e'}(t')}\left[\prod_{e''\notin E}\left(1-F_{e''}(t-\tau-x)\right)\prod_{e''\in E}F_{e''}(t-\tau-x)\right]\mathrm{d}x\\
&= -H_{e,e'} f(t-t'-\tau) \sum_{\substack{E\subseteq\partial e\\ |E|<\theta\,, e'\in E}}\left[\prod_{e''\notin E}\left(1-F_{e''}(t')\right)\prod_{e''\in E\setminus e'}F_{e''}(t')\right]\\
&\quad + H_{e,e'} f(t-t'-\tau) \sum_{\substack{E\subseteq\partial e\\ |E|<\theta\,, e'\notin E}}\left[\prod_{e''\in\partial e\setminus E\setminus e'}\left(1-F_{e''}(t')\right)\prod_{e''\in E}F_{e''}(t')\right]\end{aligned} \tag{4.31}$$

Hence the Jacobian of $\mathcal{G}$ in the neighbourhood of the limit $\boldsymbol{F}^\star$ can be written

$$\mathcal{J}_{e,e'}(t,t') = \frac{\partial \mathcal{G}[\boldsymbol{F}]_e(t)}{\partial F_{e'}(t')}\Big|_{\boldsymbol{F}=\boldsymbol{F}^\star} = H_{e,e'} f(t-t'-\tau)\Sigma_{e,e'}(t')\,, \tag{4.32}$$

where

$$\Sigma_{e,e'}(t') = \sum_{\substack{E\subseteq\partial e\\ |E|<\theta}}\left(\frac{\prod_{e''\in\partial e\setminus E}\left(1-F^\star_{e''}(t')\right)\prod_{e''\in E}F^\star_{e''}(t')}{\left(1-F^\star_{e'}(t')\right)\mathbb{I}_{e'\notin E} - F^\star_{e'}(t')\mathbb{I}_{e'\in E}}\right)\,. \tag{4.33}$$

In the case of simple contagion processes, we have $\Sigma_{e,e'}(t') \approx 1$ for large t'. This leads to the simplified expression $\mathcal{J} = H\otimes\mathcal{F}$, where $\mathcal{F}$ is the integral operator

$$\mathcal{F}[g](t) = \int_0^{t-\tau} f(t-t'-\tau)g(t')\,\mathrm{d}t'\,. \tag{4.34}$$

This operator is made diagonal by a Laplace transform, and hence the eigenfunctions of $\mathcal{J}$ are therefore of exactly the form (4.2) found previously. In particular, the presence of the Hashimoto matrix H in (4.32) implies a contribution proportional to $v_{i\to j}$ as a prefactor to the limiting form of $F_{i\to j}$. Note that although this analysis goes via the simplification found at large t', both the delay τ and the prefactors $v_{i\to j}$ are the same across the whole time range.

For complex contagions with thresholds $\theta \geq 2$, we have $\Sigma_{e,e'}(t') \approx 0$ for large t', which rules out direct use of the linear analysis outlined above. However, progress can be made with the heuristic $\Sigma_{e,e'}(t') \approx \sigma$, where $\sigma \in \mathbb{R}^+$ depends on θ, but not the edge in question or the delay time distribution. Essentially, the constant σ captures the

(multiplicative) additional "difficulty" for the contagion to spread with higher thresholds. This approximation implies a modification of the timescales obtained in the linear theory, but does not alter the dependence on the network, and hence the relative time to infection is again proportional to the logarithm of the non-backtracking centrality. Figure 4 in the main text supports this claim with numerical evidence. Computing the delay τ requires the determination of the precise form of σ. This appears far more challenging and we leave it for future work.

Other centrality measures

Many different node centrality measures have been proposed in the networks literature, and the weights they ascribe to different nodes are more or less correlated with one another depending on the metrics in question. In Figure 4-8 we show a comparison between the contagion arival time (as accurately predicted by the non-backtracking centrality) and five other well-known centrality measures. Betweenness centrality, degree centrality and PageRank all show signficant spread of contagion arrival times relavite to centrality score and hence are not useful predictors of, for exmaple, epidemic risk.

Closeness centrality is based on the mean distance between nodes in a network, corresponding presicely to the mean contagion arrival time in the limit of Dirac-delta distributed transmission times. Unsurprisingly, this metric shows a strong corelation with epidemic arrival when presented in the logarithmic scale which we have shown to be the correct. We should emphasise three points of advantage our results have over the heuristic use of closeness centrality. First, our theoretical derivations have shown (log) non-backtracking centrality is the correct measure. Second, our analytical results apply to a broad range of infection time distributions. Third, non-backtracking centrality is significantly faster to compute than closeness centrality.

In the simple test presented in Figure 4-8, the logarithm of eigenvector centrality also appears to make a usable prediction of the infection arrival time. It is well-known, however, that eigenvector centrality can become localized in networks containing high-degree "hub" nodes [4]. We illustrate this problem in Figure 4-9, showing how eigenvector centrality is distorted by the presence a hub node; the striations visible in the left panel correspond to distance from the hub node, which is given undue prominance in eigenvector centrality. Non-backtracking centrality, by contrast, continues to perform well for this example.

Temporal percolation

While the shape of the infection size curve may be described by the non-backtracking centrality distribution of the nodes, one can predict the time at which the bulk of the outbreak occurs by considering the following simple heuristic for unit rate infections. The time needed for an infected cluster of size m to grow by one node scales as $1/E_m$

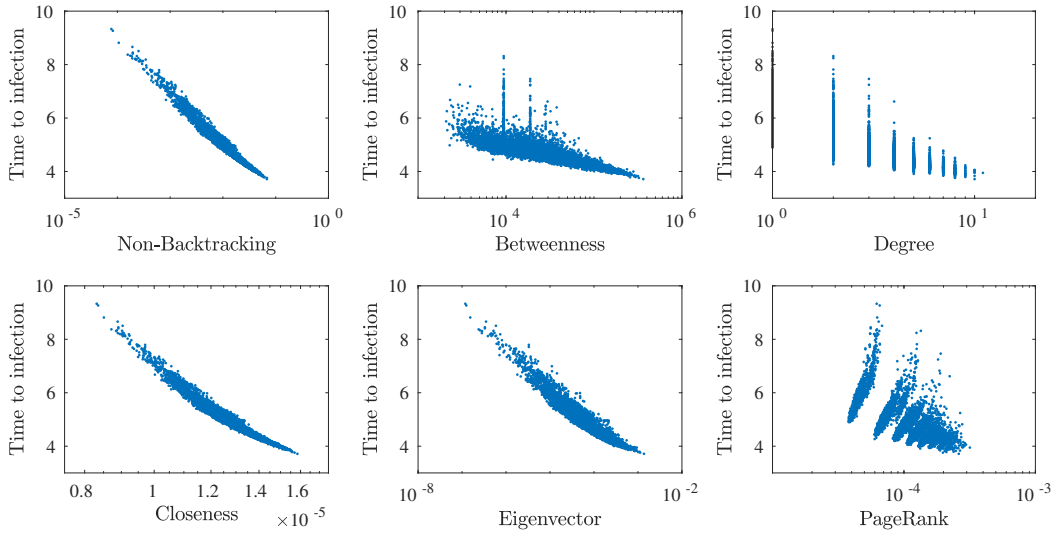

Figure 4-8: *Comparison between contagion arival time and (log) centrality of nodes under various metrics. The network used was an Erdő-Rényi random graph on $N = 10^4$ nodes with mean degree 3; contagion simulations were averaged over 1000 samples, with exponentially distributed transmission times.*

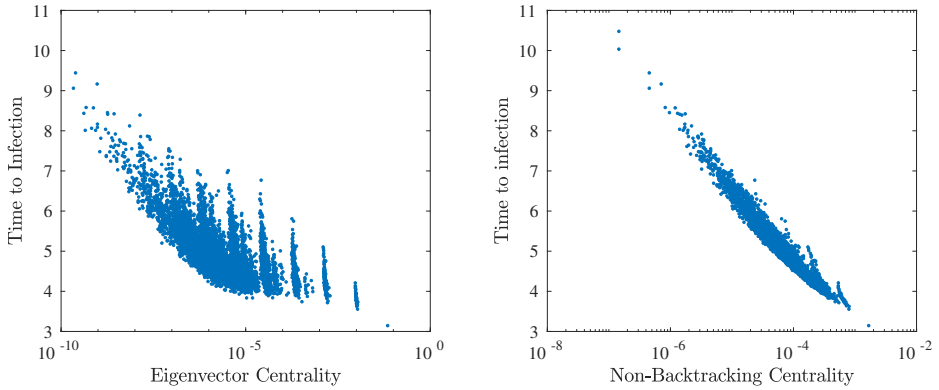

Figure 4-9: *Comparison between non-backtracking centrality and eigenvector centrality in predciting infection arival time in the presence of a hub. The network used was an Erdő-Rényi random graph on $N = 10^4$ nodes with mean degree 3, with the addition of a single "hub" node connected to 50 randomly selected other nodes. Contagion simulations were averaged over 1000 samples, with exponentially distributed transmission times.*

where E_m is the number of edges leaving the cluster. During the exponential growth phase, addition of a node to the cluster will cause the loss of one external edge (used for transmission) and an average gain of λ additional edges from the neighbours of the new node. Therefore $E_{m+1} = E_m + \lambda - 1$, and we thus find that the time needed to infect a fraction β of all nodes grows like $\log(N)/(\lambda - 1)$. This implies that rescaling time by $t' = t(\lambda - 1/\log(N)$ should collapse the curves for different large networks, as shown in Fig. 5 of the main text. Moreover, the transition between $\beta = 0$ and $\beta = 1$ becomes sharp at $t' = 1$ in the limit of large network size.

This explosive transition is, in fact, a general property of time-ordered percolation. In the supplement we show how the above reasoning can be made precise for sparse configuation-model networks with finite second moments, corresponding to graphs with non-zero percolation thresholds. Additionally, we study temporal percolation on dense graphs with a fraction q of all possible edges present, showing that the same result holds under the rescaling $t' = tqN/\log(N)$.

A sharp transition in sparse graphs

Write R_m for the time to reach m nodes. For exponential transmission times

$$\mathbb{E}[R_{m+1}] = \mathbb{E}[R_m] + \mathbb{E}\left[\frac{1}{O_m}\right], \tag{4.35}$$

where O_m is the number of outgoing edges from the cluster of m infected nodes. In a configuration model graph we can write

$$O_{m+1} = O_m + K_m - 1\,, \tag{4.36}$$

where K_m is the degree of the node added as the cluster grows from size m to $m+1$, and the -1 term corresponds to the edge used in transmission, that becomes internal to the cluster. This leads to the expression

$$O_m = K_0 + \sum_{i=1}^{m-1} K_i - (m-1)\,. \tag{4.37}$$

For a configuration model graph, K_0 is chosen according to the degree distribution and all subsequent K_i are chosen according to the branching distribution.

Introduce generating functions

$$g(x) = \mathbb{E}[z^{K_0}]\,, \quad \tilde{g}(z) = \mathbb{E}[z^{K_1}]\,, \quad \gamma_m(z) = \mathbb{E}[z^{O_m}]\,. \tag{4.38}$$

Now (4.37) implies

$$\gamma_m(z) = z^{-m} g(z)\tilde{g}(z)^{m-1}\,. \tag{4.39}$$

Asymptotically in large m we have

$$\gamma_m(z) \approx \frac{g(z)}{g'(z)} e^{m(1-z)(\lambda-1)}\,, \tag{4.40}$$

where we used the fact that $\tilde{g}'(1) = \lambda = 1/\rho_c$. It then follows that

$$\mathbb{E}\left[\frac{1}{O_m}\right] = \int_0^1 \gamma_n(z)dz \approx \frac{1}{m(\lambda-1)}\,, \tag{4.41}$$

and hence

$$\mathbb{E}[R_m] \approx \frac{\log(m)}{\lambda-1}\,. \tag{4.42}$$

A sharp transition in dense graphs

We show how the sharp transition in infected proportion is not a phenomenon exclusive to this setting but rather a characteristic of time dependent percolation in general by considering a dense network setting also.

Suppose we have for simplicity an infection spreading at exponential rate 1 on a dense network of size N and mean degree qN, starting from a single node. Taking $\mathbb{E}(R_m)$ to denote the expected time to reach m infections, it follows that the time for the number of infected to increase from m to $m+1$ will be given in the early stages by

$$\mathbb{E}(T_{n+1} - T_n) = \frac{1}{qn(N-n)} \tag{4.43}$$

and so $\mathbb{E}(R_m)$ is given, and bounded, by

$$\begin{aligned}\mathbb{E}(R_m) &= \sum_{\ell=1}^{m-1} \frac{1}{qN\ell - q\ell^2} \\ &> \sum_{\ell=1}^{m-1} \frac{1}{q(N-1)}\frac{1}{\ell} = \frac{1}{q(N-1)}\log(m)\end{aligned} \tag{4.44}$$

For an upper bound first notice that $\frac{1}{q\ell(N-\ell)}$ is decreasing with ℓ in the interval $(0, N/2]$ and so for $m \leq N/2$ the sum may be bounded by the integral, so

$$\begin{aligned}\mathbb{E}(R_m) &= \sum_{\ell=1}^{m-1} \frac{1}{q\ell(N-\ell)} < \frac{1}{qN} + \int_1^{m-1} \frac{1}{q\ell(N-\ell)}\,\mathrm{d}\ell \\ &< \frac{1}{qN}\left(1 + \log\left(\frac{(m-1)(N-1)}{N-(m-1)}\right)\right) \\ &< \frac{1}{qN}\left(1 + \log\left(\frac{Nm}{N-m}\right)\right)\end{aligned} \tag{4.45}$$

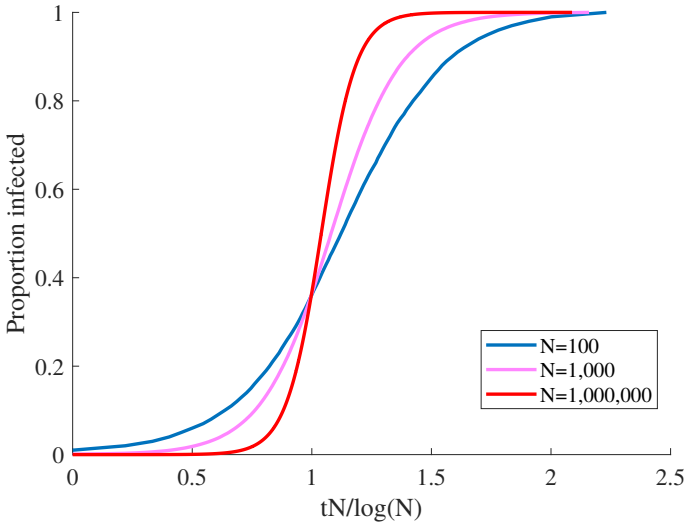

Figure 4-10: *Plot showing the proportion of infected vs time on complete graphs of varying size for an infection with exponential infection times as an average over 500 simulations from random seed nodes. Time is scaled by $N/\log(N)$ as per our calculation to show a progressively sharp transition at time 1.*

Similarly for $m > N/2$ a bound may be made by shifting the end points of the integral to get

$$\begin{aligned}\mathbb{E}(R_m) <& \frac{4}{qN^2} + \int_{N/2}^{m} \frac{1}{q\ell(N-\ell)}\,\mathrm{d}\ell \\ <& \frac{1}{qN}\left(1 + \log\left(\frac{Nm}{N-m}\right)\right)\end{aligned} \tag{4.46}$$

(note we are only interested in large N)

These bounds motivate introducing the rescaled variables

$$Q_\beta = \frac{qN}{\log(N)} T_{\lceil \beta N \rceil}\,, \quad \text{for } \beta \in (0,1)\,. \tag{4.47}$$

Then

$$1 + \frac{\log(\beta)}{\log(N)} < \mathbb{E}Q_\beta < 1 + \frac{\log(\beta)}{\log(N)} + \frac{1-\log(1-\beta)}{\log(N)}\,. \tag{4.48}$$

If we rescale time by $t' = qNt/(\log N)$ then, for large N, up to time $t' = 1$ almost nobody is infected and after time $t' = 1$ the infection reaches almost everyone.

Simulation details

For a given network $G = (V, E)$, the SI model is simulated as follows:

1. Choose a source node $s \in V$ uniformly at random
2. For each $i \in V$, compute the length of the shortest path from s to i, and store this as the distance d_i
3. For each ordered pair of neighboring vertices i and j generate a random delay $X_{i,j}$, chosen from the distribution with pdf f
4. For each $i \in V$, compute the minimum weight w_i of a path from s to i in the weighted digraph with weights given by the delays computed in step 3. That is,

$$w_i = \min \{X_{s,\ell_1} + X_{\ell_1,\ell_2} + \cdots + X_{\ell_m,i} : (s, \ell_1, \ldots, \ell_m, i) \text{ is a path from } s \text{ to } i\}.$$

Following this procedure, we generate exact samples of the arrival times of the underlying epidemic spreading process. Each sample gives a set of N pairs of the form (d_i, w_i) for $i \in V$, where d_i is the distance from the source and w_i the epidemic arrival time.

To compute the expected arrival times for the scatter plots in Fig. 4 of the main text, we simply average the w_i over many samples with different random source nodes. To compute the delay τ requires additional consideration of the distance from the source. For each n, one can compute the time for a simulated contagion to reach that distance from the source by computing $t_n = \min_i\{w_i : d_i = n\}$. Averaging this quantity over many samples produces $\langle t_n \rangle$, the mean time for a contagion to reach distance n from a random source. Figure 4-11 shows a typical example of how this quantity varies with the distance considered.

In the networks we are interested in, the number of nodes at distance n from the source grows exponentially with n (the small world property). We have developed our theory under the assumption that $n \gg 1$, but still small relative to the diameter of the network. For n too small or too large the speed of spread will be limited by a lack of multiplicity of routes of that length. In this sense the theoretical value of τ we compute is the smallest possible, corresponding to the regime in which the contagion is spreading rapidly through the bulk of the network. To measure this from simulation data we take $\tau = \min_n\{\langle t_{n+1} \rangle - \langle t_n \rangle\}$.

For simulating complex contagions with a threshold $\theta > 1$, we find it easier to use an event-based algorithm. Starting from a randomly chosen set of source nodes (larger for higher θ to give the contagion a chance to take hold), we keep track of individual contagion events to determine for each node when its threshold is reached.

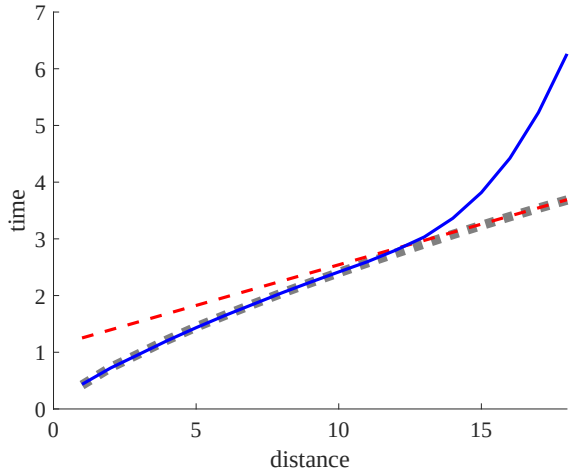

Figure 4-11: *Plot of the time $\langle t_n \rangle$ for an infection to reach a given distance n from a random source. For this figure we simulated an infection with exponential unit rate transmission time in an Erdős Rényi graph of 10^7 nodes and mean degree 3, averaged over 100 samples. The red dotted line shows the gradient τ as predicted by our theory for spreading speed. The grey dashed line shows numerical simulations of a branching process model tuned to match the network in question, effectively removing the large n finite size effects.*

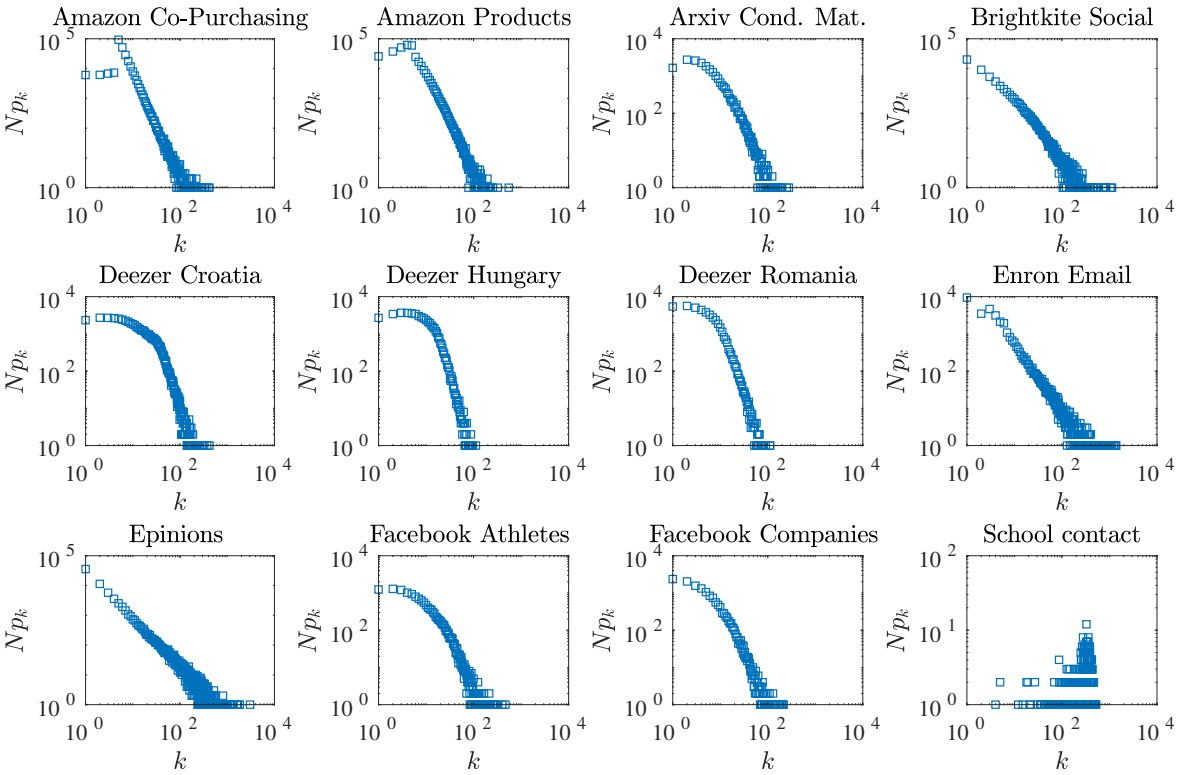

Figure 4-12: *Degree distributions of empirical networks.*

Table of data for main Figure 3

Network name	λ	τ	τ_{emp}	N	$\langle k \rangle$	Clustering	Assortativity
Deezer Romania [5]	16.0	0.0236	0.0225	41773	6.024	0.0912	0.1140
Amazon Co-purchasing [6]	17.8	0.0211	0.0188	262111	6.866	0.4198	-0.0025
Amazon Products [7]	20.7	0.0181	0.0162	334863	5.530	0.3967	-0.0588
Deezer Hungary[5]	22.9	0.0163	0.0187	47538	9.377	0.1162	0.2072
Facebook Companies [5]	30.6	0.0122	0.0145	14113	7.387	0.2392	0.0126
Arxiv Cond. Mat.[8]	35.8	0.0104	0.0145	21363	8.546	0.6417	0.1253
Facebook Athletes [5]	44.3	0.0084	0.0124	13866	12.521	0.2762	-0.0270
Deezer Croatia [5]	46.2	0.008	0.0104	54573	18.258	0.1365	0.1971
Brightkite Social [9]	99.9	0.0037	0.0086	56739	7.5	0.1734	0.0096
Enron Email [10]	115.5	0.0032	0.0055	33696	10.732	0.5092	-0.1165
Epinions [11]	181.6	0.0021	0.0044	75877	10.695	0.1378	-0.0406
School contact [12]	335.9	0.0032	0.00099	788	300.2	0.499	0.0539

REFERENCES

[1] T. Rogers, "Assessing node risk and vulnerability in epidemics on networks," *EPL (Europhysics Letters)*, vol. 109, no. 2, p. 28005, 2015.

[2] C. Moore and M. E. Newman, "Epidemics and percolation in small-world networks," *Physical Review E*, vol. 61, no. 5, p. 5678, 2000.

[3] M. Shrestha and C. Moore, "Message-passing approach for threshold models of behavior in networks," *Physical Review E*, vol. 89, no. 2, p. 022805, 2014.

[4] T. Martin, X. Zhang, and M. E. Newman, "Localization and centrality in networks," *Physical review E*, vol. 90, no. 5, p. 052808, 2014.

[5] B. Rozemberczki, R. Davies, R. Sarkar, and C. Sutton, "Gemsec: graph embedding with self clustering," *arXiv preprint arXiv:1802.03997*, 2018.

[6] J. Leskovec, L. A. Adamic, and B. A. Huberman, "The dynamics of viral marketing," *ACM Transactions on the Web (TWEB)*, vol. 1, no. 1, p. 5, 2007.

[7] J. Yang and J. Leskovec, "Defining and evaluating network communities based on ground-truth," *Knowledge and Information Systems*, vol. 42, no. 1, pp. 181–213, 2015.

[8] J. Leskovec, J. Kleinberg, and C. Faloutsos, "Graph evolution: Densification and shrinking diameters," *ACM Transactions on Knowledge Discovery from Data (TKDD)*, vol. 1, no. 1, p. 2, 2007.

[9] E. Cho, S. A. Myers, and J. Leskovec, "Friendship and mobility: user movement in location-based social networks," in *Proceedings of the 17th ACM SIGKDD international conference on Knowledge discovery and data mining*, pp. 1082–1090, ACM, 2011.

[10] J. Leskovec, K. J. Lang, A. Dasgupta, and M. W. Mahoney, "Community structure in large networks: Natural cluster sizes and the absence of large well-defined clusters," *Internet Mathematics*, vol. 6, no. 1, pp. 29–123, 2009.

[11] M. Richardson, R. Agrawal, and P. Domingos, "Trust management for the semantic web," in *International semantic Web conference*, pp. 351–368, Springer, 2003.

[12] M. Salathé, M. Kazandjieva, J. W. Lee, P. Levis, M. W. Feldman, and J. H. Jones, "A high-resolution human contact network for infectious disease transmission," *Proceedings of the National Academy of Sciences*, vol. 107, no. 51, pp. 22020–22025, 2010.

CHAPTER 5

CONCLUDING REMARKS

Networks have already proved themselves to be a promising framework for studying the spread of diseases in structured populations. However, due to the high levels of biological, environmental and societal complexity inherent in epidemic dynamics, developing an effective mathematical framework is a challenging task. In the introduction we described how both network and epidemic models have evolved through a series of progressive refinements over the last century. Today's network epidemic models are more insightful than ever, though while the gap between model and reality is closing it still remains very significant. The work presented in this thesis adds another few steps towards a general and accurate theory of epidemics.

We saw in Section 1.1 how population structure itself has become increasingly well represented by random graph models. A plethora of techniques have been developed to reflect a large range of observed network characteristics, including arbitrary degree distributions, local clustering and the existence of highly connected hubs. Typically though, the more complex the graph model, the less is known about how epidemics spread on it. Increasingly sophisticated techniques to model many aspects of infection spread, while often proven effective in some special cases, frequently lack the generalisability needed to match realistic population models. Similarly, while there have been effective advancements to model infection dynamics, such as heterogeneity and disease interactions, these techniques are often not compatible and we still have a way to go to achieve an effective and complete epidemiological theory.

In Chapter 2 we modelled a secondary infection with dependence on a primary host. In the environment of a sparse Erdős-Rényi graph, we were able to provide interesting insight into the relative infection speeds required for the secondary infection to survive. Through the application of branching process models we found that a secondary infection must progress at a similar time scale to the primary infection, and also that large secondary epidemics result from a relatively fast secondary infection, but are very rare.

While this certainly proves an interesting and insightful case study, however, the meth-

ods used are not directly applicable to networks with clustering or inhomogeneous structure. The desirable next step would be to translate the results we found here into a more general class of graph structure. A possible avenue for such advancement is by way of temporal networks. In secondary infection dynamics the primary infection creates an evolving network environment in which the infection may grow. There is then some scope for a translation of the model to a simple disease on a temporal network, the likes of which have been studied recently in [123, 124, 121] for example. What our results do suggest are phenomena that may well be generalised, and techniques that may very well be extended.

Furthermore, while the work presented here is of theoretical interest in its own right, motivations for its study were made throughout in a variety of physical processes. The natural next step would then be to consider related physical phenomena directly, with the use of real model parameters and comparative datasets.

Additionally to superinfections, such as the aforementioned Hepatitis D virus, two stage contagion dynamics may be found to appear in many other contexts; the spreading of bacteriophages between virally infected hosts; in modelling ecosystems, habitat colonisation by predatory species; within social networks, the spread of increasingly extreme politics and consequential radicalisation. In all these contexts it would be both interesting and potentiality instructive to adapt our model to reflect such interactions. This would enable us to identify the necessary relative time scales of successful secondary waves and explore our hypothesis of the rarity of large secondary outbreaks.

One question the machinery developed in Chapter 2 is unable to address, however, is how a network may not be uniformly responsive to such infection dynamics. In a recent survey paper highlighting challenges in epidemiology [125] it was observed that understanding the impact of heterogeneity is of key importance in developing a good infection model. While this is a question that has not entirely gone unanswered (contributions including [107, 91, 25]), in Chapter 3 we successfully extended this further to exploring the role of network structure with multiple interacting infections.

We demonstrated how recent techniques for analysing heterogeneous node response may be extended to a complex contagion model, giving an understanding of how topological characteristics may make different parts of the network more or less vulnerable to any one infection strain. Perhaps the most important moral of this paper is a proof of concept for the extension of a powerful technique, based on the message passing equations, to be used to model complex infection characteristics. For instance, message passing equations have, in the context of a simple single infection model, been used to find optimal immunisation sets [115]. Similar analysis may realistically also be applied to multi-infection models using the message passing variants we have developed, making them a potentially instructive tool to be used in complex disease mitigation.

This method is effective, not only for exploring heterogeneity in a very general class of graph structure but also for modelling general infection dynamics, including non-exponential lifetimes. There is also further scope to make similar adaptations to those discussed in order to consider bootstrap, or k-core, percolation dynamics for the modelling

of infections with threshold behaviour. Threshold dynamics are naturally applicable to modelling ideas spreading through social networks. In this context a multi-type infection may again be relevant to represent different levels of influence [126] and it may be possible to use our model to assess individual propensity to becoming a super influencer. Whilst this model is demonstrably adaptable, however, it has yet to be tested in a wide range of contexts and with real measured parameters to potentially produce insightful results.

There are also challenges remaining in the implementation of the approach– its formulation may lead to a large system of equations that is computationally expensive or mathematically intractable. Further research into techniques to analyse the message passing equations may represent a significant advancement in the field.

Such a contribution is presented in Chapter 4 with a calculation of infection progression speed that, when combined with the system of time dependent message passing equations, may enable the calculation of temporal vulnerability. Here we successfully used a wave front calculation to find the asymptotic speed at which an infection moves away from its source. Furthermore, we demonstrated how, as a consequence of the same calculation, the expected infection arrival time may be correlated with the non-backtracking centrality. Finally, since centrality measures are localised properties, strongly dependent only on an individuals immediate neighbourhood, it follows that the expected offset in infection time is independent of graph size. This enables us to conclude with the result that infection prevalence is relatively sharp in the limit of large graphs.

The techniques used in these calculations depend upon sparse homogeneous graph structures, though work demonstrably well as an approximation to a broad class of real world networks also. To greater understand the model's effectiveness and mathematical limitations it would certainly be advantageous to build on this work with a more rigorous understanding of the approximation made, so its results may be more reliably used.

In Chapter 4 we again restricted our discussions to exponential or Weibull infection dynamics. However, as we noted earlier, calculations such as these based on message passing equations work effectively with a much more general class of infection time distribution. Furthermore, due to the observation of timings, it is possible to observe whether the infection becomes multipley present in a given neighbourhood at any one instance. This means that we may be able to also apply the method to a class of threshold models.

It is then possible to use the methodology of Chapter 4 to consider many further classes of infection dynamics. For instance a *k-core* type infection may be modelled, where an individual may only become infected after being exposed to k separate infected neighbours. Through simulation it may by observed that individual node mean infection times are again log-linearly correlated with non-backtracking centrality, showing this to be a more general phenomena than demonstrated in Chapter 4. In fact, it seems that breaking this relationship requires infection dynamics that penalise highly connected nodes– such an example given by an adaptive threshold model where infection is dependent on having a given proportion, rather than number, of infected neighbours.

It would then make for an instructive avenue for future work to repeat similar infection

speed calculations with different infection dynamics This would allow us to better quantify and test our results for the use of a wide range of different social, biological and engineering applications.

In conclusion, we have presented a number of results on both the interactions of complex infections and the dynamics of their evolution, which together achieve further small improvements to the theory of epidemic modelling on networks. We have reason to believe that, going forward, these results will be further augmented and combined in the manner of scientific advancement to achieve a yet richer understanding of epidemic spread that may be employed in the management and mitigation of infectious disease.

BIBLIOGRAPHY

[1] H. F. Gray, "Sewerage in ancient and mediaeval times," *Sewage Works Journal*, pp. 939–946, 1940.

[2] F. Karinthy, "Chain-links," *Everything is different*, 1929.

[3] W. O. Kermack and A. G. McKendrick, "A contribution to the mathematical theory of epidemics," *Proceedings of the royal society of london. Series A, Containing papers of a mathematical and physical character*, vol. 115, no. 772, pp. 700–721, 1927.

[4] R. M. Anderson, "Discussion: the kermack-mckendrick epidemic threshold theorem," *Bulletin of mathematical biology*, vol. 53, no. 1-2, p. 1, 1991.

[5] M. J. Mäkelä, T. Puhakka, O. Ruuskanen, M. Leinonen, P. Saikku, M. Kimpimäki, S. Blomqvist, T. Hyypiä, and P. Arstila, "Viruses and bacteria in the etiology of the common cold," *Journal of clinical microbiology*, vol. 36, no. 2, pp. 539–542, 1998.

[6] C. for disease and control prevention, "Reports of selected e. coli outbreak investigations." `https://www.cdc.gov/ecoli/outbreaks.html`. [Accessed 30 July 2019].

[7] D. M. Morens, J. K. Taubenberger, and A. S. Fauci, "Predominant role of bacterial pneumonia as a cause of death in pandemic influenza: implications for pandemic influenza preparedness," *The Journal of infectious diseases*, vol. 198, no. 7, pp. 962–970, 2008.

[8] N. Lanchier and Y. Zhang, "Some rigorous results for the stacked contact process," *arXiv preprint arXiv:1410.3842*, 2014.

[9] R. A. Blythe, R. J. Allen, *et al.*, "Parasites on parasites: Coupled fluctuations in stacked contact processes," *EPL (Europhysics Letters)*, vol. 101, no. 5, p. 50001, 2013.

[10] W. B. Whitman, D. C. Coleman, and W. J. Wiebe, "Prokaryotes: the unseen majority," *Proceedings of the National Academy of Sciences*, vol. 95, no. 12, pp. 6578–6583, 1998.

[11] W. Cai, L. Chen, F. Ghanbarnejad, and P. Grassberger, "Avalanche outbreaks emerging in cooperative contagions," *Nature physics*, vol. 11, no. 11, p. 936, 2015.

[12] J. R. Gog and B. T. Grenfell, "Dynamics and selection of many-strain pathogens," *Proceedings of the National Academy of Sciences*, vol. 99, no. 26, pp. 17209–17214, 2002.

[13] J. Gog and J. Swinton, "A status-based approach to multiple strain dynamics," *Journal of mathematical biology*, vol. 44, no. 2, pp. 169–184, 2002.

[14] I. live stats. `https://www.internetlivestats.com/total-number-of-websites/`. [Accessed 30 July 2019].

[15] F. newsroom. `https://newsroom.fb.com/company-info/`. [Accessed 30 July 2019].

[16] R. Solomonoff and A. Rapoport, "Connectivity of random nets," *The bulletin of mathematical biophysics*, vol. 13, no. 2, pp. 107–117, 1951.

[17] E. N. Gilbert, "Random graphs," *The Annals of Mathematical Statistics*, vol. 30, no. 4, pp. 1141–1144, 1959.

[18] P. Erdös and A. Rényi, "On random graphs, i," *Publicationes Mathematicae (Debrecen)*, vol. 6, pp. 290–297, 1959.

[19] P. Erdös and A. Rényi, "On the evolution of random graphs," *Publ. Math. Inst. Hung. Acad. Sci*, vol. 5, no. 1, pp. 17–60, 1960.

[20] A. Nachmias and Y. Peres, "Component sizes of the random graph outside the scaling window," *arXiv preprint math/0610466*, 2006.

[21] R. M. Karp, "The transitive closure of a random digraph," *Random Structures & Algorithms*, vol. 1, no. 1, pp. 73–93, 1990.

[22] M. S. Bartlett, *An introduction to stochastic processes: with special reference to methods and applications*. CUP Archive, 1978.

[23] D. G. Kendall, "Deterministic and stochastic epidemics in closed populations," in *Proc. 3rd Berkeley Symp. Math. Statist. Prob*, vol. 4, pp. 149–165, 1956.

[24] F. Ball, "The threshold behaviour of epidemic models," *Journal of Applied Probability*, vol. 20, no. 2, pp. 227–241, 1983.

[25] O. Diekmann, J. A. P. Heesterbeek, and J. A. Metz, "On the definition and the computation of the basic reproduction ratio r 0 in models for infectious diseases in heterogeneous populations," *Journal of mathematical biology*, vol. 28, no. 4, pp. 365–382, 1990.

[26] I.-J. Bienaymé, "De la loi de multiplication et de la durée des familles," *Soc. Philomat. Paris Extraits, Sér*, vol. 5, no. 37-39, p. 4, 1845.

[27] D. G. Kendall, "Branching processes since 1873," *Journal of the London Mathematical Society*, vol. 1, no. 1, pp. 385–406, 1966.

[28] H. W. Watson and F. Galton, "On the probability of the extinction of families," *The Journal of the Anthropological Institute of Great Britain and Ireland*, vol. 4, pp. 138–144, 1875.

[29] F. Galton and H. Watson, "Educational times," *Galtons first thoughts on the problem of the extinction of families*, 1873.

[30] T. E. Harris, *The theory of branching processes*. Courier Corporation, 2002.

[31] K. B. Athreya, "Branching process," *Encyclopedia of Environmetrics*, vol. 1, 2006.

[32] K. B. Athreya and P. Jagers, *Classical and modern branching processes*, vol. 84. Springer Science & Business Media, 2012.

[33] T. Biyikoglu, J. Leydold, and P. F. Stadler, *Laplacian eigenvectors of graphs: Perron-Frobenius and Faber-Krahn type theorems*. Springer, 2007.

[34] B. A. Sevast'yanov, "Limit theorems for branching stochastic processes of special form," *Theory of Probability & Its Applications*, vol. 2, no. 3, pp. 321–331, 1957.

[35] W. T. Scott and G. E. Uhlenbeck, "On the theory of cosmic-ray showers ii. further contributions to the fluctuation problem," *Physical Review*, vol. 62, no. 11-12, p. 497, 1942.

[36] B. Bollobás and O. Riordan, "Random graphs and branching processes," in *Handbook of large-scale random networks*, pp. 15–115, Springer, 2008.

[37] T. Łuczak, "Random trees and random graphs," *Random structures & algorithms*, vol. 13, no. 3-4, pp. 485–500, 1998.

[38] B. Bollobás, "The evolution of random graphs," *Transactions of the American Mathematical Society*, vol. 286, no. 1, pp. 257–274, 1984.

[39] B. Bollobás and B. Béla, *Random graphs*. No. 73, Cambridge university press, 2001.

[40] T. Łuczak, "Component behavior near the critical point of the random graph process," *Random Structures & Algorithms*, vol. 1, no. 3, pp. 287–310, 1990.

[41] O. Riordan and N. Wormald, "The diameter of sparse random graphs," *Combinatorics, Probability and Computing*, vol. 19, no. 5-6, pp. 835–926, 2010.

[42] M. Molloy and B. Reed, "A critical point for random graphs with a given degree sequence," *Random structures & algorithms*, vol. 6, no. 2-3, pp. 161–180, 1995.

[43] F. Chung and L. Lu, "The average distances in random graphs with given expected degrees," *Proceedings of the National Academy of Sciences*, vol. 99, no. 25, pp. 15879–15882, 2002.

[44] B. Söderberg, "General formalism for inhomogeneous random graphs," *Physical review E*, vol. 66, no. 6, p. 066121, 2002.

[45] M. E. Newman, "Assortative mixing in networks," *Physical review letters*, vol. 89, no. 20, p. 208701, 2002.

[46] T. Gross, C. J. D. D'Lima, and B. Blasius, "Epidemic dynamics on an adaptive network," *Physical review letters*, vol. 96, no. 20, p. 208701, 2006.

[47] B. Rozemberczki, R. Davies, R. Sarkar, and C. Sutton, "Gemsec: graph embedding with self clustering," *arXiv preprint arXiv:1802.03997*, 2018.

[48] J. Leskovec, J. Kleinberg, and C. Faloutsos, "Graph evolution: Densification and shrinking diameters," *ACM Transactions on Knowledge Discovery from Data (TKDD)*, vol. 1, no. 1, p. 2, 2007.

[49] M. Salathé, M. Kazandjieva, J. W. Lee, P. Levis, M. W. Feldman, and J. H. Jones, "A high-resolution human contact network for infectious disease transmission," *Proceedings of the National Academy of Sciences*, vol. 107, no. 51, pp. 22020–22025, 2010.

[50] J. Leskovec and J. J. Mcauley, "Learning to discover social circles in ego networks," in *Advances in neural information processing systems*, pp. 539–547, 2012.

[51] B. Bollobás and O. Riordan, "The diameter of a scale-free random graph," *Combinatorica*, vol. 24, no. 1, pp. 5–34, 2004.

[52] A. Fronczak, J. A. Hołyst, M. Jedynak, and J. Sienkiewicz, "Higher order clustering coefficients in barabási–albert networks," *Physica A: Statistical Mechanics and its Applications*, vol. 316, no. 1-4, pp. 688–694, 2002.

[53] R. Albert and A.-L. Barabási, "Statistical mechanics of complex networks," *Reviews of modern physics*, vol. 74, no. 1, p. 47, 2002.

[54] J. Travers and S. Milgram, "An experimental study of the small world problem," in *Social Networks*, pp. 179–197, Elsevier, 1977.

[55] S. Milgram, "The small world problem," *Psychology today*, vol. 2, no. 1, pp. 60–67, 1967.

[56] M. E. Newman, S. H. Strogatz, and D. J. Watts, "Random graphs with arbitrary degree distributions and their applications," *Physical review E*, vol. 64, no. 2, p. 026118, 2001.

[57] A. Barrat and M. Weigt, "On the properties of small-world network models," *The European Physical Journal B-Condensed Matter and Complex Systems*, vol. 13, no. 3, pp. 547–560, 2000.

[58] M. Richardson, R. Agrawal, and P. Domingos, "Trust management for the semantic web," in *International semantic Web conference*, pp. 351–368, Springer, 2003.

[59] J. Leskovec, K. J. Lang, A. Dasgupta, and M. W. Mahoney, "Community structure in large networks: Natural cluster sizes and the absence of large well-defined clusters," *Internet Mathematics*, vol. 6, no. 1, pp. 29–123, 2009.

[60] J. Yang and J. Leskovec, "Defining and evaluating network communities based on ground-truth," *Knowledge and Information Systems*, vol. 42, no. 1, pp. 181–213, 2015.

[61] J. Leskovec, J. Kleinberg, and C. Faloutsos, "Graphs over time: densification laws, shrinking diameters and possible explanations," in *Proceedings of the eleventh ACM SIGKDD international conference on Knowledge discovery in data mining*, pp. 177–187, ACM, 2005.

[62] R. Pastor-Satorras and A. Vespignani, "Epidemic spreading in scale-free networks," *Physical review letters*, vol. 86, no. 14, p. 3200, 2001.

[63] A.-L. Barabási and R. Albert, "Emergence of scaling in random networks," *science*, vol. 286, no. 5439, pp. 509–512, 1999.

[64] R. Van Der Hofstad, *Random graphs and complex networks*, vol. 1. Cambridge university press, 2016.

[65] M. E. J. Newman, "Random graphs with clustering," *Phys. Rev. Lett.*, vol. 103, p. 058701, 2009.

[66] J. W. Essam, "Percolation theory," *Reports on progress in physics*, vol. 43, no. 7, p. 833, 1980.

[67] D. Stauffer and A. Aharony, *Introduction to percolation theory*. Taylor & Francis, 2018.

[68] D. Stauffer, "Scaling theory of percolation clusters," *Physics reports*, vol. 54, no. 1, pp. 1–74, 1979.

[69] J. Chalupa, P. L. Leath, and G. R. Reich, "Bootstrap percolation on a bethe lattice," *Journal of Physics C: Solid State Physics*, vol. 12, no. 1, p. L31, 1979.

[70] J. Adler, "Bootstrap percolation," *Physica A: Statistical Mechanics and its Applications*, vol. 171, no. 3, pp. 453–470, 1991.

[71] B. Karrer, M. E. Newman, and L. Zdeborová, "Percolation on sparse networks," *Physical review letters*, vol. 113, no. 20, p. 208702, 2014.

[72] D. S. Callaway, M. E. Newman, S. H. Strogatz, and D. J. Watts, "Network robustness and fragility: Percolation on random graphs," *Physical review letters*, vol. 85, no. 25, p. 5468, 2000.

[73] K. E. Hamilton and L. P. Pryadko, "Tight lower bound for percolation threshold on an infinite graph," *Physical review letters*, vol. 113, no. 20, p. 208701, 2014.

[74] T. Martin, X. Zhang, and M. Newman, "Localization and centrality in networks," *Physical Review E*, vol. 90, no. 5, p. 052808, 2014.

[75] S. P. Borgatti, "Centrality and network flow," *Social networks*, vol. 27, no. 1, pp. 55–71, 2005.

[76] B. Bollobás, C. Borgs, J. Chayes, O. Riordan, *et al.*, "Percolation on dense graph sequences," *The Annals of Probability*, vol. 38, no. 1, pp. 150–183, 2010.

[77] M. Y. Li and J. S. Muldowney, "Global stability for the seir model in epidemiology," *Mathematical biosciences*, vol. 125, no. 2, pp. 155–164, 1995.

[78] W.-m. Liu, H. W. Hethcote, and S. A. Levin, "Dynamical behavior of epidemiological models with nonlinear incidence rates," *Journal of mathematical biology*, vol. 25, no. 4, pp. 359–380, 1987.

[79] H. W. Hethcote, "The mathematics of infectious diseases," *SIAM review*, vol. 42, no. 4, pp. 599–653, 2000.

[80] A. McLean and R. M. Anderson, "Measles in developing countries part i. epidemiological parameters and patterns," *Epidemiology & Infection*, vol. 100, no. 1, pp. 111–133, 1988.

[81] A. Gray, D. Greenhalgh, L. Hu, X. Mao, and J. Pan, "A stochastic differential equation sis epidemic model," *SIAM Journal on Applied Mathematics*, vol. 71, no. 3, pp. 876–902, 2011.

[82] L. J. Allen, F. Brauer, P. Van den Driessche, and J. Wu, *Mathematical epidemiology*, vol. 1945. Springer, 2008.

[83] H. W. Hethcote and J. A. Yorke, *Gonorrhea transmission dynamics and control*, vol. 56. Springer, 2014.

[84] N. T. Bailey *et al.*, *The mathematical theory of infectious diseases and its applications*. No. 2nd ediition, Charles Griffin & Company Ltd 5a Crendon Street, High Wycombe, Bucks HP13 6LE., 1975.

[85] P. A. H. Organisation, "Countries and territories with autochthonous transmission of zika virus in the americas reported in 2015-2017." `https://www.paho.org/hq/`. [Accessed 04 September 2019].

[86] E. M. of Public Health, "Vector transmitted diseases, zika virus." `https://www.salud.gob.ec/wp-content/uploads/2015/12/vvGACETA-ZIKA_SE-32.pdf`.

[87] E. B. Wilson and J. Worcester, "The spread of an epidemic," *Proceedings of the National Academy of Sciences of the United States of America*, vol. 31, no. 10, p. 327, 1945.

[88] S. Rushton and A. Mautner, "The deterministic model of a simple epidemic for more than one community," *Biometrika*, vol. 42, no. 1/2, pp. 126–132, 1955.

[89] K. Dietz and D. Schenzle, "Mathematical models for infectious disease statistics," in *A celebration of statistics*, pp. 167–204, Springer, 1985.

[90] R. Pastor-Satorras and A. Vespignani, "Epidemic dynamics in finite size scale-free networks," *Physical Review E*, vol. 65, no. 3, p. 035108, 2002.

[91] Y. Moreno, R. Pastor-Satorras, and A. Vespignani, "Epidemic outbreaks in complex heterogeneous networks," *The European Physical Journal B-Condensed Matter and Complex Systems*, vol. 26, no. 4, pp. 521–529, 2002.

[92] J. C. Miller, A. C. Slim, and E. M. Volz, "Edge-based compartmental modelling for infectious disease spread," *Journal of the Royal Society Interface*, vol. 9, no. 70, pp. 890–906, 2011.

[93] N. Sherborne, J. C. Miller, K. B. Blyuss, and I. Z. Kiss, "Mean-field models for non-markovian epidemics on networks," *Journal of mathematical biology*, vol. 76, no. 3, pp. 755–778, 2018.

[94] F. Ball and P. Neal, "Network epidemic models with two levels of mixing," *Mathematical biosciences*, vol. 212, no. 1, pp. 69–87, 2008.

[95] J. Lindquist, J. Ma, P. Van den Driessche, and F. H. Willeboordse, "Effective degree network disease models," *Journal of mathematical biology*, vol. 62, no. 2, pp. 143–164, 2011.

[96] M. J. Keeling, "The effects of local spatial structure on epidemiological invasions," *Proceedings of the Royal Society of London. Series B: Biological Sciences*, vol. 266, no. 1421, pp. 859–867, 1999.

[97] M. E. Newman, "Properties of highly clustered networks," *Physical Review E*, vol. 68, no. 2, p. 026121, 2003.

[98] F. Ball, D. Mollison, and G. Scalia-Tomba, "Epidemics with two levels of mixing," *The Annals of Applied Probability*, pp. 46–89, 1997.

[99] M. J. Keeling and K. T. Eames, "Networks and epidemic models," *Journal of the Royal Society Interface*, vol. 2, no. 4, pp. 295–307, 2005.

[100] G. P. Garnett and R. M. Anderson, "Sexually transmitted diseases and sexual behavior: insights from mathematical models," *Journal of Infectious Diseases*, vol. 174, no. Supplement_2, pp. S150–S161, 1996.

[101] D. Chakrabarti, Y. Wang, C. Wang, J. Leskovec, and C. Faloutsos, "Epidemic thresholds in real networks," *ACM Transactions on Information and System Security (TISSEC)*, vol. 10, no. 4, p. 1, 2008.

[102] Y. Wang, D. Chakrabarti, C. Wang, and C. Faloutsos, "Epidemic spreading in real networks: An eigenvalue viewpoint," in *22nd International Symposium on Reliable Distributed Systems, 2003. Proceedings.*, pp. 25–34, IEEE, 2003.

[103] P. L. Simon, M. Taylor, and I. Z. Kiss, "Exact epidemic models on graphs using graph-automorphism driven lumping," *Journal of mathematical biology*, vol. 62, no. 4, pp. 479–508, 2011.

[104] J. A. Ward and J. Evans, "A general model of dynamics on networks with graph automorphism lumping," in *International Conference on Complex Networks and their Applications*, pp. 445–456, Springer, 2018.

[105] H. Frisch and J. Hammersley, "Percolation processes and related topics," *Journal of the society for industrial and applied mathematics*, vol. 11, no. 4, pp. 894–918, 1963.

[106] P. Grassberger, "On the critical behavior of the general epidemic process and dynamical percolation," *Mathematical Biosciences*, vol. 63, no. 2, pp. 157–172, 1983.

[107] T. Rogers, "Assessing node risk and vulnerability in epidemics on networks," *EPL (Europhysics Letters)*, vol. 109, no. 2, p. 28005, 2015.

[108] H. W. Hethcote and D. W. Tudor, "Integral equation models for endemic infectious diseases," *Journal of mathematical biology*, vol. 9, no. 1, pp. 37–47, 1980.

[109] R. K. Miller and R. K. Miller, *Nonlinear Volterra integral equations*. No. 48, WA Benjamin, 1971.

[110] G. Röst, Z. Vizi, and I. Kiss, "Pairwise approximation for sir-type network epidemics with non-markovian recovery," *Proceedings of the Royal Society A: Mathematical, Physical and Engineering Sciences*, vol. 474, no. 2210, p. 20170695, 2018.

[111] B. Karrer and M. E. Newman, "Message passing approach for general epidemic models," *Physical Review E*, vol. 82, no. 1, p. 016101, 2010.

[112] J. Pearl, *Reverend Bayes on inference engines: A distributed hierarchical approach.* Cognitive Systems Laboratory, School of Engineering and Applied Science, 1982.

[113] M. Mezard, G. Parisi, M. A. Virasoro, and D. J. Thouless, "Spin glass theory and beyond," *Physics Today*, vol. 41, p. 109, 1988.

[114] R. Kühn and T. Rogers, "Heterogeneous micro-structure of percolation in sparse networks," *EPL (Europhysics Letters)*, vol. 118, no. 6, p. 68003, 2017.

[115] F. Altarelli, A. Braunstein, L. Dall'Asta, J. R. Wakeling, and R. Zecchina, "Containing epidemic outbreaks by message-passing techniques," *Physical Review X*, vol. 4, no. 2, p. 021024, 2014.

[116] R. R. Wilkinson and K. J. Sharkey, "Message passing and moment closure for susceptible-infected-recovered epidemics on finite networks," *Physical Review E*, vol. 89, no. 2, p. 022808, 2014.

[117] R. R. Wilkinson, F. G. Ball, and K. J. Sharkey, "The relationships between message passing, pairwise, kermack–mckendrick and stochastic sir epidemic models," *Journal of mathematical biology*, vol. 75, no. 6-7, pp. 1563–1590, 2017.

[118] S. Melnik, A. Hackett, M. A. Porter, P. J. Mucha, and J. P. Gleeson, "The unreasonable effectiveness of tree-based theory for networks with clustering," *Physical Review E*, vol. 83, no. 3, p. 036112, 2011.

[119] F. Negro, "Hepatitis d virus coinfection and superinfection," *Cold Spring Harbor perspectives in medicine*, vol. 4, no. 11, p. a021550, 2014.

[120] E. Valdano, L. Ferreri, C. Poletto, and V. Colizza, "Analytical computation of the epidemic threshold on temporal networks," *Physical Review X*, vol. 5, no. 2, p. 021005, 2015.

[121] A. Koher, H. H. Lentz, P. Hövel, and I. M. Sokolov, "Infections on temporal networks- a matrix based approach," *PloS one*, vol. 11, no. 4, p. e0151209, 2016.

[122] J. P. Gleeson, J. A. Ward, K. P. O'Sullivan, and W. T. Lee, "Competition-induced criticality in a model of meme popularity," *arXiv preprint arXiv:1305.4328*, 2013.

[123] L. Speidel, K. Klemm, V. M. Eguíluz, and N. Masuda, "Temporal interactions facilitate endemicity in the susceptible-infected-susceptible epidemic model," *New Journal of Physics*, vol. 18, p. 073013, jul 2016.

[124] L. E. Rocha and N. Masuda, "Individual-based approach to epidemic processes on arbitrary dynamic contact networks," *Scientific reports*, no. 6, p. 31456, 2016.

[125] L. Pellis, F. Ball, S. Bansal, K. Eames, T. House, V. Isham, and P. Trapman, "Eight challenges for network epidemic models," *Epidemics*, vol. 10, pp. 58–62, 2015.

[126] S. Melnik, J. A. Ward, J. P. Gleeson, and M. A. Porter, "Multi-stage complex contagions," *Chaos: An Interdisciplinary Journal of Nonlinear Science*, vol. 23, no. 1, p. 013124, 2013.